



12-2017

Improving the Adhesion of Glass/Polypropylene (Glass/PP) and High-Density Polyethylene (HDPE) Surfaces by Open Air Plasma Treatment

Vidyarani Sangnal Matt Durandhara Murthy
University of Tennessee

Recommended Citation

Sangnal Matt Durandhara Murthy, Vidyarani, "Improving the Adhesion of Glass/Polypropylene (Glass/PP) and High-Density Polyethylene (HDPE) Surfaces by Open Air Plasma Treatment." Master's Thesis, University of Tennessee, 2017.
https://trace.tennessee.edu/utk_gradthes/4999

This Thesis is brought to you for free and open access by the Graduate School at Trace: Tennessee Research and Creative Exchange. It has been accepted for inclusion in Masters Theses by an authorized administrator of Trace: Tennessee Research and Creative Exchange. For more information, please contact trace@utk.edu.

To the Graduate Council:

I am submitting herewith a thesis written by Vidyarani Sangnal Matt Durandhara Murthy entitled "Improving the Adhesion of Glass/Polypropylene (Glass/PP) and High-Density Polyethylene (HDPE) Surfaces by Open Air Plasma Treatment." I have examined the final electronic copy of this thesis for form and content and recommend that it be accepted in partial fulfillment of the requirements for the degree of Master of Science, with a major in Mechanical Engineering.

Uday Vaidya, Major Professor

We have read this thesis and recommend its acceptance:

Chad Duty, Madhu S. Madhukar

Accepted for the Council:

Carolyn R. Hodges

Vice Provost and Dean of the Graduate School

(Original signatures are on file with official student records.)

**Improving the Adhesion of Glass/Polypropylene
(Glass/PP) and High-Density Polyethylene (HDPE)
Surfaces by Open Air Plasma Treatment**

**A Thesis Presented for the
Master of Science
Degree
The University of Tennessee, Knoxville**

**Vidyarani Sangnal Matt Durandhara Murthy
December 2017**

Copyright 2017 by
Vidyarani Sangnal Matt Durandhara Murthy

Acknowledgments

I would like to express my sincere and heartfelt gratitude to my thesis advisor Dr. Uday Vaidya for his expert advice and constant guidance all the time I needed.

I would like to thank wholeheartedly my committee professors, Dr. Chad Duty and Dr. Madhu Madhukar for their technical input during my study. I would like to extend my sincere thanks to Dr. John Dunlap for training me on SEM instrument. My gratitude is due to David Nuttel, process engineer at MDF, for all the help during installation of the Plasmamatreat instrument.

I would like to express my heartfelt gratitude to Tim Smith, Andy Stretcher and Wilson Lee from Plasmamatreat USA, Inc. for providing us the plasma treatment equipment and helping me successfully finish my thesis.

I would like to thank my Knoxville friends, Surbhi Kore, Kaustubh Mungale, Pritesh Yeole, Jared Hughes and Shailesh Alwekar for all the support.

Finally, I want to thank my nearest and dearest ones, my father, Durandhara Murthy, my mother, Malini Durandhara Murthy, my husband, Dr. Nitilaksha Hiremath, my brother, Hareesh Kumar, my father in-law, Dr. Phalaxayya Hiremath, my mother in-law, Sharada Hiremath for all the unconditional love and affection, motivation and encouragement, support, sacrifice, patience and confidence in me.

Abstract

The objective of this study is to investigate the bonding between glass reinforced polypropylene (glass-PP) and high-density polyethylene (HDPE) surfaces. These materials present low surface energy and surface adhesion problems. The atmospheric plasma treatment process enhances the adhesion between glass-PP and HDPE surfaces by increasing their surface energies. In this work, glass-PP and HDPE were subjected to the atmospheric/air plasma treatment by varying different parameters such as plasma intensity and number of treatments. Optimal plasma treatment conditions were then determined based on the bond strength between the surfaces after plasma treatment. Also, characterization techniques such as FTIR (Fourier Transform Infrared spectroscopy), SEM (Scanning Electron Microscopy), TGA (Thermogravimetric analysis) and surface energy determination via wettability inks were performed to understand the surface modification and chemical changes after plasma treatment. Furthermore, the effect of plasma treatment on glass/PP surface versus a neat PP surface was characterized to understand the effect of plasma treatment on fiber reinforced polymer versus neat polymer. The improvement of bond strength in glass/PP- HDPE panels was found to be higher than neat PP (neat Polypropylene)-HDPE panels. The G_{1c} (Mode 1 interlaminar fracture toughness) value of glass/PP- HDPE panels increase from 0.1 N/mm to 5.5 N/mm whereas, the G_{1c} value of neat PP- HDPE panels increase from 0.4 N/mm to 2.8 N/mm.

Table of contents

| | |
|---|----|
| CHAPTER 1- INTRODUCTION..... | 1 |
| CHAPTER 2- LITERATURE REVIEW..... | 5 |
| 2.1 Adhesives..... | 5 |
| 2.2 Adhesion..... | 6 |
| 2.3 Interface boundaries..... | 7 |
| 2.4 Wetting..... | 7 |
| 2.5 Factors affecting adhesion..... | 9 |
| 2.6 Bonding mechanisms..... | 11 |
| 2.6.1 Physical bonding..... | 11 |
| 2.6.2 The absorption theory..... | 12 |
| 2.6.3 The electrostatic attraction theory..... | 12 |
| 2.6.4 Chemical bonding..... | 12 |
| 2.6.5 Diffusion or interdiffusion theory..... | 12 |
| 2.6.6 Mechanical bonding or mechanical interlock theory..... | 13 |
| 2.7 Surface pretreatments for polymers and polymeric composites..... | 13 |
| 2.7.1 Corona discharge treatment..... | 14 |
| 2.7.2 Flame treatment..... | 14 |
| 2.7.3 Plasma treatment..... | 15 |
| CHAPTER 3- MATERIALS AND METHODS..... | 21 |
| 3.1 Materials..... | 21 |
| 3.2 Methods..... | 24 |
| 3.2.1 Plasma treatment and adhesively bonded panels fabrication..... | 24 |
| 3.2.2 Mechanical characterization..... | 27 |
| 3.2.3 Surface energy determination..... | 31 |
| 3.2.4 FTIR (Fourier Transform Infrared)-ATR (Attenuated Total Reflection) spectroscopy..... | 31 |
| 3.2.5 Scanning Electron Microscope (SEM)..... | 32 |
| 3.2.6 Thermogravimetric analysis (TGA)..... | 32 |
| 3.3 Objective 1: Effect of adhesive on bonding between glass-PP and HDPE surfaces..... | 33 |
| 3.4 Objective 2: Effect of various plasma nozzles and plasma intensities on bonding between glass/PP and HDPE surfaces..... | 34 |
| 3.5 Objective 3: Effect of various plasma treatment heights and plasma intensities on bonding between glass/PP and HDPE surfaces..... | 35 |

| | |
|--|----|
| 3.6 Objective 4: Effect of number of plasma treatments on bonding between glass/PP and HDPE surfaces | 35 |
| 3.7 Objective 5: Effect of aging/time on plasma treatment of glass/PP and HDPE surfaces ... | 36 |
| 3.8 Objective 6: Comparison of the effect of plasma treatment on the glass/PP and neat PP surfaces..... | 37 |
| CHAPTER 4- RESULTS AND DISCUSSION | 38 |
| 4.1 Effect of adhesive on bonding between glass-PP and HDPE surfaces | 38 |
| 4.2 Effect of plasma treatment from various nozzles on the mode 1 interlaminar fracture toughness of the adhesively bonded glass/PP and HDPE panel | 40 |
| 4.3 Effect of various plasma treatment heights and plasma intensities on bonding between glass/PP and HDPE surfaces..... | 42 |
| 4.4 Effect of number of plasma treatments on bonding between glass/PP and HDPE surfaces | 45 |
| 4.5 Effect of aging/time on the plasma treatment of glass/PP and HDPE surfaces | 48 |
| 4.6 Comparison of the effect of plasma treatment on the glass/PP and neat PP surfaces..... | 49 |
| CHAPTER 5- EMPIRICAL CURVE FITTING OF SURFACE ENERGY EXPERIMENTS ... | 52 |
| CHAPTER 6- CONCLUSIONS | 55 |
| REFERENCES | 56 |
| APPENDIX..... | 60 |
| VITA..... | 88 |

List of tables

| | |
|---|----|
| Table 3.1 Openair® Plasma generator equipment settings | 24 |
| Table 3.2 Various plasma nozzle heads used for the treatment [Plasmatreat ®]..... | 35 |
| Table A.1 Showing the effects of surface pretreatments on bond strength and durability of the polymers [3] | 61 |
| Table A.2 Effect of various surface pretreatment methods on the surface chemistry modifications of homopolymer polypropylene | 61 |
| Table A.3 Roughness values for corona discharge, flame, fluorination, vacuum plasma, air plasma pretreatments for homopolymer Polypropylene [31]..... | 62 |
| Table A.4 Composition of epoxy adhesive part A provided by the epoxy.com | 62 |
| Table A.5 Composition of epoxy adhesive part A provided by the epoxy.com | 62 |
| Table A.6 G_{1c} calculations for adhesively bonded sandwich panel using acrylic adhesive | 64 |
| Table A.7 G_{1c} calculations for adhesively bonded sandwich panel using epoxy adhesive..... | 64 |
| Table A.8 Summary of G_{1c} values for adhesively bonded sandwich panel using acrylic and epoxy adhesive | 65 |
| Table A.9 G_{1c} calculations for adhesively bonded sandwich panel with plasma surface pre-treatment from nozzle #22826..... | 69 |
| Table A.10 G_{1c} calculations for adhesively bonded sandwich panel with plasma surface pre-treatment from nozzle #22892..... | 70 |
| Table A.11 G_{1c} calculations for adhesively bonded sandwich panel with plasma surface pre-treatment from nozzle #22890..... | 70 |
| Table A.12 G_{1c} calculations for adhesively bonded sandwich panel with plasma surface pre-treatment from nozzle #10147 | 71 |
| Table A.13 G_{1c} calculations for adhesively bonded sandwich panel with plasma surface pre-treatment from nozzle #22826 | 71 |
| Table A.14 Summary of G_{1c} values for adhesively bonded sandwich panels with plasma surface pre-treatment from five different nozzles | 72 |
| Table A.15 Surface energies of glass/PP and HDPE surfaces after plasma treatment with five different nozzles..... | 72 |
| Table A.16 G_{1c} calculations for adhesively bonded sandwich panel with plasma surface pre-treatment with treatment height of 0.0254m (1”) using nozzle #22826 | 74 |
| Table A.17 G_{1c} calculations for adhesively bonded sandwich panel with plasma surface pre-treatment with treatment height of 0.019m (0.75”) using nozzle #22826 | 74 |
| Table A.18 G_{1c} calculations for adhesively bonded sandwich panel with plasma surface pre-treatment with treatment height of 0.012m (0.5”) using nozzle #22826 | 75 |
| Table A.19 Summary of G_{1c} values for adhesively bonded sandwich panels with plasma surface pre-treatment from three treatment heights nozzles # 22826..... | 75 |
| Table A.20 Surface energies of glass/PP and HDPE surfaces after plasma treatment using nozzle#22826 for three treatment heights | 76 |
| Table A.21 G_{1c} calculations for adhesively bonded glass-PP and HDPE sandwich panel without plasma surface pre-treatment | 77 |

| | |
|--|----|
| Table A.22 G_{1c} calculations for adhesively bonded glass-PP and HDPE sandwich panel with one plasma surface pre-treatment from nozzle# 22826 | 79 |
| Table A.23 G_{1c} calculations for adhesively bonded glass-PP and HDPE sandwich panel with two plasma surface pre-treatments from nozzle# 22826 | 79 |
| Table A.24 G_{1c} calculations for adhesively bonded glass-PP and HDPE sandwich panel with three plasma surface pre-treatments from nozzle# 22826 | 80 |
| Table A.25 G_{1c} calculations for adhesively bonded glass-PP and HDPE sandwich panel with four plasma surface pre-treatments from nozzle# 22826 | 80 |
| Table A.26 G_{1c} calculations for adhesively bonded glass-PP and HDPE sandwich panel with five plasma surface pre-treatments from nozzle# 22826 | 81 |
| Table A.27 Summary of G_{1c} values for adhesively bonded sandwich panels with 0 through 5 number of plasma surface pre-treatments from nozzle # 22826 | 81 |
| Table A.28 Surface energies of glass/PP and HDPE surfaces before and after 1 through 5 number | 83 |
| Table A.29 Effect of aging/time on the plasma treatment of glass/PP and HDPE surfaces | 83 |
| Table A.30 G_{1c} calculations for adhesively bonded neat PP and HDPE sandwich panel before plasma surface pre-treatment | 84 |
| Table A.31 G_{1c} calculations for adhesively bonded neat PP and HDPE sandwich panel after plasma surface pre-treatment | 84 |
| Table A.32 G_{1c} calculations for adhesively bonded glass-PP and HDPE sandwich panel without plasma surface pre-treatment | 85 |
| Table A.33 G_{1c} calculations for adhesively bonded glass-PP and HDPE sandwich panel after plasma surface pre-treatment | 86 |
| Table A.34 Summary of G_{1c} values for adhesively bonded neat PP-HDPE and Glass-PP-HDPE sandwich panels before and after plasma treatment | 87 |
| Table A.35 Surface energies of glass-PP and neat PP surfaces before and after plasma treatment | 87 |
| Table A.36 Surface energies of glass-PP panels after plasma treatment | 87 |

List of figures

| | | |
|-------------|--|----|
| Figure 1. 1 | Flowchart indicating the plan of work..... | 4 |
| Figure 2.1 | Contact angle and surface tension (γ) for a liquid drop on a solid surface | 9 |
| Figure 2.2 | Types of mechanisms of bonding: (a) Bond formed by electrostatic attraction, (b) Chemical bond formed between groups A on one surface and group B on the other surface, (c) bond formed by molecular entanglement following interdiffusion and, (d) Mechanical bond formed when a liquid polymer wets a rough solid surface. [20].... | 11 |
| Figure 3.1 | Schematic of a sandwich structure | 21 |
| Figure 3.2 | Image of the sandwich panel fabricated for the present study using glass/PP as face sheet and HDPE as core material..... | 22 |
| Figure 3.3 | Image showing the front of glass/PP sheets and HDPE sheet used for the sandwich structure..... | 22 |
| Figure 3.4 | Chemical structure of Tetrahydrofurfuryl methacrylate indicating ester functional group | 23 |
| Figure 3.5 | Chemical structure of part A of epoxy resin comprising of Diglycidyl ether of bisphenol A (DEBA) component..... | 23 |
| Figure 3.6 | Schematic of plasma generation [Plasmatreat.com]..... | 25 |
| Figure 3.7 | Plasmatreat equipment setup at MDF..... | 26 |
| Figure 3.8 | Schematic of the fabrication process of adhesively bonded sandwich panel using plasma treatment of substrates before adhesion..... | 27 |
| Figure 3.9 | Double cantilever beam specimen with loading blocks (a) Schematic (b) Actual specimen used for testing..... | 28 |
| Figure 3.10 | Schematic of Double Cantilever Beam specimen preparation, (a) image of the sandwich panel (b) Five specimens cut from the sandwich panel (c) Roughening of cut specimens and aluminum blocks in a sander (d) Plasma treatment of specimens (e) Application of adhesive to specimens for bonding them with aluminum blocks (f) Clamping of the specimens and aluminum blocks (g) DCB specimen after complete curing of the adhesive | 29 |
| Figure 3.11 | ATR-FTIR spectroscopy equipment | 31 |
| Figure 4.1 | Summary of G_{1C} values for adhesively bonded sandwich panel using acrylic and epoxy adhesive..... | 38 |
| Figure 4.2 | Summary of G_{1C} values for adhesively bonded sandwich panels with plasma surface pre-treatment from five different nozzles | 40 |
| Figure 4.3 | Plasma coming out from nozzle (a) #22824..... | 41 |
| Figure 4.4 | Plasma coming out from nozzle #22892 indicating large treatment area and varied plasms intensity within the treatment area..... | 42 |

| | |
|--|----|
| Figure 4.5 Summary of G_{1C} values for adhesively bonded sandwich panels with plasma surface pre-treatment from three treatment heights nozzles # 22826..... | 43 |
| Figure 4.6 Plasma treatment height of (a) 0.012m (0.5 inches) (b) 0.019m (0.75 inches) (c) 0.0254 m (1 inch) indicating varied treatment areas and plasma intensities from three treatment heights from the same nozzle..... | 44 |
| Figure 4.7 Summary of G_{1C} values for adhesively bonded sandwich panels with 0 through 5 number of plasma surface pre-treatments from nozzle# 22826..... | 45 |
| Figure 4.8 SEM image of glass-PP surface (a) before treatment (b) after 1 plasma treatment (c) after 5 plasma treatments | 46 |
| Figure 4.9 Degradation of the glass-PP surface with multiple plasma treatments as indicated by the discoloration for higher number of treatments..... | 47 |
| Figure 4.10 Effect of aging/time on the plasma treatment of glass/PP and HDPE surfaces | 48 |
| Figure 4.11 Summary of G_{1C} values for adhesively bonded sandwich neat PP-HDPE and Glass-PP-HDPE panels before and after plasma treatment | 49 |
| Figure 4.12 SEM images of glass-PP surface before and after plasma treatment | 51 |
| Figure 4.13 SEM images of neat PP surface before and after plasma treatment..... | 51 |
| | |
| Figure 5.1 Glass-PP panels fabrication via compression molding | 52 |
| Figure 5.2 Thermogravimetric analysis curves of fabricated glass-PP panels | 53 |
| Figure 5.3 Effect of plasma treatment on surface energy and fiber volume fraction of glass-PP surface..... | 54 |
| | |
| Figure A.1 Schematic of open air plasma movement in a serpentine pattern..... | 63 |
| Figure A.2 Surface energy determination by wettability inks (a) good wetting (b) poor wetting 63 | |
| Figure A.3 Load- displacement curves from ASTM D5528 testing for adhesively bonded sandwich panel using (a) acrylic adhesive (b) epoxy adhesive | 63 |
| Figure A.4 FTIR transmittance versus wavenumber plot for acrylic adhesive | 65 |
| Figure A.5 FTIR transmittance versus wavenumber plot for epoxy adhesive | 66 |
| Figure A.6 FTIR transmittance versus wavenumber plot for glass-PP surface after plasma treatment | 66 |
| Figure A.7 FTIR transmittance versus wavenumber plot for HDPE surface after plasma treatment | 67 |
| Figure A.8 Schematic of plasma stream coming out (a) from nozzle #10147 (b) from nozzle #22826..... | 67 |
| Figure A.9 Load- displacement curves from ASTM D5528 testing for adhesively bonded sandwich panels with plasma treatment from nozzle (a) 22826 (b) 22892 | 68 |
| Figure A.10 Load- displacement curves from ASTM D5528 testing for adhesively bonded sandwich panels with plasma treatment from nozzle (a) 22890 (b) 10147 | 68 |
| Figure A.11 Load- displacement curves from ASTM D5528 testing for adhesively bonded sandwich panels with plasma surface pre-treatment from nozzle 22824 | 69 |
| Figure A.12 Load- displacement curves from ASTM D5528 testing for adhesively bonded sandwich panels with plasma surface pre-treatment (a) from treatment height of | |

| | |
|--|----|
| 0.025m (1") using nozzle #22826 (b) from treatment height of 0.019m (0.75") using nozzle #22826 | 73 |
| Figure A.13 Load- displacement curves from ASTM D5528 testing for adhesively bonded sandwich panels with plasma surface pre-treatment from 0.012m (0.5") treatment heights using nozzle #22826 | 73 |
| Figure A.14 Load- displacement curves from ASTM D5528 testing for adhesively bonded glass-PP and HDPE sandwich panels without plasma surface pre-treatment | 76 |
| Figure A.15 Load- displacement curves from ASTM D5528 testing for adhesively bonded glass-PP and HDPE sandwich panels with (a) 1 plasma treatment (b) 2 plasma treatments | 77 |
| Figure A.16 Load- displacement curves from ASTM D5528 testing for adhesively bonded glass-PP and HDPE sandwich panels with (a) 3 plasma treatments (b) 4 plasma treatments | 78 |
| Figure A.17 Load- displacement curves from ASTM D5528 testing for adhesively bonded glass-PP and HDPE sandwich panels with 5 plasma treatments | 78 |
| Figure A.18 Failed sandwich structure without surface treatment to glass-PP and HDPE surfaces | 82 |
| Figure A.19 Failed sandwich structure with plasma treatment to glass-PP and HDPE surfaces . | 82 |
| Figure A.20 Load- displacement curves from ASTM D5528 testing for adhesively bonded neat PP and HDPE sandwich panels (a) before plasma surface pretreatment (b) after plasma pretreatment | 85 |
| Figure A.21 Load- displacement curves form ASTM D5528 testing for adhesively bonded glass-PP and HDPE sandwich panels (a) before plasma treatment (b) after plasma treatment | 86 |

Chapter 1

Introduction

Adhesively bonded joints in comparison to other joining methods offer advantages such as higher joint stiffness, superior fatigue performance and reduction of added weight penalty due to elimination of bolts and other stiffeners. Because of fatigue considerations, whenever possible, it is preferable to bond rather than mechanically fasten composite structures. Weight reduction without sacrifice in any joint stiffness is a critical factor in construction of an aircraft, rail vehicles and automobile industry [1]. Therefore, these industries extensively benefit from the adhesive bonding technology. A common example of an adhesive system found in the automotive industry is the attachment of a paint coating to a polymer bumper bar. Such bumper bars are frequently made with polypropylene (PP); a material exhibiting poor surface adhesive properties in its native state.

Adhesively bonded joints in polymeric composite substrates have the following advantages: (a) the capability of joining dissimilar polymers, (b) bonding very thin sections to heavy sections without distortion, (c) lower stress concentrations than mechanical joints, (d) weigh less than mechanically bonded joints, (e) less sensitivity to cyclic loading, (f) permit smooth external surfaces at the joint and (g) offer economic advantages, often by reducing the hand labor necessary for other bonding techniques. [1]

Polyolefins are a family of thermoplastics with a good balance of physical and chemical properties. Due to their low cost, light-weight, easy processing and recycling characteristics, they are suitable for the manufacture of composites. Most industrially applied polyolefins and composites have low surface free energy in the range of 28 mN/m – 30 mN/m and lack polar functional groups on their surfaces, resulting in inherently poor adhesion properties [2]. Since most of automotive and aerospace industries use low surface energy polymers and their composites extensively, they have been investigating adhesives and the associated adhesion mechanisms. Polypropylene and HDPE, as other polyolefins, are characterized by high chemical inertness, as a consequence of its nonpolar nature, and a very low surface energy resulting in very low wetting and adhesion properties [3] [4]. For this reason, these polymers find enormous difficulties for different industrial processes such as painting and adhesion, which are highly related to surface wetting properties. Thus, the

use of these polymers and their composites in technological applications requires, in many cases, require a surface pretreatment to modify surface activity, thus enhancing good adhesion levels [3] [4].

There are several technologies to promote surface changes and improve adhesion behavior. It has been theoretically verified that for complete wetting the surface energy of the adhesive must be lower than the surface energy of the adherend [5]. Therefore, the primary objective of a surface pretreatment is to increase the surface energy of the adherend as much as possible. The purpose of surface pretreatments to the polymeric substrate is to: (a) produce a surface free from contaminants, (b) sufficiently roughen the surface, (c) produce a fresh stable oxide layer on the surface. Surface pretreatments always modifies the surface rather than affecting the bulk properties. As a result of surface pretreatment, wettability and/or of the adhesive properties of the surface could be increased significantly [6, 7].

The adhesive properties of glass/PP and HDPE surfaces can thus be improved by surface pretreatments before the application of adhesive. There are various pretreatment methods for polyolefins reported in the literature for example, mechanical pretreatment, chemical pretreatment, photochemical pretreatment and plasma treatment [3]. Physical processes such as plasma technologies (corona plasma, cold plasma, atmospheric plasma, etc.) are interesting solutions from a technical point of view [8] [9]. They increase surface activation by two main processes: one mechanism is surface activation by insertion of polar groups (mainly oxygen-based species) into free radicals. The second mechanism is characterized by changes in surface roughness thus promoting changes in surface topography [9] [10].

Since Glass/PP and HDPE surfaces tend to be inert with few or no functional groups to bond like most of the polymers, plasma treatment activates the surfaces by inducing functional groups to the surfaces. The plasma treatment involves a low-pressure plasma gas, which is electrically conductive and consists of excited atoms, ions and free radicals. The plasma particles react not only with each other but also with the surfaces, which are exposed to the gas, giving rise to the following effects: (a) surface cleaning, (b) degradation of the polymer chains, (c) removal of material from the surface, (d) formation of radicals on the surface, and (e) change of tacticity of

the polymer chains. The combined effect of these processes results in an improvement of the adhesion properties of the surface [11] [12] [13] [14] [9].

Although various studies have been conducted in the past, on investigating the effect of plasma treatment on various polymers. This study is unique because it involves investigation of effect of plasma treatment in improving the adhesion of glass-PP and HDPE surfaces by measuring its G_{1c} values. The study is important since both glass-PP and HDPE surfaces are industrially applicable polymers. In the present work, sandwich panels were fabricated by bonding HDPE, glass-PP material. Sandwich structures are commonly used for automotive, aerospace and construction industry. In automotive and aerospace industry, they are used as floor panels and body panels. Advantages of these structures are that they offer high strength to weight ratio increasing efficiency by reducing fuel consumption. HDPE, and PP are commodity plastics and glass-PP is used since unidirectional glass fiber composites offer higher specific strength. Therefore, a combination of glass-PP and HDPE material will provide an optimum structure with improved performance at lower costs. Since it is difficult to bond glass-PP and HDPE surfaces in their native states, plasma surface treatment was used to enhance their bonding.

The objective of this thesis work is to do an in-depth analysis of the bonding between the glass/PP and HDPE surfaces. As per Fig1.1, the low surface energy polymeric surfaces glass/PP and HDPE were subjected to the atmospheric/air plasma treatment by varying different parameters such as plasma intensity and number of treatments. Further, the surface energy of the plasma treated surfaces were determined. Then, all the treated samples were bonded using an acrylic adhesive and further tested to determine the mode 1 interlaminar fracture toughness. The objective of the work is to study:

1. Effect of the adhesive on plasma treatment and bonding between glass/PP and HDPE surfaces.
2. Effect of various plasma intensities as a function of various nozzle dimensions and treatment areas on bonding between glass/PP and HDPE surfaces.
3. Effect of various plasma intensities as a function of treatment height and treatment areas on bonding between glass/PP and HDPE surfaces.
4. Effect of number of plasma treatments on bonding between glass/PP and HDPE surfaces.
5. Effect of aging/time on the plasma treatment of glass/PP and HDPE surfaces.
6. Comparison of the effect of plasma treatment on glass/PP surface versus neat PP surfaces.

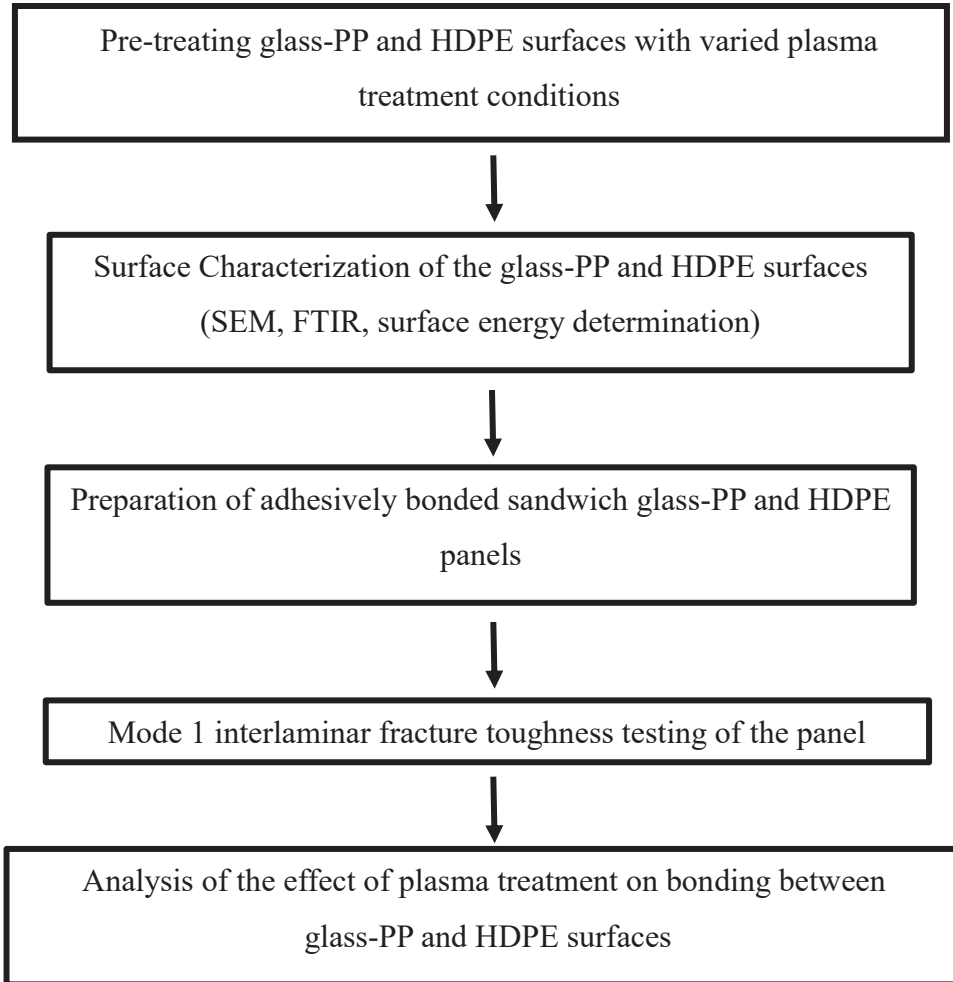


Figure 1. 1 Flowchart indicating the plan of work

Chapter 2

Literature Review

2.1 Adhesives

An adhesive is defined as a polymeric substance with viscoelastic behavior, capable of holding adherends together by surface attachment to produce a strong bond. The adhesive used in adhesive bonding of two adherends can be of the following categories: (a) thermoplastic resins, (b) thermoset resins, (c) artificial elastomers, and (d) even some ceramics. They can be applied as drops, beads, pellets, tapes, or coatings (films) and are available in the form of liquids, pastes, gels, and solids [1].

There are several other classifications of the adhesive material [15] [16]. For example, adhesives can be classified by; (a) organic chemistry, (b) intended applications and (c) high-temperature composites as adherends [1]. Even though the selection of an adhesive for a particular adherend system can be difficult, proper study on the adhesive chemistry should provide a feasible solution to understand its compatibility with the given adherend system.

Adhesive systems based on organic chemistry are categorized into five different systems that accomplish the objectives: [1] (a) Solvent-based adhesives, (b) Latex adhesives, (c) Pressure-sensitive adhesives, (d) Hot-melt, and (e) Reactive adhesives. Whereas intended applications range [15] from (a) load-bearing (structural adhesives) to (b) light-duty holding (nonstructural or fixturing adhesives, to (c) sealing (the forming of liquid or gas-tight joints). Commonly used structural (i.e., load-bearing) adhesives include [1] (a) epoxies, (b) cyanoacrylates, (c) anaerobics, (d) acrylics, (e) urethanes, (f) silicones, (g) high-temperature adhesives, and (h) hot melts. The bond created by using these adhesives can bear maximum load when stressed without failure.

Epoxy and acrylic adhesive systems are studied in this work for the advantages they offer for polymeric bonding. Acrylic adhesive includes a reactive chemical group called Tetrahydrofurfuryl methacrylate which includes ester functional group in its chemical structure. Epoxy adhesive includes modified Diglycidyl-Ether of bisphenol A as a reactive chemical group with oxirane functional group in its chemical structure.

Some of the advantages of the acrylic adhesives are summarized herein [17]: (a) Acrylic polymers possess enhanced resistance to aging, which results from the ability of these polymers to absorb ultraviolet light in the solar spectrum and re-dissipate it as harmless energy in the infrared wavelength range [2], (b) good strength, toughness, and versatility, (c) ability to bond a variety of materials, including plastics, metals, ceramics, and composites, even though oily or dirty surface [16], (d) good resistance to water and humidity, (e) room temperature curing and a non-mix application system [1]. The acrylic based adhesive is two component adhesives where both the components react to produce a strong thermoset bond at room temperature when adhesively joined. The curing can be accelerated by heat, and in some cases cures with ultraviolet light. The disadvantages of these adhesives include (a) low high-temperature strength, (b) flammability, (c) an unpleasant odor when still uncured, and (d) comparatively expensive [1].

Epoxyes are a broad family of polymer materials characterized by the presence of epoxy groups in their molecular structure. The thermosetting epoxyes are the oldest, most common, and most diverse of the adhesive systems, and can be used to join most engineering materials, including metal, glass, composite, and ceramic. Epoxy adhesives can be either one-stage (curing agent already mixed in) or two-stage where the user mixes in the curing agent just before use. The form of the one-stage material is most often a sheet, very much like a prepreg without the reinforcement, or in a paste. Both room temperature and elevated temperature curing systems are used based on the application. The present study involves room temperature curing. The advantages of epoxy adhesive are: [1] (a) strong, versatile adhesives that can be designed to offer high adhesion, (b) good tensile and shear strength, (c) high rigidity, (d) good chemical resistance, (e) excellent bonding, (f) good creep resistance, (g) easy curing with little shrinkage, and (h) good tolerance to elevated temperatures. After curing at room temperature, shear strengths can be as high as 35 to 70 MPa [1].

2.2 Adhesion

In a simple system, bonding at an interface is due to adhesion between the adhesive and adherend. A measurable amount of work is necessary in order to separate such adhesively bonded surfaces. [18] There must be good molecular contact between the adhesive and an adherend to ensure good bonding. Since the nature of bonding is dependent on chemistry of each constituent in terms of

atomic arrangement, the interface between the adherends should have specific properties. A certain amount of energy is required to break an adhesive bond or to separate two surfaces, this energy is the measure of the strength of the adhesive bond [1]. Often separation of two surfaces involves breakage of chemical or van der Waals bonds and the plastic deformation of one or both bulk materials on either side of the interface.

Adhesion results [15] from (a) the mechanical bonding between the adhesive and adherend, and (b) chemical forces either primary covalent bonds or polar secondary forces between the two. Properties of an adhesive joint determined by the properties of an adhesive itself i.e., Brittle polymers give brittle joints, polymers with high shear strengths give bonds of high shear strength, heat resistant polymers produce bonds with good heat resistance, and so on. Whenever there is a failure within the adhesive it is called as cohesive failure which often happens with good bond, where the adhesive is weaker than the substrate [1].

2.3 Interface boundaries

The properties of the surfaces in any phase is different than that of the properties of bulk of the phases. The atoms near the surface are not in equilibrium states, because they do not completely belong to either of the phases. This is because of the rapid changes that occurs near the phase boundaries. The forces on a molecule in the bulk often gets cancelled whereas the forces on a molecule at the surface do not cancel and are always unbalanced. Because of this unbalance, equilibrium atomic bonding arrangements disrupt leading to an excess energy called surface free energy γ [19]. Surface free energy is defined as the energy necessary to form a unit area of new surface or the energy necessary to move a molecule from the bulk to the surface. This excess surface energy may be minimized by minimizing surface area. This tendency is called surface tension if the surfaces are liquid and a vapor, γ_{LV} . The surface free energy of the surface is proportional to the surface area. Thus, a drop of liquid will tend to assume a spherical shape to minimize its surface area and, thereby, its surface free energy.

2.4 Wetting

Good bonding requires wetting of the adherend surface by an adhesive. Wetting is promoted by polar secondary forces between adhesive and substrate [17], this is why low-polarity/non-polymers

are difficult to bond with adhesives. Thermodynamic work of adhesion W_a explains adhesion as, [8]:

$$W_a = \gamma_{SV} + \gamma_{LV} - \gamma_{SL} \dots\dots\dots (1)$$

where γ_{SV} , γ_{LV} and γ_{SL} are the specific surface energies, or surface tensions of the solid-vapor, liquid-vapor and solid-liquid interfaces, respectively. This concept of thermodynamic work of adhesion can be used to explain the wetting of a solid surface by a liquid drop which is illustrated in figure 2.1. Balducci explains the contact angle as θ as an angle between the liquid drop and solid substrate intersection. Zisman [5] introduced a parameter called critical surface tension of wetting γ_c as, only liquids with $\gamma_{LV} < \gamma_c$ will spontaneously spread on the solid. The contact angle θ defines the wettability of a solid surface. Three different conditions for wetting are defined in Figure 2.1:

(a) partial wetting occurs when $0^\circ < \theta < 180^\circ$; and the Young's equation defines that three surface tensions should have force equilibrium until force equilibrium is established i.e.,

$$\gamma_{SV} = \gamma_{SL} + \gamma_{LV} \cos \theta \dots\dots\dots (2)$$

Here, the net free energy is lowered by replacing an S-V surface by an S-L and an L-V surface together.

(b) complete wetting occurs when,

$$\gamma_{SV} = \gamma_{SL} + \gamma_{LV} \cos \theta \dots\dots\dots (3)$$

and $\theta = 0$; and $\gamma_{LV} + \gamma_{SL} = \gamma_{SV}$

(c) no wetting occurs when, $\theta = 180^\circ$;

$$\gamma_{SV} + \gamma_{LV} < \gamma_{SL} \dots\dots\dots (4)$$

Proper wetting and interfacial bonding requires the following [15] : (a) surface pretreatment before joining, and (b) a low viscosity adhesive to flow over the surface and then harden (cure) to provide a strong bond. An equilibrium value of θ cannot be obtained due to constant inhomogeneity of the surface. Therefore, a range of contact angles exist between the maximum or advancing angle, θ_a , and the minimum or receding angle, θ_r . This phenomenon is called the contact-angle hysteresis [1].

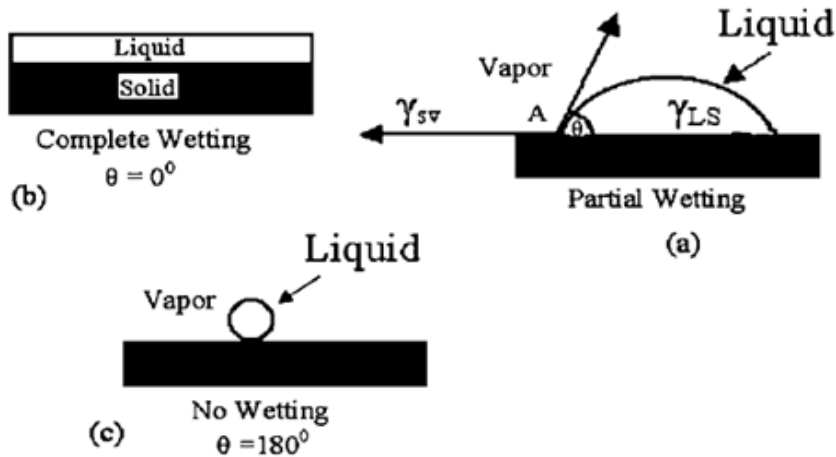


Figure 2.1 Contact angle and surface tension (γ) for a liquid drop on a solid surface

The static contact angle data can be determined using a Video Contact Angle (VCA) Analyzer [18] or goniometer. The VCA can be used to register angles up to 180° on both sides of the drop without moving the substrate. The surface energy information is then calculated, in terms of dispersive and polar or non-dispersive components, using the geometric mean equation combined with Young's equation [1]. The other way of finding surface energy is via wettability inks. The surface tension of these inks is predetermined and they predict the surface energy of the solid substrates without having to calculate the contact angles [25].

2.5 Factors affecting adhesion

Various factors are responsible and critical to attain good adhesion between the adherend and adhesive. Critical parameters required for good adhesion according to Balden are: (1) Thermodynamic energy of adhesion, (2) molecular weight, (3) transcrystallinity, (4) surface energy of adherends, and (5) surface roughness. Various studies have been performed to explain the criticality of these factors on adhesion, few such examples were reviewed and presented in this section.

(1) Molecular weight

Creton [20] has studied the effect of molecular weight on the adhesion properties (i.e., peel resistance, quick tack, and shear resistance) of the adhesives (i.e., polymer-to-polymer substrates). A high molecular weight will favor adhesive separation, by slowing the process of chain

disentanglement, which is responsible for cohesive fracture [21]. However, the molecular weight can also influence the micromechanical deformation mechanisms within the adhesive layer which are eventually responsible for the measured energy of adhesion [20].

(2) Transcrystalline layer

Schonhorn and Ryan [22] studied the adhesion in epoxy adhesive-polyethylene film-epoxy adhesive pieces. They concluded that the presence of a large transcrystalline surface layer in the polyethelene film considerably enhances the adhesive-joint strength. Conclusions from Ishida and Bussi [14] are also in agreement for the fact that transcrystalline layer preserves the expected properties of the surface rather than brings any enhancement. Therefore, when no transcrystalline zone is present, a weak boundary layer is formed, which decreases considerably the expected quality of adhesion [23]. Transcrystallinity prevents such a detrimental effect by extending the bulk properties of the matrix to the surface region. If the transcrystalline zone is damaged, this protective effect is lost.

(3) Surface energy of adherends

Various studies have been done to understand the effect of surface energy of adherends on the bond strength. Toyama et al. [24] studied the peel strength of a poly (n-butyl acrylate) on a variety of polymeric adherends. They found a maximum in the peel strength when the surface tensions of the adhesive, γ_a , and of the adherends, γ_s , were closely matched. However there have been other studies suggesting these results: (a) the surface energy of the adherend should not be below that of the adhesive (b) if the surface energy of the adherend is comparable or higher than that of the adhesive, the influence of surface forces on the measured adhesion is relatively small compared to the effect of the viscoelastic losses in the adhesive layer [20].

(4) Surface roughness

The effect of surface roughness is also important for the adhesion [25] [26]. A research showed that the measured adhesion of an adhesive is dependent on its surface roughness down to fractions of a micrometer, and that a surface roughness of the order of a micrometer could decrease the measured adhesion by a factor of 10 [27].

Harris and Beevers [5] have proposed a simple model to explain the restrictions for spreading of a droplet on a surface. The model included surface roughness such as peaks, ridges and asperities

form barriers which restrict the spreading of the droplet. [27] and Yost et al. [18] have pointed out that complete/sufficient wetting is difficult for surfaces with smaller contact angles.

Wenzel [19] proposed that wetting is influenced more by the amount of effective surface area that can interact with the liquid, than the surface roughness. He derived the ratio of the true surface area divided by the projected geometric area (Wenzel’s roughness factor, r) and used this to provide an expression for the contact angle as $\cos\theta_{\text{rough}} = r\cos\theta_{\text{smooth}}$.

2.6 Bonding mechanisms

It is necessary to understand all the different possible bonding mechanisms, one or more of which may be acting at any given instant. There are following bonding mechanisms or types existing in the literature, which are particularly useful in explaining certain phenomena associated with adhesive bonding [20,9]: (a) physical bonding, (b) chemical bonding, (c) diffusion or interdiffusion theory, and (d) mechanical bonding or mechanical interlock theory as indicated by Fig 2.2.

2.6.1 Physical bonding

Physical bonding involves weak, secondary or van der Waals forces, dipolar interactions, hydrogen bonding and other low energy forces [20]. Physical bonding contains the following bonding types: (a) the absorption theory, and (b) the electrostatic attraction theory.

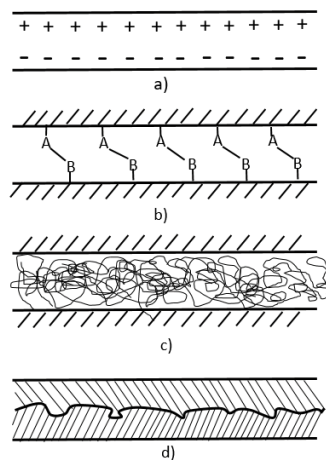


Figure 2.2 Types of mechanisms of bonding: (a) Bond formed by electrostatic attraction, (b) Chemical bond formed between groups A on one surface and group B on the other surface, (c) bond formed by molecular entanglement following interdiffusion and, (d) Mechanical bond formed when a liquid polymer wets a rough solid surface. [20]

2.6.2 The absorption theory

According to this theory, an adhesive must wet the adherend surface to form a good bond. This theory has led to the development of materials with lower surface tension than that of the adherend [21].

2.6.3 The electrostatic attraction theory

This theory postulates that because of the interaction of the adhesive and the adherend, an electrostatically charged double layer of ions develops at the interface. According to the electrostatic attraction theory, forces of attraction occur between two surfaces carrying net opposite charges [9] Fig.2.2. (a) The fact that electrical discharges are observed when an adhesive is peeled from a substrate is cited as evidence of these attractive forces [21]. A difference in electrostatic charge between constituents at the interface may contribute to the force of attraction bonding. The strength of the interface will depend on the charge density [9]. This attraction is unlikely to make a major contribution to the final bond strength of the interface [20].

2.6.4 Chemical bonding

The chemical bonding theory is the oldest and best known of all bonding theories. The nature of the chemical bonding is the key to the physical and chemical behavior of matter. Atomic or molecular transport, by diffusional processes, is involved in chemical bonding. This encompasses all types of covalent, ionic, and metallic bonding. Chemical bonding involves primary forces and the bond energy in the range of approximately 40–400 kJ/mol [22]. Figure 2.2 (b) explains that a chemical bond is formed between a chemical grouping on the adhesive surface and a compatible chemical group in the adherend.

A chemical reaction at the interface is of interest for polymer matrix composites. Surface treatments to these polymer matrix composites such as glass fiber/ carbon fiber reinforced polymeric composites often involve chemicals that modify surfaces with different chemical compositions and oxide formations. These morphological changes influence the nature of the chemical bonds. Subsequently, a relationship exists between chemical composition of the surface and the bond durability [7].

2.6.5 Diffusion or interdiffusion theory

A bond between two surfaces may be formed by interdiffusion of atoms or molecules across the surface. It is possible to form a bond between two polymer surfaces by the diffusion of the polymer

molecules on one surface into the molecular network of the other surface, as illustrated schematically in Fig.2.2 c. Therefore, the strength of the bond formed through such diffusion will depend on the amount of molecular entanglement and the number of molecules involved. This bonding mechanism is applicable to cases in which the adhesive contains a solvent for the adherend [21]. The phenomena of interdiffusion has been called autohesion in relation to adhesives.

However, interdiffusion in some situations is not beneficial because it produces undesirable compounds when the oxide films present on the fibers are completely disrupted under extremely high temperature and pressure [22]. Effective diffusion barriers such as coatings on fibers is always employed to prevent or reduce the damage due to interdiffusion. It is generally agreed that the highest strength is achieved when, upon stressing, the fracture occurs in the body of the adherend or within the adhesive, not at the interface. Per this theory, for an adhesive to perform satisfactorily, the weak boundary layer at the interface should be eliminated. Generally, this can be achieved by surface treatments [21].

2.6.6 Mechanical bonding or mechanical interlock theory

Some bonding may occur purely by the mechanical interlocking of two surfaces as illustrated in Fig.2.2d. According to this theory, when a liquid adhesive is placed between two surfaces, it penetrates the crevices and pores and then solidifies and further interlocks with the surface layers on both sides and provides a mechanical bond. The fact that fresh, roughened surfaces provide the best bond support this theory. In general, mechanical bonding is a low-energy bond in comparison to a chemical bond [1]. Even though pure mechanical bonding is not sufficient to produce a good bond, it could add to the overall bonding, in the presence of reaction bonding. Roughness or an increase in the surface often enable mechanical interlocking of the adhesive to the adherend. It has been shown that because of the high stability of the fresh oxide layer to moisture degradation, good durable bonds can be achieved by surface roughening [28].

2.7 Surface pretreatments for polymers and polymeric composites

There are many methods available to pretreat polymeric substrates. These include both physical and chemical surface pretreatments. The methods used to pretreat a polymer are [6, 7]: (a) chemical or electrochemical, (b) mechanical treatments such as grit blasting, peel-ply and tear-ply (c)

thermal treatments such as flame treatment, corona discharge treatment, and laser treatment, (d) photochemical treatment (e) plasma treatment.

Several surface pretreatment methods used for thermoplastic and thermoset polymeric materials are presented [3] [4] [29] [30] in Table A.1 in Appendix. It should be noted that thermoplastic materials are more difficult to bond than thermoset materials. The integrity of the bond in any fiber reinforced polymeric material will be dominated by matrix properties, rather than the fiber properties. According to the Table A.1 in Appendix, corona discharge treatment, flame treatment and plasma treatment are recommended for the thermoplastic polymers. Hence these treatment methods are briefly described in the sections below.

For thermoplastic composites, only, the change in surface chemistry along with change in surface topography provides strong bond strengths. For example, the primary aim of the surface treatment in thermoplastic composites is to increase the surface energy of the adherend as much as possible. This can be achieved by a decrease water contact angle and an increase in surface tension. Various factors such as cost, effectiveness, and stability of the treated surface in service are taken into consideration while selecting a surface pretreatment method [3].

2.7.1 Corona discharge treatment

The corona discharge surface pretreatment method involves exposure of the substrate surface to excited atoms, ions and free radicals at atmospheric pressure. According to various studies, [25] corona treatment has found to increase surface tension and the surface chemistry by oxidizing the polymer matrix to increase bond strengths. Corona discharge has been used successfully to treat glass-fiber-polypropylene composites for bonding. It is also used to treat polyolefin films to make them good surfaces for adhesion to printing inks. Optimization of the treatment to obtain maximum surface energy, using standard wettability inks and was found to be $58 \text{ dyn} \cdot \text{cm}^{-1}$. For example, the process parameters for homopolymer polypropylene, HF 133 M were as follows [31]: number of passes = 1, treatment width=0.18 m, speed=15min⁻¹, electrode-sample gap = 1 mm and power = 33 W (power density= $120 \text{ Wm}^{-2} \text{ min}^{-1}$).

2.7.2 Flame treatment

This is a widely-used surface pretreatment method for thermoplastics such as polyolefins. Flame treatment involves surface modification by introducing oxygen containing functional groups to the

surface [32]. An oxidizing flame used in flame treatments contains excited atoms, ions and free radicals, which oxidize the surface of the adherend to increase hydrophilicity and thus increase the bond strength. Few critical parameters in successful flame treatment are the distance from the surface to be treated, the air/gas ratio and the dwell time.

Sutherland et al [28] has demonstrated and optimized a flame treatment method for maximum surface energy, which was found to be 56 dyn cm^{-1} . For example, the process parameters for homopolymer polypropylene, HF 133 M were as follows [31]: number of passes = 8, speed = 25 m min^{-1} , propane flow = 3.751 min^{-1} , air flow = 881 min^{-1} , cone height = 4 mm, burner gap = 13 mm, power density = 207.5 mJmm^{-1} and burner length = 265 mm.

2.7.3 Plasma treatment

Plasma treatment has been used for more than 20 years to pretreat polymers [3]. Various works have been reported so far on plasma surface pretreatment method to treat polymers and polymeric composite materials that enhance surface adhesion. Plasma treatment of the polymer surface and then adjusting parameters such as gas flow, power, pressure and treatment time allows for many refinements to be made to the surface without changing the bulk properties[10]. Variables in plasma treatments such as gas composition and plasma conditions determine how ions, electrons, fast neutrons and radicals affect the etching, activation and cross linking between polymer surfaces [9]. Plasma polymerization is used to create highly adherent thin polymer films on the surface, allowing adhesion between two surfaces which would not otherwise adhere[8] [9]. For example, plasma treatments involving various gases have been found to enhance the surface tension, oxide the polymer matrix and increase the bond strength of PEEK composite [33] [29].

Green et al. [31] have studied the effects of corona discharge, flame, fluorination, low pressure vacuum plasma and atmospheric plasma surface pre-treatments on the polypropylene (PP). It was observed from their study that these five surface pretreatment methods showed significant changes in surface topology and surface chemistry by incorporation of oxygen groups into the near-surface region (Table A.2 in Appendix). Even though all five treatments showed similar bond strength to polyurethane adhesives, surface chemistry and topography varied widely across the five pretreatments. From the Table A.2 it can be observed that the vacuum plasma induced the maximum amount of oxygen into the surface (12.99 at%). Also, vacuum plasma and air plasma

have been found to include both oxygen and nitrogen functional groups. The following trend was observed (from left to right of decreasing oxygen content) amongst the five surface pretreatments.

Vacuum plasma > air plasma > fluorination > flame > corona discharge

Surface roughness characterization of the surface pretreated samples were done using the AFM (atomic force microscopy) microscopy and the roughness values are reported in Table A.3 in Appendix. The roughness was described by the R_A value, which is the ratio of the actual surface length to the surface length of a smooth surface. The results showed that vacuum plasma created heterogeneous surface with a high surface density of equally sized and spaced nodules. Air plasma was found to induce a “micro-rough” surface with features of ~80 nm diameter.

Table A.3 Roughness values for corona discharge, flame, fluorination, vacuum plasma and air plasma pretreatments for homopolymer polypropylene, HF 135 M [31]. Air, oxygen, nitrogen, microwave and direct current (DC) plasma treatments are being more widely used to increase adhesion through surface oxidation[11] [12] [13] [14] [9]. The type of plasma used in the surface modification of polymers has a significant effect on the wettability and the overall adhesion properties of the polymer.

Wertheimer [34] described a processing method and equipment of large-scale low-pressure plasma that could be used to treat polyolefin components. For example, the process parameters for homopolymer polypropylene, HF 133 M were as follows [31]: pressure = 2.6×10^{-2} mbar, voltage = 2500 V, current= 2.3 A, pump-down time = 5 min, plasma reaction time = 35 s and hold time following plasma = 60 s. Surface modification experiments using plasma treatment require low pressures which in turn require costly vacuum systems.

New techniques involving atmospheric pressure plasmas have been introduced to modify the surfaces of polymers and polymer blends. Studies using a combination of surface analytical techniques such as XPS, AFM, SIMS and optical contact angle analysis have shown that low pressure treatment or atmospheric pressure treatment results in surface properties favoring strong adhesion [10].

Atmospheric plasma pre-treatment or “air” plasma pre-treatment method functions similar to vacuum plasma except for the fact that substrates can be treated in atmospheric conditions

eliminating vacuum chambers [35]. US-Patent 5837958 [36] describes the air plasma treatment method. In air plasma treatment method, a plasma jet is being formed using atmospheric air which then comes out of a nozzle or pairs of nozzles. The sample is then placed below the nozzles within the plasma cone and pre-treated. This allows polymer surfaces to be cleaned, etched or chemically modified [37]. The process parameters were set to create the greatest surface energy using wettability inks, which was identified as being in excess of $120 \text{ dynes cm}^{-1}$. For example, the process parameters for homopolymer polypropylene, HF 133 M were as follows [31]: gas = air at atmospheric pressure, input pressure = 2 bar, output jet pressure = 13.9 mbar, rotation speed of nozzle = 1500 rpm and treatment speed = 10 mm min^{-1} .

J. Abenojar et., al [38] evaluated the effect of air plasma treatment on the thermal stability of LDPE and its composites reinforced with 15 and 30% (by wt.) of boron. Results showed that the air plasma treatment is adequate to treat these materials as it does not degrade the material, but it modifies the chemistry and nano roughness the surface, increasing its wettability. Jong-Kyu Park et al., [39] developed a source for an atmospheric pressure ejected plasma (APEP) pre-treatments of polymers to improve the adhesion ability between polymers. Proper operational conditions were found by *T*-peel tests performed with various plasma parameters and high peel strength up to 3.5 kg cm was achieved at those conditions.

Microwave plasma [40] post-discharge treatment is a pretreatment method also functions similar to any other plasma treatment methods except that the polymer substrate is not exposed to high-energy entities such as electrons or high-energy ions to reduce the destructive impact they can have on the substrate. Accordingly, this method shows lesser surface roughness unless for drastic treatment conditions (high power and long treatment times) [41].

Lennon et al. [7] have investigated the effects of microwave plasma surface treatments of polyamides (PA) film, polyamide 12 and polyamide 11 (PA11 as substrates (i.e., polymer-polymer system), using the two surface pretreatment processes: the ammonia and nitrogen mixtures by changing the O/N mixtures and NH gases. The effects of nitrogen, power and treatment time on the surface energy was studied. It was observed that the wettability depends not on the quantity of oxygen in the mixture but simply on its presence. Addition of oxygen showed an increase in wettability with a reduction of the water contact angle on the PA11 from 75° to approximately 45° .

From the investigation of the effect of plasma power on wettability it was concluded that 200 W treatment gave best wettability and further increase in power does not have any effect. They also concluded that a rapid increase in surface energies was observed between 100 and 360 s plasma exposure times. Optimal treatment conditions with respect to the wettability and the chemical composition of the surface can therefore be determined as 100 cm min, 200 W, 360 s, which can be used to evaluate the adhesion of the substrate [7]. It was also observed from the pull off test that the O/N plasma treatment increases strongly the toughness of the PA/adhesive interface.

In another study, the effect of microwave plasma treatment on the bonding strength of CFRP/aluminum foam composites was investigated. Results showed when the CFRP was plasma-treated using oxygen gas, the bending and shear strength was improved by 7.5% and 650%, respectively, compared to the case without plasma treatment. The improved bonding strength of the plasma-treated CFRP/aluminum foam composites was attributed to the increased surface roughness of the CFRP and the newly formed, CO and COO functionalities on the CFRP [42].

Jiangnan Lai [39] showed that microwave-induced argon plasma modified the surfaces of polycarbonate (PC), polypropylene (PP), polyethylene terephthalate (PET) samples both in composition by CO functional group and roughness.

Similarly, Grimond et al. [9] used atmospheric pressure glow discharge plasmas (air corona and nitrogen) to modify the surface properties of PP films. They found that nitrogen increased the surface energy of the substrate to a greater extent due to the added presence of amine, amide and hydroxyl functional groups. Massines et al. [9] used atmospheric pressure glow discharge plasma successfully to deposit silane groups on the surface of PP films as a method of enhancing the film surface properties. Kwon et al. [9] investigated plasma modified PP and found that the maximum surface energy was achieved with a plasma treatment time of 90 s, power of 100W, gas flow rate of 6 LPM and ageing time of 5 min.

Bhowmik et al. [9] used a combination of contact angle and XPS measurements to conclude that DC glow discharge treatment of PP surface increased the surface energy and increased the surface oxygen to carbon ratio. As surface energy is directly related to the work of adhesion, the increase in surface energy corresponds to a theoretical increase in adhesion [9]. An investigation of surface energy changes for polymethylmethacrylate (PMMA) demonstrated that both DC glow discharge

and microwave plasma treatments considerably increased the surface free energy of the sample. However, only the DC glow discharge method improved coating adhesion [9]. UV/ozone treatment is also reported by researchers to increase the oxygen containing functional groups on the surface [9] [43].

Plasma treatment of polymers using nitrogen/oxygen mixtures has been studied in the past [44]. It has been observed by several studies that [31, 32] the use of nitrogen/oxygen mixtures is more efficient than the use of oxygen alone as they lead to a higher concentration of atomic oxygen. The comparison with the NH plasma treatment was made with the optimum conditions as that of O/N treatments. In case of O/N treatment the optimal treatment conditions were a power of 200 W with a gas flow of 100 cm³ min during 180 s were chosen whereas for ammonia treatment the optimal conditions were 200 cm³ min—600 W—180 s. In conclusion, after plasma treatment and whatever the gas used, a great increase of the adhesion properties was noticed for whatever the epoxy reactive system.

An investigation into the characteristics of PP modified by an Ar/O₂ plasma found that the Ar plasma treatment was more effective in improving film wettability [9]. Allyl cyanide and a mixture of xylene, air and oxygen plasmas have also been used successfully to improve the degree of adhesion between polymers and their matrix [45].

Oxygen plasma treatment of high-density polyethylene (HDPE) with different crystalline fractions has shown that an increased crystalline order lowers oxidation, and hence the ageing of the polar functional groups on the sample surface [9]. However, Hegemann et al. [9] has shown in a series of experiments based on different surface treatments of polymers that although oxygen containing plasma treatments increased the wettability characteristics of the surfaces, this could be quickly lost to the atmosphere through ageing. They observed that N₂ plasma treatments of polycarbonate showed the lowest ageing effects but a surface deposition of SiO_x layers was the best way to maintain a lasting hydrophilic surface. They identified a more permanent hydrophilic treatment for polymer surfaces. In this study SiO_x layers were deposited onto the surface of polycarbonate (PC) substrates, and were shown through contact angle measurements to be less prone to ageing effects when compared to the plasma treatments.

Oxygen plasma has also been used to treat the surface of both polycarbonate (PC) and PMMA to induce the deposition of diamond like carbon (DLC). It was shown that the DLC film adhered

better to PC than to PMMA, and thus interfacial layers were deposited onto the surface of PMMA in order to increase its adhesion [46].

In a study [47], PP bumper bar substrates were treated with oxygen plasma and it was found that to optimize adhesion and wettability the plasma power was required to be below 500W for an exposure time of 300. It was found that as the plasma power increased above 500W, hydrophilic functional groups were still forming on the surface of the polyolefins (determined through XPS analysis), however surface roughness (AFM measurements) began to decrease. The surface morphology (as determined by an assembly of round grains) values increased past this point.

Hegemann et al., [39] studied the effect of plasma treatments in a rf discharge of Ar, He, or N₂ on etching, cross-linking, and activating polymers like PC, PP, EPDM, PE, PS, PET and PMMA. According to their results, wetting and friction properties of polymers can be improved by a simple plasma treatment, demonstrated on PC and EPDM, respectively. Plasma-deposited layers strongly adhere to the polymers to avoid the rapid failure of stressed components. The plasma treatment should be adjusted for different polymers to minimize degradation and aging effects.

Chapter 3

Materials and Methods

3.1 Materials

A sandwich composite comprises of a core material of certain thickness sandwich between two face sheets of certain thickness. The schematic of a typical sandwich composite is shown in the figure 3.1.

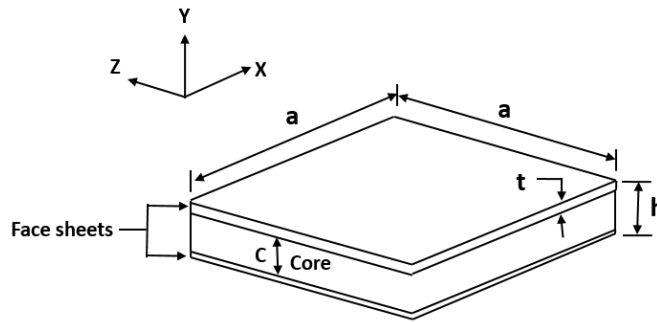


Figure 3.1 Schematic of a sandwich structure

The schematic in the Fig.3.1 involves a representative sandwich structure with a core material sandwich between two face sheets. The present study focuses on bonding between the core material and one face sheet. Fig. 3.2 shows the representative the sandwich structure fabricated in the present study. The face material used for this was a compression molded glass fiber reinforced polypropylene (referred as glass/PP panel). The panel was fabricated by laying up 6 layers of unidirectional glass/PP tapes to obtain $0^{\circ}/90^{\circ}$ cross ply with 64% fiber weight fraction. The sample size of 0.15 m*0.15m for both the face sheet and the core material was used. The thickness of the face sheet was 0.002m and the thickness of the core was 0.01m. High Density Polyethylene (HDPE) was used as a core material and glass-PP was used as a face sheet. The schematic of the face sheet and core material are shown in Fig. 3.2 and 3.3. In one of the investigations, neat PP material will be used as a face sheet instead of glass/PP sheet. The neat PP (neat Polypropylene) sheets were fabricated by the extrusion compression molding (ECM) technique at the Manufacturing Demonstration Facility (MDF) of Oak Ridge National Laboratory (ORNL) at Knoxville.



Figure 3.2 Image of the sandwich panel fabricated for the present study using glass/PP as face sheet and HDPE as core material



Figure 3.3 Image showing the front of glass/PP sheets and HDPE sheet used for the sandwich structure

The following steps were involved in the production of neat PP panels via ECM process:

1. PP pellets were conveyed to the hopper and fed to the plasticizing unit. The plasticizing unit comprises of four heating zones which were pre-heated to 215.5°C (420°F), 215° C (419°F), 204°C (400°F) and 196 °C (385°F) temperatures respectively.
2. A deep-flighted screw plasticizes the PP material gently. The screw then retracts and places the prepared melt in the enclosed space in front of it.
3. The plasticizing unit enters the opened mold.
4. The closure device at the plasticizing unit opens, the screw pushes the melt out and places it in the form of a strand in the mold.
5. The closure device at the plasticizing unit cuts off the melt strand and the unit retract from the mold.
6. The press closes and the melt is distributed under a pressure of 18143 Kgs (20 tons) was applied for 120 seconds under low shear stress in the cavity between the top and bottom of the mold.

7. At the end of the cooling time the press opens. Parallel to this the plasticizing unit has prepares fresh melt.

8. The finished molding is demolded manually. With the placement of melt in the mold the production cycle for the next molding begins.

The bonding between the face sheet and the core sheet were studied for two adhesive systems; (1) Acrylic adhesive (2) Epoxy adhesive.

The Acrylic adhesive used for the study is Henkel's Loctite AA 3035 B also known as Loctite AA 3035 BNDER 400ML PTB. The adhesive is comprised of 30-60% Tetrahydrofurfuryl methacrylate and 10-30% of Alkyl methacrylate. The functional group in the chemical structure of the Tetrahydrofurfuryl methacrylate is ester group which is indicated by the red circle the Fig.3.4. The epoxy adhesive used for the present study was purchased from Epoxy.com with the product number #2005 Part A and #2005 Part B. Composition of the part A and part B of the adhesive is presented in the Table A.4 and Table A.5 in Appendix. Two component epoxy system used for the present study involves room temperature curing. Fig 3.5 represents the chemical structure of the Diglycidyl ether of bisphenol A (DEBA) group of the epoxy adhesive system.

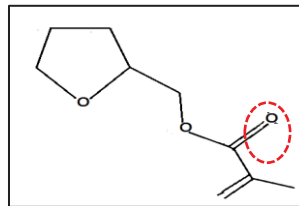


Figure 3.4 Chemical structure of Tetrahydrofurfuryl methacrylate indicating ester functional group

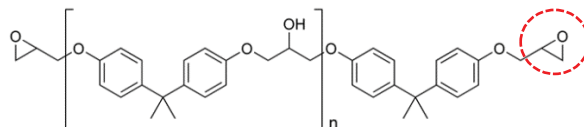


Figure 3.5 Chemical structure of part A of epoxy resin comprising of Diglycidyl ether of bisphenol A (DEBA) component.

3.2 Methods

3.2.1 Plasma treatment and adhesively bonded panels fabrication

Openair[®] Plasma technology is used for the surface treatment of the glass/PP and HDPE samples. The Openair[®] Plasma treatment equipment was donated by the Plasmatreat USA Inc. to the IACMI (Institute of Advanced Composites Manufacturing) located in the MDF (Manufacturing demonstration facility) of the ORNL (Oak Ridge National Lab). The model number of the equipment used for the treatment is Openair[®] Plasma generator FG5001- V5. O. The operating conditions of the plasmatreat equipment is indicated in Table 3.1.

The generator FG5001 provides the output voltage for the high voltage transformers (1000V). The transformers HTR12 and HTR22 increase the output voltage of the generator (1Kv) on the one hand and to an ignition voltage of 20Kv and to a burn voltage of 2Kv. The RF electric arc resulting in the plasma jet is focused using compressed air in the jet outlet opening.

The plasma is generated inside the plasma jet with high voltage and blown out through the jet head using the working gas that is fed in. The plasma jet directed at the material serves the generation and spread of plasma. The plasma jet used in our equipment is RD1004 rotating jet. Here, an eccentrically arranged set opening is set in rotation. This results in an enlargement of plasma exit angle. Using this jet, relative speeds of up to 0.36 ms^{-1} can be achieved.

The activation of the surface of the construction part differs depending on the speed, the material to be treated and the distance of the jet to the part surfaces. Fig.3.6 shows the schematic of the plasma generation within the plasma jet.

Table 3.1 Openair[®] Plasma generator equipment settings

| Equipment settings | |
|---------------------------|--|
| Model | FG5001-V5. O |
| Generator | FG5001 |
| Output power | 1kVA |
| Air pressure | 45 Psi |
| Room temperature | 15-20°C (60-70 F) |
| Treatment rate | 0.01125 ms^{-1} (11.25 mms^{-1}) |

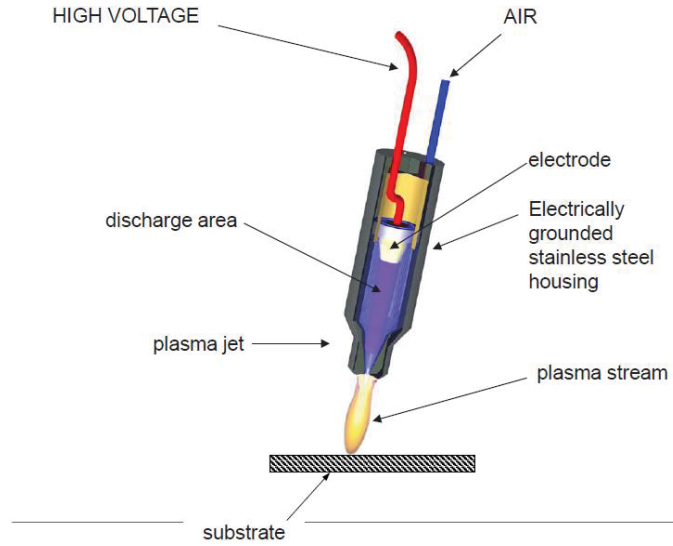


Figure 3.6 Schematic of plasma generation [Plasmatreat.com]

The plasma stream that comes out of the nozzle is directed towards the substrate to be treated. The generation of plasma is schematically represented in Fig.3.6. For the purposes of uniform controlled treatment of the surfaces, a x-y robotic arm with a controller unit is attached to the system on top of which the substrates to be treated are placed. The controller unit of the x-y robotic arm is programmed to adjust the speed of the platform movement and path of the movement. The treatment speed was adjusted to be 0.01125 ms^{-1} and serpentine path was chosen for treatment.

Fig.3.7 shows the plasma jet mounted vertically straight to table and can be adjusted to required height. A x-y robotic arm is attached to the same table. The controller has a capability of moving up to 0.5m in x direction and 0.4m in y direction. The speed of the controller can be adjusted between 10 ms^{-1} to 14 ms^{-1} . For experiments in the present study, controller speed of 11.25 ms^{-1} was used. The x-y robotic arm is connected to a controller that is connected to a computer. The plasma treatment speed and the arm movement pattern can be adjusted via computer. A platform having dimensions of $0.35\text{m} \times 0.35\text{m}$ is mounted on the controller arm. The specimen having dimensions of $0.15\text{m} \times 0.15\text{m}$ to be treated was placed on this platform.

After placing the sample on the platform and beneath the plasma nozzle, treatment speed (speed of x-y robotic arm/platform) and treatment pattern (relative movement of the x-y robotic

arm/platform) was adjusted in the computer. The pattern indicated in the Fig.A.1 in Appendix is used for the treatment of the substrates used in the present study.

Fig.3.8 shows the fabrication of the adhesively bonded sandwich panel subjected to plasma pretreatment. The glass/PP and HDPE panels were cut to the dimensions of $0.15\text{m} \times 0.15\text{m}$ and cleaned with acetone to remove any visible surface contaminants. Then the samples were placed on a x-y robotic platform underneath the plasma jet for the treatment. Treatment of the specimen was carried out. The activation of the surface differs depending on the speed, the material to be treated and the distance of the jet to the part surfaces. HDPE and glass-PP surfaces were treated one after the other.

Followed by the plasma treatment, adhesive was applied on the treated HDPE surface and glass-PP surface was placed on top of the HDPE surface and allowed for curing under pressure. Room temperature curing was carried out by the application of a load of 907.185 Kgs in the carver compression press at FCMF (Fibers and Composites Manufacturing Facility), at The University of Tennessee, Knoxville. After allowing the adhesive to cure for 24 hours inside the press (which is in accordance with the data provided by the adhesive manufacturers). Once the curing of the adhesive is completed, the adhesively bonded sandwich panel is removed from the press and is shown in the last section of the Fig. 3.8. Panels fabricated by such a process are ready to go for mechanical testing. ASTM D5528-13 testing was conducted to understand the bond strength of the adhesively bonded panels.

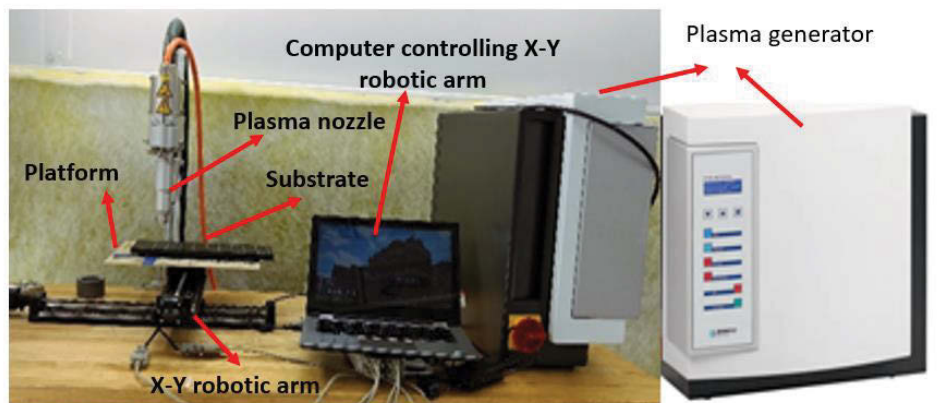


Figure 3.7 Plasmatreat equipment setup at MDF

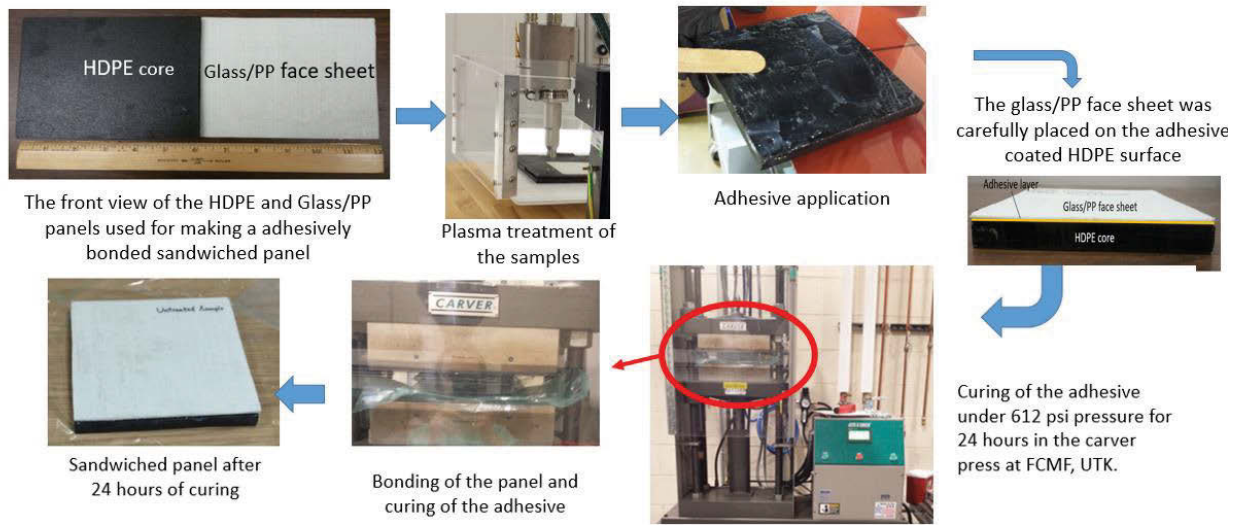


Figure 3.8 Schematic of the fabrication process of adhesively bonded sandwich panel using plasma treatment of substrates before adhesion

3.2.2 Mechanical characterization

(ASTM D5528-13 standard test method for Mode 1 interlaminar fracture toughness of unidirectional fiber-reinforced polymer matrix composites)

This test method describes the determination of the opening Mode I interlaminar fracture toughness, G_{Ic} , of continuous fiber-reinforced composite materials using the double cantilever beam (DCB) specimen as show in the figure below. This is the test method recommended for the unidirectional glass/PP tape laminates and single-phase polymer matrices. Susceptibility to delamination is one of the major weaknesses of many advanced laminated composite structures. Knowledge of a laminated composite material's resistance to interlaminar fracture is useful for product development and material selection. Furthermore, a measurement of the Mode I interlaminar fracture toughness, independent of specimen geometry or method of load introduction, is useful for establishing design allowable used in damage tolerance analyses of composite structures made from these materials. This test method can serve the following purposes:

1) To establish quantitatively the effect of fiber surface treatment, local variations in fiber volume fraction, and processing and environmental variables on G_{Ic} of a particular composite material.

- 2) To compare quantitatively the relative values of G_{Ic} for composite materials with different constituents.
- 3) To compare quantitatively the values of G_{Ic} obtained from different batches of a specific composite material, for example, to use as a material screening criterion or to develop a design allowable.
- 4) To develop delamination failure criteria for composite damage tolerance and durability analyses.

Double cantilever beam (DCB) specimens (both schematic and actual) used for ASTM D5528-13 testing are shown in the figure 3.9. In the Fig.3.9a and Fig.3.9b, L = length of the sample, b = Sample width, a_0 = Delamination length and h = thickness of the sample. Fig.3.10 shows the schematic of the preparation of specimens for testing. The sandwich panel fabricated is of the dimensions of $0.15\text{m} \times 0.15\text{m}$, five specimens having dimensions of $0.0254\text{m} \times 0.127\text{m}$ are cut from the fabricated panel. Aluminum loading blocks were used for loading the DCB specimens. These aluminum blocks were adhesively bonded to DCB specimens. To enable proper adhesion of aluminum blocks to specimens, both specimens and aluminum loading blocks were roughened before plasma treatment in a sander having a grit size of 120 grit. Sanding belt from Warrior company was used where aluminum oxide is used an abrasion material. RMS values of roughness (R_a) attained via 12 grit size sand paper are found to be 52 micron in literature[48].

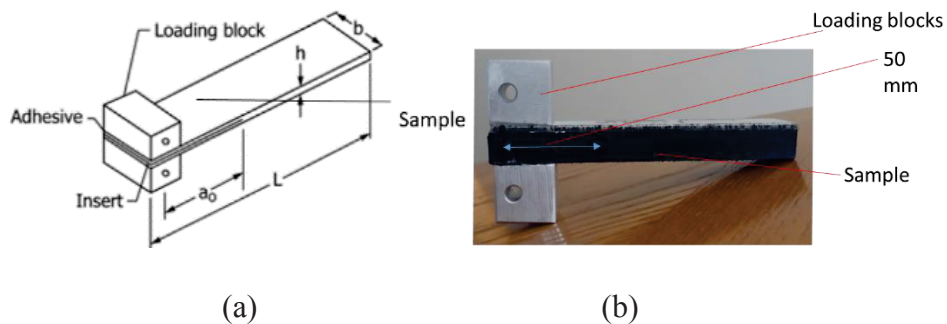


Figure 3.9 Double cantilever beam specimen with loading blocks (a) Schematic (b) Actual specimen used for testing

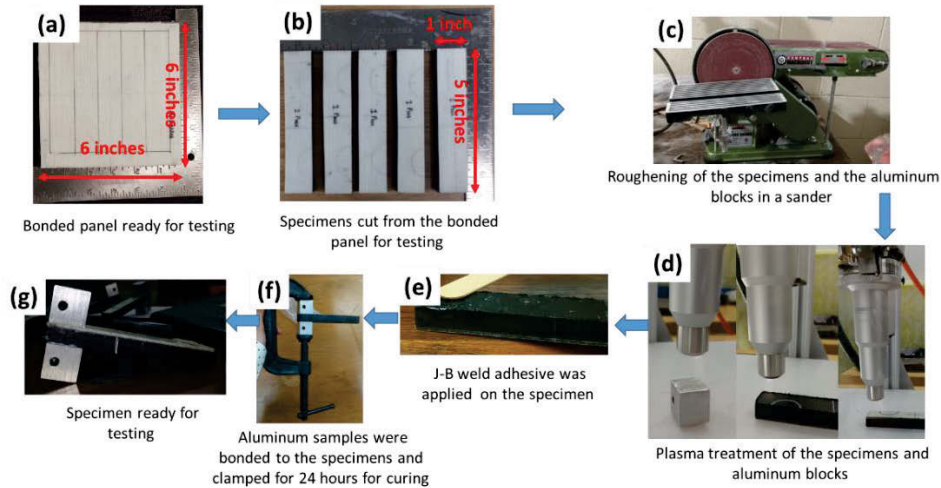


Figure 3.10 Schematic of Double Cantilever Beam specimen preparation, (a) image of the sandwich panel (b) Five specimens cut from the sandwich panel (c) Roughening of cut specimens and aluminum blocks in a sander (d) Plasma treatment of specimens (e) Application of adhesive to specimens for bonding them with aluminum blocks (f) Clamping of the specimens and aluminum blocks (g) DCB specimen after complete curing of the adhesive

Once all the specimens and aluminum blocks are roughened, both specimens and aluminum blocks are treated with plasma with nozzle #22826 with treatment height 0.19m and an exposure time of 5secs. Aluminum blocks are bonded to the specimens using a steel reinforced epoxy adhesive called JB weld soon after plasma treatment. The adhesive was purchased from the J-B weld company and was synthesized to bond variety of materials including metals, plastics, wood, concrete, ceramics and fiberglass. This is a room temperature cure two-part adhesive with Epoxy steel resin and an epoxy steel hardener. The chemical composition of the adhesive includes: (1) bisphenol-A-(epichlorohydrin) (2) Epoxy resin titanium dioxide (3) 2,4,6-tris (diethylaminomethyl)phenol (4) crystalline silica.

The specimens and aluminum blocks were clamped after adhesive application and allowed to cure for 24 hours by clamping them together to obtain the DCB specimens that are ready for testing.

The DCB specimen shown in Fig. 3.9a and Fig.3.9b consists of a rectangular uniformly thick, unidirectional laminated composite specimen. Opening forces are applied to the DCB specimen by means of loading blocks bonded to one end of the specimen. The ends of the DCB are opened

by controlling either the opening displacement or the crosshead movement, while the load and delamination length are recorded. A record of the applied load versus opening displacement is recorded on an X-Y recorder, or equivalent real-time plotting device or stored digitally. The Mode I interlaminar fracture toughness is calculated using a modified beam theory. The testing procedure involved the following steps:

- The average values of the width and thickness measurements of all the DCB specimens to be tested were recorded.
- The first 0.05m (50 mm) is the delamination length which was marked.
- The load blocks were mounted on the specimen in the grips of the loading machine.
- The specimen was loaded at a constant crosshead rate of 2 mm/min until the marked delamination length is attained and the load displacement values were continuously recorded.

Three data reduction methods for calculating G_{Ic} values have been evaluated in the past. These consisted of a modified beam theory (MBT), a compliance calibration method (CC) and a modified compliance calibration method (MCC). Because G_{Ic} values determined by the three different data reduction methods differed by no more than 3.1 %, none of the three were clearly superior to each other. However, the MBT method yielded the most conservative values of G_{Ic} for 80 % of the specimens tested. Hence, the MBT data reduction method is recommended.

Modified Beam Theory (MBT) Method:

The beam theory expression for the strain energy release rate of a perfectly built-in (that is, clamped at the delamination front) double cantilever beam is as follows:

$$G_{Ic} = \frac{3P\delta}{2ba}$$

G_{Ic} = Mode I interlaminar fracture toughness

P = load,

δ = load point displacement,

b = specimen width, and

a = delamination length.

3.2.3 Surface energy determination

A simple method to measure the surface tension of materials such as plastic, glass, and recycled or composite materials, is the determination using test inks. Test inks from Plasmatrete USA, Inc. are used to measure the surface tension of the plasma treated PP, glass-PP and HDPE surfaces in this study. Plasmatrete test inks having the trade name ‘Surface Test Inks C28 to C72’ used in this study are manufactured according to DIN Draft 53364 or ISO 8296.

Formamide test inks (A Series) is used in the present study. The test ink is applied quickly to the surface using the integrated brush of the bottle. If the brush stroke edges are stable for two seconds, the surface is easily wettable (Fig.A.2a in Appendix). Then, the surface tension of the substrate is at least equal to the value of the test ink. If the brush strokes of the test ink contract (Fig.A.2bIn Appendix), the next lower test ink should be used. This way, surface tension value of substrates is gradually approached.

3.2.4 FTIR (Fourier Transform Infrared)-ATR (Attenuated Total Reflection) spectroscopy

Fourier Transform Infrared Spectroscopy, also known as FTIR Analysis or FTIR Spectroscopy, is an analytical technique used to identify chemical groups associated with a material. The FTIR Analysis method uses infrared light to scan test samples and observe chemical properties. With an ATR setup, the infrared beam is reflected within the ATR crystal. Infrared spectroscopy probes the molecular vibrations. Functional groups can be associated with characteristic infrared absorption bands, which correspond to the fundamental vibrations of the functional groups. The vibrational frequencies of a given chemical/functional group are expected in specific regions which depend on the type of atoms involved and the type of chemical bonds. Tables are available for the main chemical groups. Within these vibration regions, the frequencies of the chemical groups are modulated by the specific environment of the group.

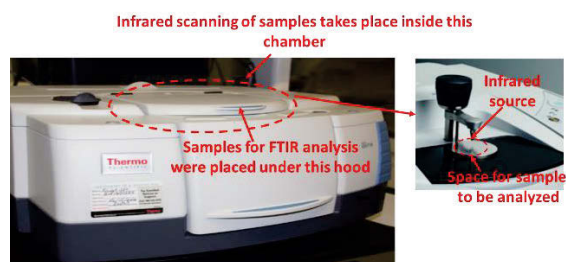


Figure 3.11 ATR-FTIR spectroscopy equipment

Therefore, to establish a clear relationship between the infrared mode frequency and the structural properties of a given residue, it is necessary to perform a detailed analysis of experimental results using theoretical chemistry approaches.

The Nicolet iS50 FT-IR Spectrometer used in this study shown in Fig. 3.11 measures the absorption spectrum in the mid-IR region ($5000\text{-}400\text{ cm}^{-1}$). This is a powerful technique that provide chemical information of materials that absorb specific frequencies that are characteristic of their structure. The spectrometer has a deuterated triglycine sulfate (DTGS) detector and a mercury cadmium telluride (MCT) detector for applications requiring higher sensitivity and faster response.

3.2.5 Scanning Electron Microscope (SEM)

The scanning electron microscope (SEM) uses a focused beam of high-energy electrons to generate a variety of signals at the surface of solid specimens. These signals include secondary electrons that produce SEM images, secondary electrons are most valuable for showing morphology and topography on samples. The data collected over a selected area is then generated into 2-dimensional image that displays spatial variations in these properties. The SEM instrument used in this work was Auriga 200 at the University of Tennessee, Microscopy Center.

3.2.6 Thermogravimetric analysis (TGA)

Thermogravimetric analysis or thermal gravimetric analysis (TGA) is a method of thermal analysis in which the mass of a sample is measured over time as the temperature changes. TGA is conducted on an instrument referred to as a thermogravimetric analyzer. A thermogravimetric analyzer continuously measures mass while the temperature of a sample is changed over time. Mass, temperature, and time in thermogravimetric analysis are considered base measurements while many additional measures may be derived from these three base measurements.

A typical thermogravimetric analyzer consists of a precision balance with a sample pan located inside a furnace with a programmable control temperature. The temperature is generally increased at constant rate to incur a thermal reaction in a controlled atmosphere. The thermogravimetric data collected from a thermal reaction is compiled into a plot of mass or percentage of initial mass on the y axis versus either temperature or time on the x-axis. This plot, which is often smoothed, is referred to as a TGA curve. The thermogravimetric analyzer used in this study is Mettler Toledo

with model number -TGA/SDTA 851^e. The equipment is located in characterization lab in FCMF, UTK.

3.3 Objective 1: Effect of adhesive on bonding between glass-PP and HDPE surfaces

Adhesively bonded glass/PP and HDPE sandwich panels were fabricated using two adhesive systems, acrylic and epoxy. Two adhesively bonded sandwich panels were prepared from each acrylic and epoxy adhesives.

Adhesively bonded sandwich panel using acrylic adhesive were prepared from glass/PP and HDPE surfaces. Both the surfaces were cleaned with acetone before plasma treatment. The plasma treatment equipment was used to treat both the glass/PP and HDPE surfaces with the same processing parameters mentioned in Table.3.2. The nozzle #22826 was selected out of the five nozzles i.e., #10141, #22824, #22826, #22892 and #22890 for the treatment of glass-PP and HDPE surfaces. The details of these five nozzles are presented in the Table 3.2. Treatment height used for this study were nozzle 0.019m. Both the surfaces were treated one after the other with the aid of an x-y robotic arm. Soon after the treatment, the two-part Loctite adhesive was applied uniformly throughout the 0.15m × 0.15m core surface. The face sheet was placed on top of adhesive layer on core surface followed by the curing in the compression press with the loading of 3023.95 kgsm⁻² (10 tons/square foot) for 24 hours.

Adhesively bonded sandwich panel using acrylic adhesive with no surface treatment to glass/PP and HDPE surfaces was fabricated to understand the effect of plasma treatment. In this method, substrates were cleaned with acetone and then the two-part acrylic adhesive was applied uniformly and cured as per the conditions mentioned in the adhesively bonded sandwich panel fabrication with plasma pre-treatment to the substrates.

Adhesively bonded sandwich panel using epoxy adhesive were prepared from glass/PP and HDPE surfaces. The method used for the fabrication of the adhesively bonded sandwich panel using epoxy adhesive is similar to that of the adhesively bonded sandwich panel using acrylic adhesive. Part A and part B epoxy adhesive were mixed externally with the volume ratio of 1:1. The face sheet was placed on top of adhesive layer on core surface followed by the curing in the compression press with the loading of 3023.95 kgsm⁻² (10 tons/square foot) for 5 hours.

Adhesively bonded sandwich panel using epoxy adhesive with no surface treatment to glass/PP and HDPE surfaces was fabricated to understand the effect of plasma treatment. In this method, substrates were cleaned with acetone and then the two-part epoxy adhesive was applied uniformly and cured as per the conditions mentioned in the adhesively bonded sandwich panel fabrication with plasma pre-treatment to the substrates.

All the four fabricated samples were subjected to the mode 1 interlaminar fracture toughness test. The sample preparation and testing conditions were described in the previous sections. The purpose of testing these samples was to study the effect of surface pretreatment as well as various adhesives on adhesion of glass/PP and HDPE samples.

FTIR (Fourier Transform Infrared)-ATR (Attenuated total reflection) spectroscopy was conducted at the JIAM (Joint Institute for Advanced Materials) facility at the University of Tennessee, Knoxville to understand the chemistry of adhesives, substrates and bonding between adhesives and substrates. SEM imaging was conducted to understand the effect of plasma treatment on the surface topography of glass/PP and HDPE samples.

3.4 Objective 2: Effect of various plasma nozzles and plasma intensities on bonding between glass/PP and HDPE surfaces

In this study, the interlaminar fracture toughness G_{Ic} for adhesively bonded HDPE and glass/PP surfaces treated with various plasma jet nozzles were calculated and compared to choose the nozzle head best suited for treating our substrates. Table.3.2 represents the information of the various plasma jet nozzle heads used for the present investigation.

Adhesively bonded sandwich panels with plasma pre-treatment were fabricated as per the conditions mentioned before. A total of five panels were fabricated using each of the five nozzle heads presented in the Table.3.2. The activation of the surface differs depending on the intensity of the nozzle, speed of treatment and the height of treatment. The intensity of the plasma stream coming out is dependent on the nozzle type. In this study, the effect of various plasma intensities was studied keeping treatment height and speed of treatment constant. Further, all the fabricated sandwich panels were subjected to Mode 1 interlaminar fracture toughness test to compare the effect of various plasma stream intensities on the treatment.

Table 3.2 Various plasma nozzle heads used for the treatment [Plasmatreat ®]

| Nozzle heads used for the treatment | | | | | | | |
|--|-------|----------------------|-----------------------------------|--|-------|----------------------|-----------------------------------|
| Jet nozzle head | Angle | Treatment width (mm) | Treatment area (mm ²) | Jet nozzle head | Angle | Treatment width (mm) | Treatment area (mm ²) |
| 22892  | 32° | 55 | 2374.6 | 22824  | 5° | 10 | 78.5 |
| 22890  | 25° | 35 | 961.6 | 10147  | 0° | 8 | 50.24 |
| 22826  | 14° | 25.4 | 506.4 | | | | |

3.5 Objective 3: Effect of various plasma treatment heights and plasma intensities on bonding between glass/PP and HDPE surfaces

The objective of this study is to investigate the optimum height of plasma treatment required to obtain better bonding of the adhesively bonded glass/PP and HDPE sandwich panel. Three treatment heights from nozzle #22826 were selected for the investigation: 0.0254m (1"), 0.019m (0.75") and 0.0127m (0.5"). The choice of the treatment heights was made as per the safe workable distance mentioned in the plasma treat equipment user manual. As mentioned before, the activation of the surface differs depending on the intensity of the nozzle, speed of treatment and the height of treatment. In this study, the effect of various plasma intensities was studied keeping treatment height and speed of treatment constant. The fabrication of the adhesively bonded sandwich panels with plasma pre-treatment was similar as mentioned before. Three panels were fabricated with the substrates for each panel being treated from different height.

Further, all the fabricated sandwich panels were subjected to Mode 1 interlaminar fracture toughness test to compare the effect of various plasma stream intensities on the treatment.

3.6 Objective 4: Effect of number of plasma treatments on bonding between glass/PP and HDPE surfaces

The objective of this study is to understand the effect of number of plasma treatments on the bonding of adhesively bonded HDPE and glass/PP sandwich panel. Also, to calculate and compare the interlaminar fracture toughness G_{IC} for the adhesively bonded HDPE and glass/PP surfaces

treated with plasma for various number of treatments/passes. Number of treatments/passes is the number of exposures to plasma for a particular exposure time. Exposure time is the time for which the sample is exposed to plasma.

The experiment was conducted to determine the mode 1 interlaminar fracture toughness of the following types of adhesively bonded sandwich panels: (1) Adhesively bonded sandwich panels without surface pretreatment (2) Adhesively bonded sandwich panels with various number of plasma treatments.

The fabrication of adhesively bonded sandwich panels without surface pretreatment and with one plasma treatment is as mentioned before. The nozzle used for the treatment is nozzle #22826 and treatment height maintained was 0.019m (0.75"). For one pass/one treatment of the plasma, the surfaces were treated for only one time. Similarly, for 2, 3, 4 and 5 passes/treatments the surfaces were treated accordingly. All the fabricated samples were tested to determine Mode 1 interlaminar fracture toughness. The results were compared to understand the effect of surface treatment.

Furthermore, to understand the effect of plasma treatment on the surface modification of glass/PP and HDPE samples, SEM (Scanning Electron Microscopy) imaging was conducted.

3.7 Objective 5: Effect of aging/time on plasma treatment of glass/PP and HDPE surfaces

Another significant phenomenon with plasma treatment of polymers is the degradation of the surface properties through ageing. It has been suggested that this is due to the reorientation of polar chemical groups into the bulk of the material, which in turn reduces the surface energy.

The objective of this work is to understand the effect of plasma treatment on the surface energies of glass/PP and HDPE surfaces with respect to time. In this study, glass/PP and HDPE surfaces were subjected to plasma treatment with nozzle #22826 with a nozzle height of 0.019m (0.75") and one treatment. Followed by the plasma treatment, surface energies of treated glass/PP and HDPE surfaces is measured for the following increments time: 0 sec (ie., immediately after the treatment), 300 secs (5 min), 600 secs (10 min), 900 secs (15 min), 1800 secs (30 min), 3600 secs (1 hr), followed by every 3600 secs (1hr) until a period of 24 hours is completed and then until 10 days with an increment of a day. The average humidity condition was 70% and the temperature

varied between 21°C-26°C (70° F -80° F). Change in surface energies of the glass/PP and HDPE surfaces were calculated using the surface energy test inks.

3.8 Objective 6: Comparison of the effect of plasma treatment on the glass/PP and neat PP surfaces

The objective of this study is to compare the effect plasma treatment on fiber in the glass/PP surface with the neat PP surface (where fibers are absent). Four adhesively bonded sandwich panels were fabricated and tested in the present investigation: (1) Panel 1- glass/PP and HDPE surfaces without surface pretreatment (2) Panel 2- glass/PP and HDPE surfaces with plasma treatment (3) Neat PP and HDPE surfaces without surface pretreatment (4) Neat PP and HDPE surfaces with plasma treatment.

The fabrication of adhesively bonded sandwich panel with neat PP as face sheet and HDPE as core is similar to the processing of the adhesively bonded sandwich panels with glass/PP as face sheet and HDPE as core. The nozzle used for the study is nozzle #22826 with only one treatment and treatment height of 0.019m (0.75"). All the fabricated samples were tested to determine Mode I interlaminar fracture toughness and to compare the effect of plasma treatment on neat PP surface versus glass/PP surface.

Chapter 4

Results and Discussion

4.1 Effect of adhesive on bonding between glass-PP and HDPE surfaces

ASTM D5528-13 testing was conducted on five specimens from each (epoxy and acrylic) adhesively bonded sandwich glass-PP and HDPE panels. The load displacement curves from testing of all the five specimens from each of them are presented below.

As shown in Fig.A.3(a). and Table A.6 in Appendix, adhesively bonded sandwich panel using acrylic adhesive shows an average G_{Ic} value of 5.5 N/mm with a standard deviation of 1.29. Whereas, adhesively bonded sandwich panel using epoxy adhesive shows an average G_{Ic} value of 1.25 N/mm with a standard deviation of 0.67 (Fig.A.3(b) and Table A.7).

Fig.4.1 and Table.A.8 in Appendix summarizes the G_{Ic} values obtained from the Table 4.1 and 4.2. Observations made from Fig.4.2 and Table 4.3, helps to understand the adhesive system that is best suited to bond glass-PP and HDPE surfaces after plasma treatment.

The observation from the mechanical testing can be correlated to the chemical reactivity of acrylic and epoxy adhesives with the glass/PP and HDPE surfaces. FTIR spectroscopy was conducted to understand the chemistry of bonding of acrylic and epoxy adhesives with glass/PP and HDPE surfaces [9].

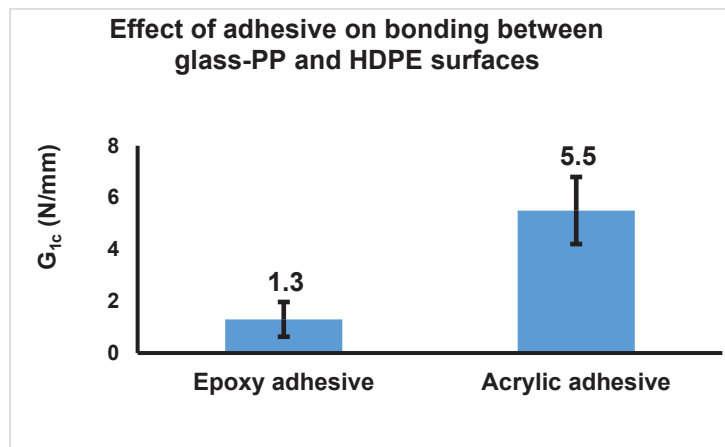


Figure 4.1 Summary of G_{Ic} values for adhesively bonded sandwich panel using acrylic and epoxy adhesive

The FTIR analysis shown in Fig.A.4 in Appendix of acrylic adhesive confirmed the presence of ester group (functional group of tetrahydrofurfuryl component of acrylic adhesive) at a transmittance of 1157.91 cm^{-1} wavenumber [49]. The FTIR analysis of epoxy adhesive confirmed the presence of oxirane group (functional group of diglycidyl ether of bisphenol A (DEBA) component of epoxy adhesive) at transmittance of 915.02 cm^{-1} and 827.27 cm^{-1} wavenumbers [50] (Fig.A.5 in Appendix).

Plasma treatment of surfaces often induces the formation of oxygen-containing functional groups such as hydroxyl groups, resulting in increased surface wetting and improved adhesion [9]. A combination of ToF-SIMS, XPS and ATR-IR has been used together to analyze PP films which had been treated with an air dielectric plasma. The investigation found that the molecular organization at the sample surface along with chemical conversion of the oxidized species were responsible for the improvements in hydrophilicity.

Fig.A.6 in Appendix is the analysis of the FTIR data of the glass-PP surface after plasma treatment. The data indicates the presence of OH group on the surface of the glass-PP at a wavenumber transmittance of 2949.41 cm^{-1} , 2916.72 cm^{-1} , 2866 cm^{-1} and 2837.80 cm^{-1} . Fig.A.7 in Appendix is the analysis of the FTIR data of the HDPE surface after plasma treatment. The data indicates the presence of OH group on the surface of the HDPE at a wavenumber transmittance of 1330.30 cm^{-1} , 2914.35 cm^{-1} and 2846.94 cm^{-1} [Chemistry libretext.com].

The ester group present in the tetrahydrofurfuryl component of acrylic adhesive is highly unstable due to the presence of double bonded oxygen atom. OH group is produced on the glass/PP and HDPE surfaces due to the plasma treatment, [51] (as indicated in Fig. A.6 and Fig.A.7) this OH group reacts with the ether group present in the tetrahydrofurfuryl component to produce a stable component thus producing a strong bond between glass/PP and HDPE.

Whereas, the oxirane group present in the diglycidyl ether of bisphenol A (DEBA) component is a stable component due to the presence of stable single covalently bonded oxygen atom. OH, group is produced on the glass/PP and HDPE surfaces due to the plasma treatment, this OH group even though highly reactive, is unable to form a stable component with oxirane group due to the less reactivity of oxirane group in the epoxy adhesive. Thus, glass/PP-acrylic-HDPE bond is stronger than the glass/PP-epoxy-HDPE bond.

Therefore, considering observations made from mode 1 interlaminar fracture toughness testing of the adhesively bonded sandwich panels and FTIR analysis of the adhesives and plasma treated glass-PP and HDPE surfaces, it can be concluded that the acrylic adhesive is more reactive to glass-PP and HDPE surfaces than epoxy adhesive.

4.2 Effect of plasma treatment from various nozzles on the mode 1 interlaminar fracture toughness of the adhesively bonded glass/PP and HDPE panel

ASTM D5528-13 testing was conducted on five specimens from each adhesively bonded sandwich glass-PP and HDPE panels with plasma surface pre-treatment from five different nozzles. The load displacement curves from testing for all the five specimens from each of them are presented below.

As shown in the Fig.A.9 to A.11 and Table A.9 to A.14 in Appendix, G_{1c} values of the adhesively bonded sandwich panels with surface pretreatment using five different plasma nozzles are: # nozzle10147 is 0.73 N/mm with a standard deviation of 0.8, nozzle # 22892 is 4.79 N/mm with a standard deviation of 3.3, nozzle #22890 is 1.42 N/mm with a standard deviation of 1.49, nozzle #22824 is 0.35 N/mm with a standard deviation of 0.21, # 22826 is 5.5 N/mm with a standard deviation of 1.3. Amongst all the five nozzles used for the plasma treatment, adhesively bonded sandwich panel surfaces treated from nozzle #22826 shows the highest value of G_{1c} of 5.5 N/mm with the lowest standard deviation of 1.3. To further understand this observation, the intensity of the plasma from the various nozzles should be investigated.

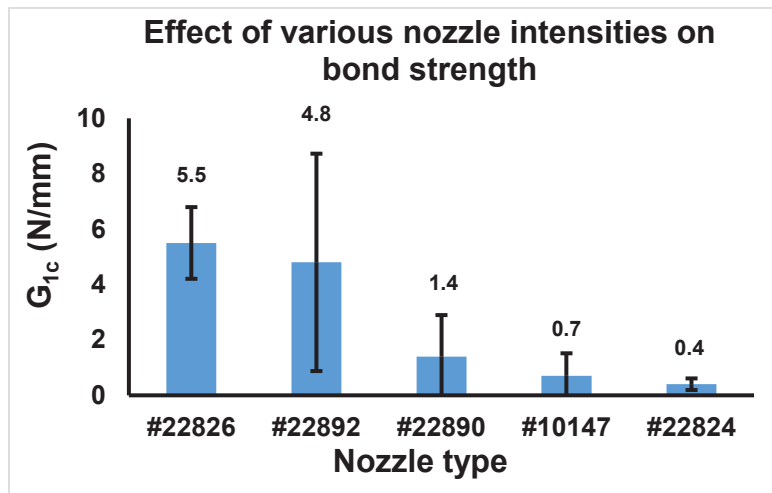


Figure 4.2 Summary of G_{1c} values for adhesively bonded sandwich panels with plasma surface pre-treatment from five different nozzles

Intensities of plasma stream coming out from each nozzle has an effect on this behavior. For example, plasma stream coming out from a 0° nozzle (#10147) is more intense compared to the plasma stream coming out from a 25° nozzle (#22826) angle as indicated in Fig. A.8 in Appendix. Therefore, surface energy values of the Glass-PP and HDPE surfaces after plasma treatment with each nozzle should be calculated to understand the effect of these plasma intensities on the treated surfaces.

Fig.4.3 and Fig 4.4 are the images of the plasma coming out from various nozzles. This information was used to understand the effect of plasma intensities on the bond strength values represented in Table A.14 and Fig.4.2.

Even though the G_{1c} values of the panels treated from nozzle #22826 and Nozzle #22892 are comparable, panels treated from nozzle #22892 show higher values of standard deviation than nozzle #22826. This could be due to the non- uniform treatment form the nozzle #22892, the intensities of the plasma within the treatment area varies resulting in a non- uniform treatment.

Hence this nozzle is not suitable for the treatment of the panels where uniform bond strength is expected. Furthermore, surface energy determination was conducted to understand the effect of these nozzle intensities. Surface energy values of the glass/PP and HDPE surfaces treated with various nozzles are presented in the Table A.15 in Appendix.

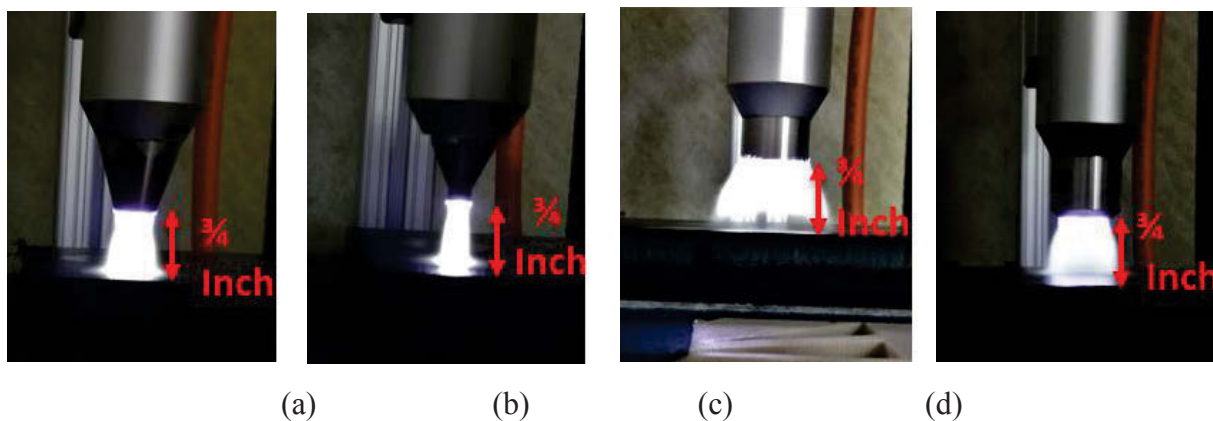


Figure 4.3 Plasma coming out from nozzle (a) #22824

(b) #10147 (c) #22890 (d) #22826 indicating varied treatment areas/intensities of plasma from each nozzle



Figure 4.4 Plasma coming out from nozzle #22892 indicating large treatment area and varied plasms intensity within the treatment area

According to the data presented in the Table A.15, the highest increase in surface energy of glass-PP and HDPE surfaces seen after plasma treatment was using nozzle # 22892 and nozzle #22826. Both the nozzles increase the surface energy of glass-PP surface from 28 mN/m to 58 mN/m, HDPE surface from 30 mN/m to 72 mN/m. However, the surface energy value recorded after plasma treatment for the nozzle #22892 was not uniform throughout the surface. The surface energy varied between 50-58mN/m. This is a validation to the earlier made observation from Fig.4.14, the treatment by the nozzle #22892 is non-uniform.

It can be concluded that Nozzle #22826 is best suited for the treatment of glass-PP and HDPE surfaces. Observations from the ASTM D5528 testing, surface energy determination and treatment area investigation support this conclusion

4.3 Effect of various plasma treatment heights and plasma intensities on bonding between glass/PP and HDPE surfaces

According to the data presented in the Fig.A.12 and A.13 in Appendix and Table A.16 to A.18 in Appendix, G_{1c} values of the adhesively bonded sandwich panels with surface pretreatment from three treatment heights using nozzle #22826 were determined.

Determined G_{1c} values are as follows: treatment height of 0.0254m (1 inch)- 1.695 N/mm with a standard deviation of 1.890, treatment height of 0.019m (0.75 inches)- 5.449 N/mm with a standard deviation of 1.2942 and treatment height of 0.012m (0.5 inches)- 1.784 N/mm with a standard deviation of 1.5826.

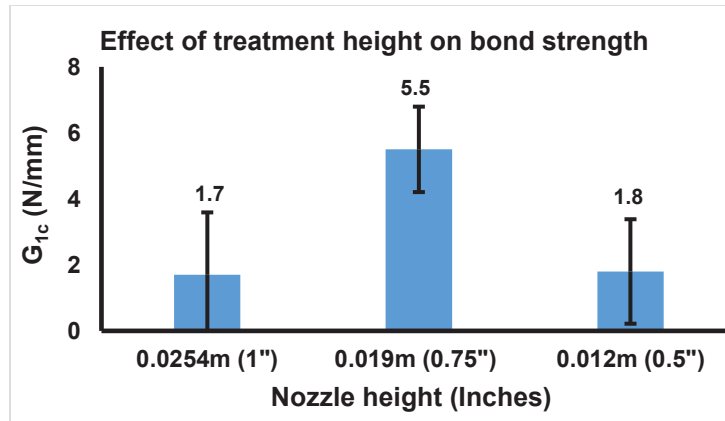


Figure 4.5 Summary of G_{1c} values for adhesively bonded sandwich panels with plasma surface pre-treatment from three treatment heights nozzles # 22826

Fig.4.5 and Table A.19 in Appendix summarizes the G_{1c} values of adhesively bonded sandwich panels whose surfaces area treated with three treatment heights. Amongst all the three treatment heights used to plasma treat glass/PP and HDPE surfaces, adhesively bonded sandwich panel surfaces treated from a treatment height of 0.019m (0.75 inches) using nozzle #22826 showed the highest value of G_{1c} of 5.5 N/mm with the lowest standard deviation of 1.3. To further understand this observation, the intensity of the plasma coming out from these three different heights from the nozzle #22826 should be studied.

The intensities of plasma stream coming out from a nozzle from different heights influences this behavior. As seen in Fig.4.6, plasma stream coming out from a height of 0.5 inches is more intense than the plasma stream coming out from a height of 0.019m (0.75 inches) and 0.0254m (1 inch). Plasma coming out from 0.012m (0.5 inches) treatment height might have degraded the surface of the polymer, since the polymers used in the study are not heat resistive. Therefore, for the better understanding of the results in the Table.A.19 and Fig.4.5, surface energy values of the Glass-PP and HDPE surfaces after plasma treatment with each nozzle height should be calculated to understand the effect of these plasma intensities on the treated surfaces.

Surface energy values of the glass/PP and HDPE surfaces treated with nozzle #22826 from three treatment heights are presented in the Table A.20 in Appendix. According to the data presented in the Table A.20, surface energy of the HDPE surface after plasma treatment from nozzle#22826 increases to 72mN/m nozzle irrespective of three treatment heights that were chosen for this study.

However, the surface energy of the glass/PP surface after plasma treatment from nozzle#22826 increases from 28mN/m to 40 mN/m for treatment height of 0.0254m (1 inches), 58 mN/m from treatment height of 0.019m (0.75 inches). The increase in surface energy after plasma treatment from 0.012m (0.5 inches) was 46 mN/m.

This might be because shorter treatment distances may allow the polymer surface to degrade due to the higher intensities of plasma. According to a theory on ageing is that polar chemical groups diffuse into the polymer matrix, a side effect being surface degradation through the rapid interaction of the polymer with radicals or ions [38].

The plasma stream coming out from three treatment heights form the nozzle 22826 are shown in the Fig.4.6. It can be seen from the figure that the shorter treatment distances increase the plasma intensity. Therefore, a shorter treatment distance degrades the surface of the glass-PP whereas, a treatment height higher than 0.019m (0.75 inches) does not sufficiently increase the surface energy. According to the data presented in Tables A.19 and A.20, it can be concluded that a treatment height of 0.0254m (0.75 inches) using nozzle#22826 is best suited for the treatment of the glass-PP and HDPE surfaces for increasing their bonding properties.

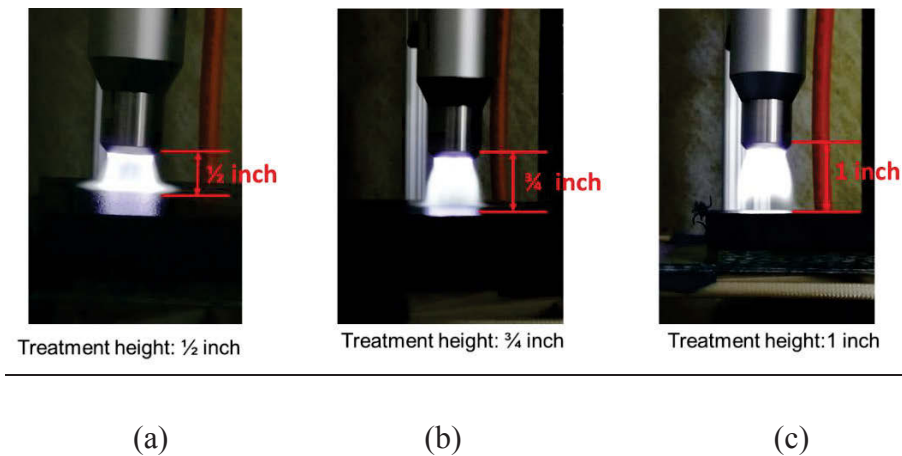


Figure 4.6 Plasma treatment height of (a) 0.012m (0.5 inches) (b) 0.019m (0.75 inches) (c) 0.0254 m (1 inch) indicating varied treatment areas and plasma intensities from three treatment heights from the same nozzle

4.4 Effect of number of plasma treatments on bonding between glass/PP and HDPE surfaces

In the Fig.A.14 to A.17, Table A.21 to A.27 in Appendix and Fig.4.7, mode 1 interlaminar fracture toughness test, G_{1c} values of the adhesively bonded sandwich panels before and after various number of plasma treatments nozzle #22826 were determined and presented.

Determined G_{1c} values are as follows: before treatment- 0.1 N/mm with a standard deviation of 0.1, one plasma treatment- 5.5 N/mm with a standard deviation of 1.3, two plasma treatments- 3.6 N/mm with a standard deviation of 2.9, three plasma treatments- 4.3 N/mm with a standard deviation of 0.4, four plasma treatments- 3.86 N/mm with a standard deviation of 1.68 N/mm and five plasma treatments- 3.29 N/mm with a standard deviation of 1.6.

G_{1c} values significantly increased after plasma treating the surfaces i.e., G_{1c} value increased from 0.1 N/mm to 5.5 N/mm. Furthermore, amongst all the five (1-5) number of plasma treatments to glass-PP and HDPE surfaces, adhesively bonded sandwich glass-PP and HDPE panel surfaces with only one plasma treatment using nozzle #22826 showed the highest value of G_{1c} of 5.5 N/mm with the lowest standard deviation of 1.3.

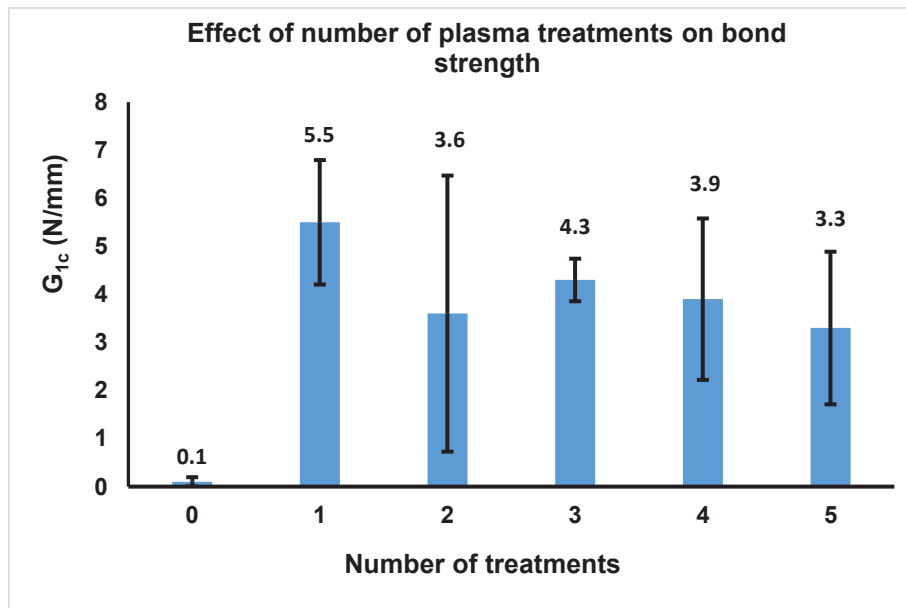


Figure 4.7 Summary of G_{1c} values for adhesively bonded sandwich panels with 0 through 5 number of plasma surface pre-treatments from nozzle# 22826

Fig.A.18 in Appendix shows the typical failed surface of mode 1 interlaminar fracture toughness test of glass-PP and HDPE bonded sandwich panels without surface treatment. From the image, it is evident that, the adhesive is stuck on to either of the surfaces and the failure is not as desired. Fig.A.19 in Appendix shows typical failed surface of mode 1 interlaminar fracture toughness test of glass-PP and HDPE bonded sandwich panels with plasma treatment to surfaces corroborating the failure in the adhesive region.

SEM images that were captured after 0 through 5 number of treatments were studied to understand the observations made from mechanical testing data. SEM images of the treated HDPE showed no noticeable changes in surfaces before and after plasma treatments, however glass-PP SEM images are presented to understand the effect of plasma treatment.

SEM images in Fig.4.8 revealed the surface modification on the glass-PP surfaces after plasma treatment which was not seen in untreated glass-PP surface. However, no further surface modification of the glass-PP surface for the increased number of plasma treatments could not be observed through SEM images.

The surface modification of the glass-PP surface after one plasma treatment could be due to two reasons. One might be the etching of the fibers on the surface of the glass-PP by the plasma other being localized debonding of glass fibers and the polypropylene matrix.

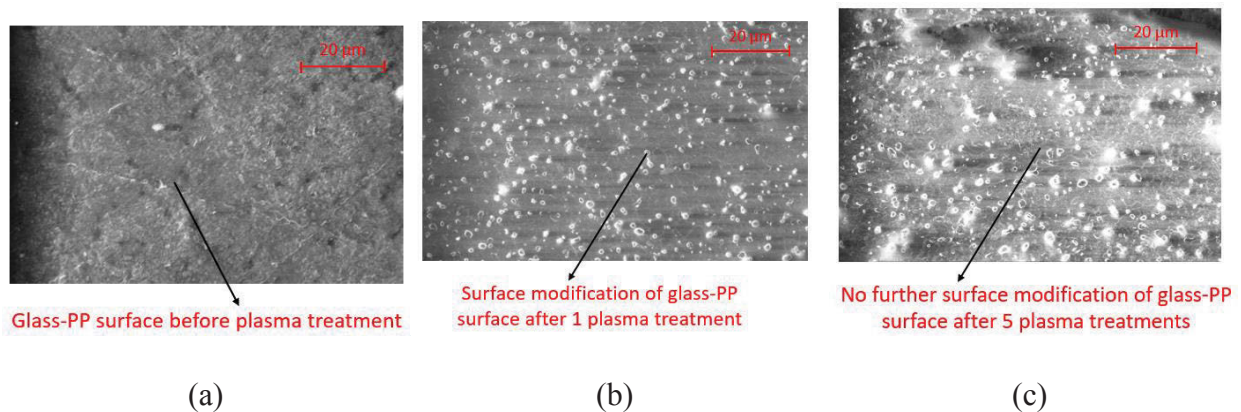


Figure 4.8 SEM image of glass-PP surface (a) before treatment (b) after 1 plasma treatment (c) after 5 plasma treatments

From the SEM images, it can be concluded that the plasma treatment significantly modifies the glass-PP surface therefore enhancing its Bondability and wetting properties. However, for the better understanding of this behavior, surface energy determination was performed. The surface energy values after 0-5 number of plasma treatments were determined via wettability inks and are presented in the Table A.28 in Appendix.

According to the data presented in Table.A.28, plasma treatment increases the surface energies of the glass-PP and HDPE surfaces. The original surface energies of both glass-PP and HDPE surfaces before plasma treatment was found to be 28mN/m. After plasma treating these two surfaces using nozzle #22826 from a treatment height of 0.019m (0.75 inches), the surface energy of HDPE surface changes to 72mN/m and the surface energy of glass-PP surface changed to 58 mN/m. The change in surface energy for HDPE surface was found to be a constant i.e., 72mN/m for further increase in number of treatments.

However, as the number of treatments for glass-PP surface increased from 2-5 number of treatments, the surface energy reduced to 52-24mN/m. This may be due to the thermal degradation of the glass-PP surface by the multiple plasma treatments. The heat transferred to the glass-PP surface due to the multiple plasma treatments might have thermally degraded the surface and reduced the surface energy as indicated in Fig.4.9. In Fig.4.9, image of the glass-PP surface after 1-5 plasma treatments have been captured. It can be clearly observed that the surface degrades with the multiple plasma treatments as indicated by the discoloration of the surface.

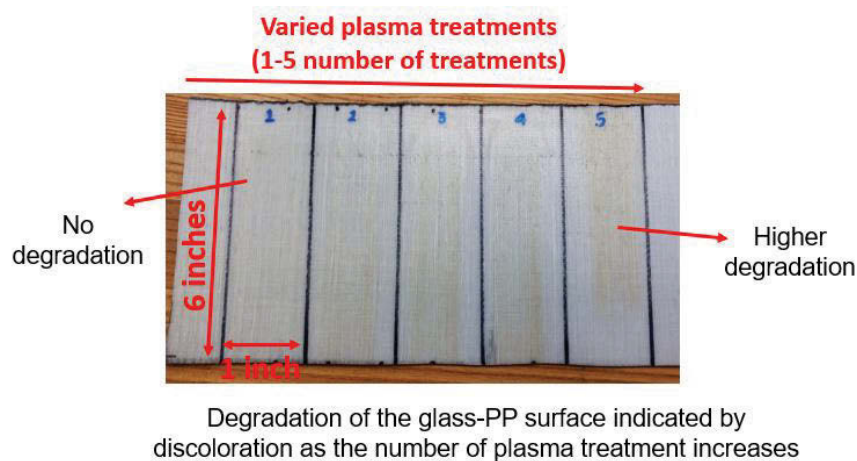


Figure 4.9 Degradation of the glass-PP surface with multiple plasma treatments as indicated by the discoloration for higher number of treatments

Therefore, only one plasma treatment using nozzle#22826 from a treatment height of 0.75 inches for both glass-PP and HDPE surfaces is sufficient enough to enhance their surface energies and thus obtain better bond ability with each other. This is in according to the results from the literature. According to Awaja et al., short plasma treatment times are required to increase the bond strength between two substrates. It has been shown that a short plasma pretreatment of the surface of PP (in some cases less than 6 s) can result in a higher bond strength [52] [53]. Long-term plasma exposure causes formation of weak boundary layers, causing the splitting of CH₃ groups from the tertiary C atoms, and can also cause inner chain scissions, whereas short time exposure will only cause outer chain scissions [9].

4.5 Effect of aging/time on the plasma treatment of glass/PP and HDPE surfaces

Uptake of environmental contaminants, re-orientation of surface groups and further chemical reactions at the surface with time, in many cases, result in an “ageing” effect. This aging effect on the plasma treated glass-PP and HDPE surfaces is evaluated in this study. The objective of this work was to understand the depth and durability of the treatment. The data generated from this study can be used by industries whenever large-scale plasma treatment is desired.

According to the data presented in Table A.29 in Appendix and Fig.4.10, no changes in surface energy was observed for the plasma treated HDPE surface for a period of 10 days. However, for the plasma treated glass-PP surface, surface energy reduced by 3.5 % (56mN/m) and further 3.5 % (54 mN/m) reduce in surface energy was observed after a period of 7 days. A total of 7% reduction in the surface energy was observed at the end of 10th day on glass-PP surface.

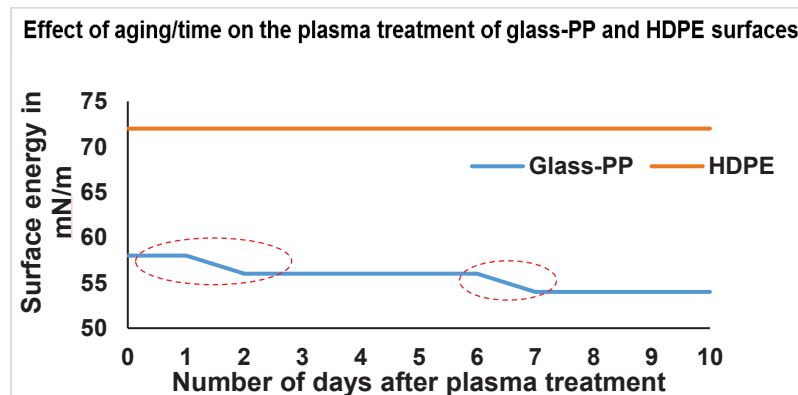


Figure 4.10 Effect of aging/time on the plasma treatment of glass/PP and HDPE surfaces

4.6 Comparison of the effect of plasma treatment on the glass/PP and neat PP surfaces

According to the data presented in Fig.A.21 in Appendix and Table A.30 to A.31 in Appendix, G_{1c} values of the adhesively bonded glass PP and HDPE sandwich panels before and after plasma treatments were as follows: before treatment- 0.1 N/mm with a standard deviation of 0.1 and after treatment- 5.5 N/mm with a standard deviation of 1.3. The G_{1c} values of the adhesively bonded glass-PP and HDPE panels increased significantly (i.e., 53 times) after the plasma treatment.

According to the data presented in Fig.A.20 and Table A.32 to A.33 in Appendix, G_{1c} values of the adhesively bonded neat PP and HDPE sandwich panels before and after plasma treatments were determined. The determined G_{1c} values are as follows: before treatment- 0.36 N/mm with a standard deviation of 0.5 and after treatment- 2.8 N/mm with a standard deviation of 1.1. The G_{1c} values of the adhesively bonded neat PP and HDPE panels also increased slightly after plasma treatment (i.e., 7 times higher).

According to the summary of the G_{1c} values presented in Table A.34 in Appendix and Fig.4.11, The G_{1c} value of neat-PP, HDPE adhesively bonded sandwich panel was found to be higher than glass-PP, HDPE adhesively bonded sandwich panel before plasma treatment. This could be because of the better adhesive -polymer interaction in neat PP panels in comparison to glass-PP panels. Fibers present in glass-PP surface (without any surface treatment) hamper adhesive-polymer interaction and thus form a bond weaker than the neat PP-adhesive bonding. Therefore, the G_{1c} values of neat PP, HDPE adhesively bonded sandwich panel was found to be higher than the glass-PP, HDPE adhesively bonded sandwich panel before plasma treatment.

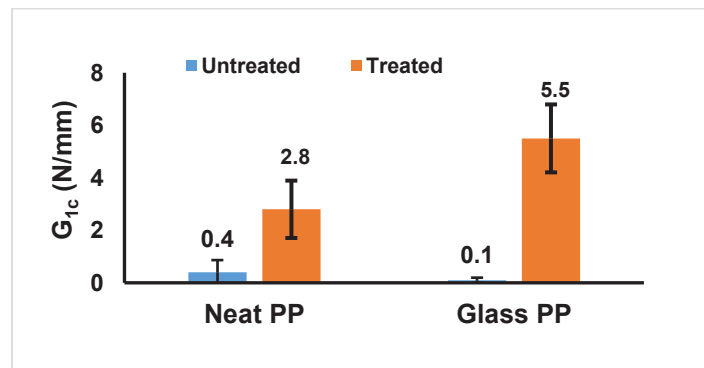


Figure 4.11 Summary of G_{1c} values for adhesively bonded sandwich neat PP-HDPE and Glass-PP-HDPE panels before and after plasma treatment

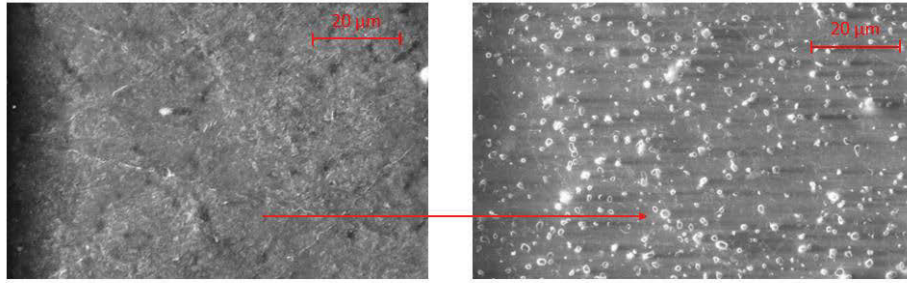
G_{1c} values of both the Glass-PP, HDPE and neat-PP, HDPE adhesively bonded sandwich panels increased after plasma treatment. G_{1c} values of the glass-PP, HDPE adhesively bonded sandwich panels increased by 53 times after plasma treatment whereas, G_{1c} values of the neat PP, HDPE adhesively bonded sandwich panels increased by only 7 times after plasma treatment. Scanning Electron Microscopy (SEM) imaging was conducted for the better understanding of this behavior.

The effect of plasma treatment on the fibers versus neat polymer matrix was evaluated using SEM images. In Fig.4.12 surface modification in the glass-PP surface was observed after plasma treatment. This could be due to the etching of glass fibers in glass-PP surface or due to the debonding of the glass fibers and the polypropylene matrix. However, this surface modification of neat PP surface was not observed in SEM images after plasma treatment as seen in Fig.4.13. This could be due the absence of the fibers in the neat polymer matrix. Surface energy values further complement this observation.

According to the surface energy data presented in the Table.A.35 in Appendix, surface energies of both the glass-PP and neat PP surfaces were found to be 28 mN/m before plasma treatment. After plasma treatment, the surface energy of neat PP surface increased to 46 mN/m and the surface energy of the glass-PP surface increased to 58mN/m.

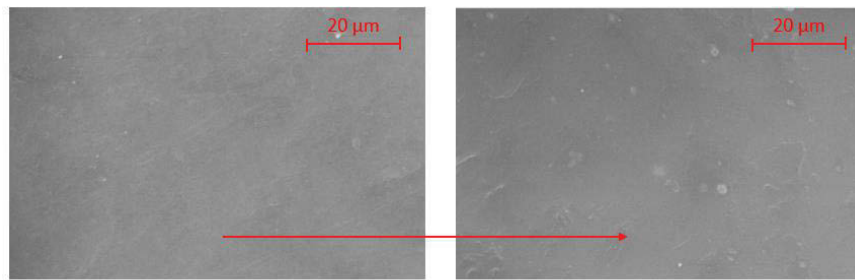
According to the data presented in Table A.34 and SEM images in Fig.12 ad Fig.13, surface energy of the glass-PP surface increased from 28mN/m to 58mN/m after plasma treatment, this is due to the increased surface area/roughness/modification. Similar increase in surface energy of neat PP surface was not observed after the plasma treatment, an increase from 28 mN/m to only 46 mN/m was observed, this is due to the absence of fibers and absence of surface modification after plasma treatment as seen in SEM images.

In conclusion, plasma treatment is more effective in glass reinforced polypropylene matrix compared to neat polypropylene matrix.



Surface modification of glass-PP surface after plasma treatment

Figure 4.12 SEM images of glass-PP surface before and after plasma treatment



No surface modification of neat PP surface after plasma treatment

Figure 4.13 SEM images of neat PP surface before and after plasma treatment

Chapter 5

Empirical Curve Fitting of Surface Energy Experiments

Experimental results from the surface energy determination of glass-PP panels with varied glass fiber weight fractions were used to develop this empirical curve fitting. This curve fitting helps to predict change in surface energy of glass-PP surface with varied fiber volume fractions after plasma treatment.

The glass-PP material used in this work so far was a commercial product with 64% fiber fraction. For the study on empirical curve fitting, glass-PP panels with varied fiber fractions were required. These glass-PP panels were fabricated via compression molding process at FCMF.

Compression molding is used for transforming sheet molding compounds into finished products in matched molds. The compression molding process begins with the placement of a precut and weighed amount of material, usually a stack of several plies onto the bottom of a preheated mold cavity. The mold is quickly closed after the material placement and the top half of the mold is lowered with a constant rate until the pressure on the charge increases to a preset value. With increasing pressure and temperature, the resin in the mold wets all the fibers and fill the entire mold cavity. After a reasonable degree of cure is achieved under pressure, the mold is opened and the part is removed. The schematic of the fabrication of glass-PP panels via compression molding is shown in Figure 5.1

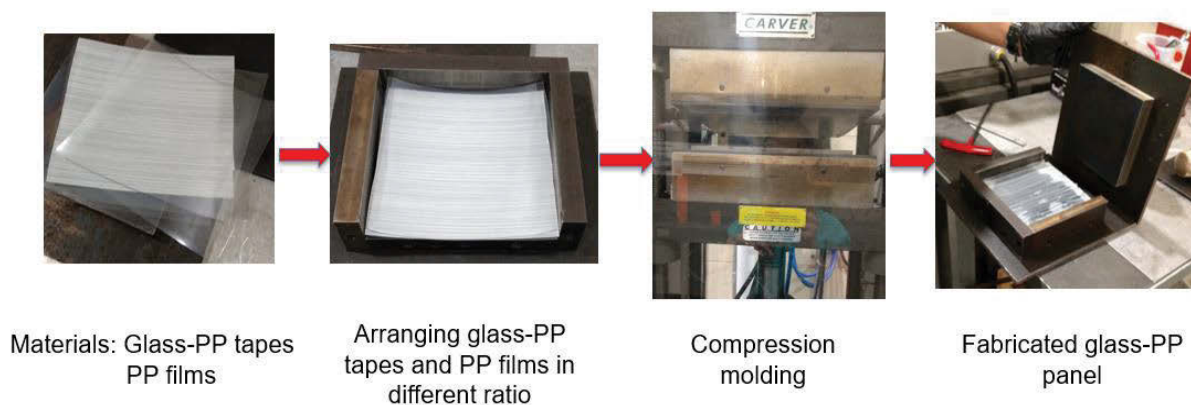


Figure 5.1 Glass-PP panels fabrication via compression molding

Materials used in this study for compression molding were, glass-PP unidirectional tape with 64 fiber wt% and neat PP films. Both glass-PP tapes and PP films were arranged layer by layer in different ratios and processed to obtain glass-PP panel with varied fiber wt%. Compression molding was carried out in a compression molding carver press located in FCMF, UTK. Processing conditions used in panel fabrication was temperature of 160°C and load of 15119 kgs/m². Glass-PP panels of thickness 0.0012m and dimensions of 0.15m * 0.15m were fabricated. Thermogravimetric analysis (TGA) was conducted to determine the fiber wt% in each of the fabricated panels. The thermogravimetric data collected is compiled into a plot of mass or percentage of initial mass on the y axis versus either temperature on the x-axis. This plot is referred to as a TGA curve and is shown in Fig.5.2. Fig.5.2 represents the fiber weight fractions of the various glass-PP panels fabricated via compression molding process. The following fiber wt % were fabricated: 13%, 16%, 31%, 36%, 47% and 58%.

All of the processed glass-PP panels were plasma treated with the following processing conditions: plasma treatment rate 0.01125 m/sec, nozzle# 22826, treatment height of 0.019m (0.75 inches). Surface energy determination of all the plasma treated glass-PP panels was conducted. Surface energy was determined via surface energy test inks. Table A.36 in Appendix represents the surface energies of the glass-PP panels after plasma treatment with varied glass fiber weight fractions thus determined.

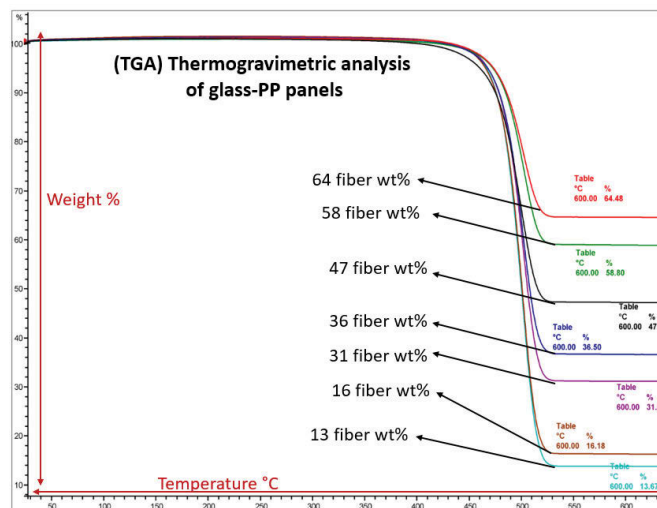


Figure 5.2 Thermogravimetric analysis curves of fabricated glass-PP panels

The data obtained from the Table A.36 is plotted in the graph in Fig.5.3. The surface energy of the glass-PP panel remains constant before plasma treatment i.e., 28 mN/m irrespective of the glass fiber weight fraction in glass-PP panels. However, surface energy after plasma treatment increases with increase in glass fiber wt %. Table A.36 and Fig. 5.3 represent the change in those surface energies.

The solid line in the Fig.5.3 represent surface energy values before plasma treatment and dash/dotted line represents the change in surface energy values after plasma treatment. The equation of the dash/dotted line is used to predict the change in surface energy after plasma treatment for glass-PP panels with varied glass fiber wt%.

The equation of the orange trendline is obtained as,

$$\text{Surface energy in } \left(\frac{mN}{m}\right) = 0.2065 (\text{glass fiber wt}\%) + 45.41 \dots \dots \dots (a)$$

Equation (a) helps to predict the surface energy value after plasma treatment for any glass-PP panel with glass fiber weight fractions varied between 0-64 %.

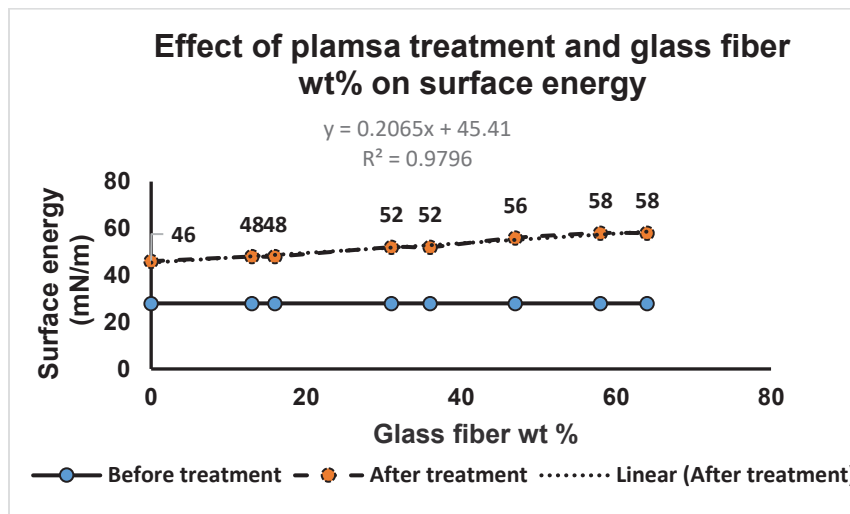


Figure 5.3 Effect of plasma treatment on surface energy and fiber volume fraction of glass-PP surface

Chapter 6

Conclusions

Open air plasma treatment increases the bond strength of the glass-PP, neat PP and HDPE surfaces by increasing their surface energies. SEM images of the plasma treated glass-PP surface reveal the surface modification after plasma treatment. Acrylic adhesive is more suitable than the epoxy adhesive for the adhesion of glass-PP and HDPE surfaces with the aid of open air plasma treatment. The optimized plasma treatment conditions for the glass-PP and HDPE surface adhesion are as follows: Nozzle # 22826 of the open-air plasma treatment equipment from the plasmatreat[®], treatment height of 0.19m, number of treatments-1 at the treatment rate of 0.001125m/sec and the power of plasma 1kVA. Plasma treatment to the glass-PP and HDPE surfaces with the optimized treatment conditions increases the surface energy of HDPE surface from 30 mN/m to 72 mN/m and glass-PP surface from 30 mN/m to 58 mN/m and thus increasing their (Adhesively bonded sandwich panel with glass-PP and HDPE surfaces) G_{1c} value from 0.1 N/mm to 5.5 N/mm. The effect of plasma treatment on glass-PP and HDPE surface tested for a period of 10 days reveal that the surface energy of HDPE surface remains constant i.e., 72 mN/m over a period of 10 days. However, Surface energy of glass-PP surface decreases from 58 mN/m to 56 mN/m i.e., 3.5% decrease after 2 days of treatment. Further, the surface energy reduces to 54mN/m indicating an overall 6.9% decrease after 7 days of treatment. Comparative study of the glass-PP surface versus neat PP surface revealed that the presence of glass fibers enhances the effect of plasma treatment.

References

1. Baldan, A., Adhesively-bonded joints and repairs in metallic alloys, polymers and composite materials: adhesives, adhesion theories and surface pretreatment. *Journal of materials science*, 2004. 39(1): p. 1-49.
2. 2017; Available from: <https://www.plasmatreat.com/>
3. Comyn, J., et al., Corona-discharge treatment of polyetheretherketone (PEEK) for adhesive bonding. *International journal of adhesion and adhesives*, 1996. 16(4): p. 301-304.
4. Blackman, B., A. Kinloch, and J. Watts, The plasma treatment of thermoplastic fibre composites for adhesive bonding. *Composites*, 1994. 25(5): p. 332-341.
5. Harris, A. and A. Beevers, The effects of grit-blasting on surface properties for adhesion. *International Journal of Adhesion and Adhesives*, 1999. 19(6): p. 445-452.
6. Gutowski, T.G., et al. The mechanics of composites deformation during manufacturing processes. in *American Society for Composites, First Technical Conference*. 1986.
7. Molitor, P., V. Barron, and T. Young, Surface treatment of titanium for adhesive bonding to polymer composites: a review. *International Journal of Adhesion and Adhesives*, 2001. 21(2): p. 129-136.
8. Dilsiz, N., N. Erinc, and E. Bayramli, Surface energy and mechanical properties of plasma-modified carbon fibers. *Carbon*, 1995. 33(6): p. 853-858.
9. Abenojar, J., et al., Atmospheric plasma torch treatment of polyethylene/boron composites: Effect on thermal stability. *Surface and Coatings Technology*, 2014. 239: p. 70-77.
10. Wei, Q., Surface characterization of plasma-treated polypropylene fibers. *Materials Characterization*, 2004. 52(3): p. 231-235.
11. Occhiello, E., et al., Oxygen-plasma-treated polypropylene interfaces with air, water, and epoxy resins: Part I. Air and water. *Journal of Applied Polymer Science*, 1991. 42(2): p. 551-559.
12. Mühlhan, C. and H. Nowack, Plasma pretreatment of polypropylene for improved adhesive bonding. *Surface and Coatings Technology*, 1998. 98(1-3): p. 1107-1111.
13. Nihlstrand, A., T. Hjertberg, and K. Johansson, Plasma treatment of polyolefins: Influence of material composition: 1. Bulk and surface characterization. *Polymer*, 1997. 38(14): p. 3581-3589.
14. Kwon, O.-J., et al., Surface characteristics of polypropylene film treated by an atmospheric pressure plasma. *Surface and Coatings Technology*, 2005. 192(1): p. 1-10.
15. Brazel, C.S. and S.L. Rosen, *Fundamental principles of polymeric materials*. 2012: John Wiley & Sons.
16. DeGarmo, E.P., et al., *Materials and process in manufacturing*. 1997: Prentice Hall.
17. Strong, A.B., *Fundamentals of composites manufacturing: materials, methods and applications*. 2008: Society of Manufacturing Engineers.
18. Creton, C., *Materials Science of Pressure-Sensitive Adhesives*. *Materials Science and Technology*, 1997.
19. Wulff, J., et al., The structure and properties of materials. *Journal of The Electrochemical Society*, 1967. 114(9): p. 243C-250C.
20. Aubrey, D., G. Welding, and T. Wong, Failure mechanisms in peeling of pressure-sensitive adhesive tape. *Journal of Applied Polymer Science*, 1969. 13(10): p. 2193-2207.
21. Schonhorn, H. and F.W. Ryan, Effect of morphology in the surface region of polymers on adhesion and adhesive joint strength. *Journal of Polymer Science Part B: Polymer Physics*, 1968. 6(1): p. 231-240.

22. Ishida, H. and P. Bussi, Morphology control in polymer composites. *Materials science and technology*, 1993.
23. Toyama, M., T. Ito, and H. Moriguchi, Studies on tack of pressure-sensitive adhesive tapes. *Journal of applied polymer science*, 1970. 14(8): p. 2039-2048.
24. Fuller, K. and D. Tabor. The effect of surface roughness on the adhesion of elastic solids. in *Proceedings of the Royal Society of London A: Mathematical, Physical and Engineering Sciences*. 1975. The Royal Society.
25. Packham, D., *Surface analysis and pretreatment of plastics and metals*: Edited by: DM Brewis Applied Science Publishers, 1982 (£ 24.00). 1983, Elsevier.
26. Packham, D.E., *Handbook of adhesion*. 1992: Addison-Wesley Longman Ltd.
27. Huh, C. and S. Mason, Effects of surface roughness on wetting (theoretical). *Journal of colloid and interface science*, 1977. 60(1): p. 11-38.
28. Pilato, L.A. and M.J. Michno, *Analysis/Testing*, in *Advanced Composite Materials*. 1994, Springer. p. 97-107.
29. Kempe, G. and H. Krauss. Adhesion bonding techniques for highly loaded parts of continuous carbon-fiber reinforced polyetheretherketone (CF-PEEK/APC2). in *ICAS, 18th Congress*. 1992.
30. Arnold, J., et al. Surface treatment of titanium for adhesive bonding. in *Proc. 29th International SAMPE Technical Conference*. 1997.
31. Hill, J.M., et al., Effects of aging and washing on UV and ozone-treated poly (ethylene terephthalate) and polypropylene. *Journal of adhesion science and technology*, 1995. 9(12): p. 1575-1591.
32. Sutherland, I., et al., Studies of vapour-phase chemical derivatisation for XPS analysis using model polymers. *Journal of Materials Chemistry*, 1994. 4(5): p. 683-687.
33. Baalman, A., et al., Surface treatment of polyetheretherketone (PEEK) composites by plasma activation. *The Journal of Adhesion*, 1994. 46(1-4): p. 57-66.
34. Fornsel, P., *Methods and apparatus for treating the surface of a workpiece by plasma discharge*. 1998, Google Patents.
35. Massines, F., N. Gherardi, and F. Sommer, Silane-based coatings on polypropylene, deposited by atmospheric pressure glow discharge plasmas. *Plasmas and polymers*, 2000. 5(3): p. 151-172.
36. Kinloch, A., *Adhesion and adhesives: science and technology*. 2012: Springer Science & Business Media.
37. Kern, W., *Thin film processes II*. Vol. 2. 2012: Academic press.
38. Chung, H., et al., Effect of oxygen plasma treatment on the bonding strength of CFRP/aluminum foam composite. *Journal of Alloys and Compounds*, 2009. 481(1): p. 214-219.
39. Lai, J., et al., Study on hydrophilicity of polymer surfaces improved by plasma treatment. *Applied Surface Science*, 2006. 252(10): p. 3375-3379.
40. Wertheimer, M., J. Klemberg-Sapieha, and H. Schreiber, Advances in basic and applied aspects of microwave plasma polymerization. *Thin Solid Films*, 1984. 115(2): p. 109-124.
41. Awaja, F., et al., Adhesion of polymers. *Progress in polymer science*, 2009. 34(9): p. 948-968.
42. Hegemann, D., H. Brunner, and C. Oehr, Plasma treatment of polymers for surface and adhesion improvement. *Nuclear instruments and methods in physics research section B: Beam interactions with materials and atoms*, 2003. 208: p. 281-286.

43. Park, J.-k., et al., Pre-treatments of polymers by atmospheric pressure ejected plasma for adhesion improvement. *Surface and Coatings Technology*, 2003. 174: p. 547-552.
44. Fowkes, F.M., Attractive forces at interfaces. *Industrial & Engineering Chemistry*, 1964. 56(12): p. 40-52.
45. Tran, C.Q. and H.-S. Choi, Surface Treatment of Polypropylene using a Large Area Atmospheric Pressure Plasma-solution System. *Korean Chemical Engineering Research*, 2011. 49(3): p. 271-276.
46. Schulz, U., U.B. Schallenberg, and N. Kaiser, Antireflection coating design for plastic optics. *Applied optics*, 2002. 41(16): p. 3107-3110.
47. Jung, C.-K., et al., Development of painting technology using plasma surface technology for automobile parts. *Thin Solid Films*, 2006. 506: p. 316-322.
48. Surface Finish. 2015 [cited 2017; Available from: <https://microgroup.com/wp-content/uploads/2015/01/Surface-Finish.pdf>
49. Maynard, P., et al., Adhesive tape analysis: establishing the evidential value of specific techniques. *Journal of Forensic Science*, 2001. 46(2): p. 280-287.
50. González, M.G., J.C. Cabanelas, and J. Baselga, Applications of FTIR on epoxy resins-identification, monitoring the curing process, phase separation and water uptake, in *Infrared Spectroscopy-Materials Science, Engineering and Technology*. 2012, InTech.
51. Van Ooij, W., D. Surman, and H. Yasuda, Plasma-polymerized coatings of trimethylsilane deposited on cold-rolled steel substrates Part 2. Effect of deposition conditions on corrosion performance. *Progress in organic coatings*, 1995. 25(4): p. 319-337.
52. Boschmans, B., et al., Static secondary ion mass spectrometry (S-SIMS) analysis of atmospheric plasma treated polypropylene films. *Applied surface science*, 2006. 252(19): p. 6660-6663.
53. Urbaniak-Domagala, W., Pretreatment of polypropylene films for following technological processes, part 2: The use of low temperature plasma method. *Journal of Applied Polymer Science*, 2011. 122(4): p. 2529-2541.

Appendix

Table A.1 Showing the effects of surface pretreatments on bond strength and durability of the polymers [3]

| | Treatment type | Material | Bond strength |
|---|---------------------------|-----------------------------|---------------------------------------|
| 1 | Abrasion and solvent wipe | Thermoset and thermoplastic | Increased by 2.2 times for thermosets |
| 2 | Grit blasting | Thermoset and thermoplastic | Increased by 2 times for thermosets |
| 3 | Acid etching | Thermoset and thermoplastic | Slight increase for 1.75 times |
| 4 | Peel ply | Thermoset | Increased by 1.4 times for thermosets |
| 6 | Corona discharge | Thermoplastic | Increased by 3 times |
| 7 | Plasma treatment | Thermoplastic | Increased by 10 times |
| 8 | Flame treatment | Thermoplastic | Increased by 2.7 times |
| 9 | Laser treatment | Thermoset and thermoplastic | Increased by 1.3 times |

Table A.2 Effect of various surface pretreatment methods on the surface chemistry modifications of homopolymer polypropylene

| Pre-treatment | C (at. %) | N (at. %) | O (at. %) | Si (at. %) | F (at. %) | O:C |
|----------------------|------------------|------------------|------------------|-------------------|------------------|------------|
| None | 99 | 0 | 0.5 | 0.5 | 0 | 0.005 |
| Corona | 93.16 | 0 | 6.69 | 0.15 | 0 | 0.072 |
| Flame | 91.75 | 0 | 7.58 | 0.51 | 0 | 0.083 |
| Fluorination | 79.1 | 0 | 10.3 | 0 | 10.24 | 0.130 |
| Vacuum plasma | 84.55 | 2.46 | 12.99 | 0 | 0 | 0.154 |
| Air plasma | 87 | 0.84 | 12.16 | 0 | 0 | 0.140 |

Table A.3 Roughness values for corona discharge, flame, fluorination, vacuum plasma, air plasma pretreatments for homopolymer Polypropylene [31]

| Pretreatment | RA (nm) |
|---------------------|----------------|
| Corona discharge | 1.325 |
| Flame fluorination | 1.173 |
| Vacuum plasma | 0.616 |
| Air plasma | 1.201 |

Table A.4 Composition of epoxy adhesive part A provided by the epoxy.com

| Ingredient | Weight % |
|--|-----------------|
| Modified diglycidyl ether of bisphenol A | 40-70 |
| Alkyl glycidyl ether | 10-30 |
| Precipitated silica | 10-30 |
| Hydroxy modified resin | 1-5 |
| Hydrocarbon resin | 1-5 |
| Naphthalene | 0.06 |

Table A.5 Composition of epoxy adhesive part A provided by the epoxy.com

| Ingredient | Weight % |
|------------------------|-----------------|
| Nonyl phenol | 30-60 |
| N-Aminoethylpiperazine | 10-30 |
| Precipitated silica | 10-30 |
| Hydroxy modified resin | 1-5 |
| Hydrocarbon resin | 1-5 |
| Naphthalene | 0.06 |

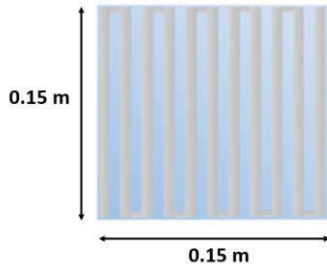


Figure A.1 Schematic of open air plasma movement in a serpentine pattern

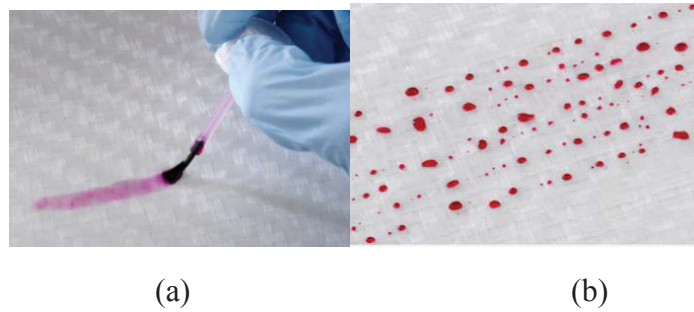


Figure A.2 Surface energy determination by wettability inks (a) good wetting (b) poor wetting

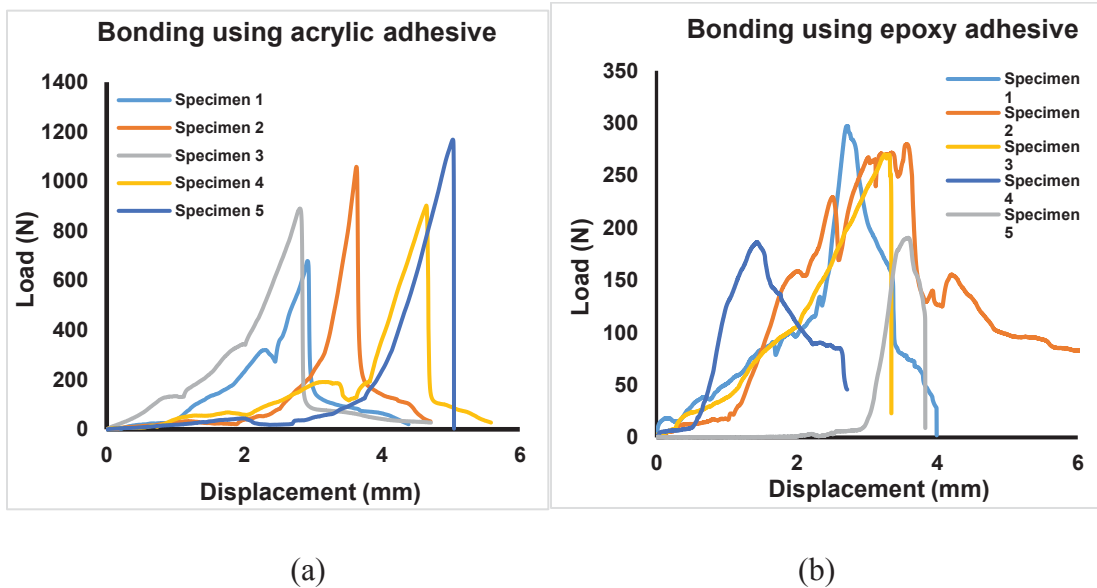


Figure A.3 Load- displacement curves from ASTM D5528 testing for adhesively bonded sandwich panel using (a) acrylic adhesive (b) epoxy adhesive

Table A.6 G_{Ic} calculations for adhesively bonded sandwich panel using acrylic adhesive

| G_{Ic} calculations of adhesively bonded sandwich panel using acrylic adhesive | | | | | |
|--|----------------------------|---------------------------------------|---|----------------------------------|---|
| | Peak Load (N) P | Delamination length (mm) a | Load point displacement (mm) g | Specimen width (mm) b | Mode 1- Interlaminar fracture toughness G_{Ic} (N/mm) |
| 1 | 678.9 | 50 | 4.4 | 25.4 | 3.5 |
| 2 | 1058.8 | 50 | 4.7 | 25.4 | 5.9 |
| 3 | 890.2 | 50 | 4.7 | 25.4 | 4.9 |
| 4 | 902.5 | 50 | 5.6 | 25.4 | 5.9 |
| 5 | 1168.4 | 50 | 5.0 | 25.4 | 6.9 |
| Mean | 939.8 | 50 | 4.8 | 25.4 | 5.5 |
| SD | 185.9 | 00 | 0.45 | 00 | 1.2942 |

Table A.7 G_{Ic} calculations for adhesively bonded sandwich panel using epoxy adhesive

| G_{Ic} calculations of adhesively bonded sandwich panel using Epoxy adhesive | | | | | |
|--|----------------------------|---------------------------------------|---|----------------------------------|---|
| | Peak Load (N) P | Delamination length (mm) a | Load point displacement (mm) g | Specimen width (mm) b | Mode 1- Interlaminar fracture toughness G_{Ic} (N/mm) |
| 1 | 297.3 | 50 | 3.99 | 25.4 | 1.40 |
| 2 | 279.9 | 50 | 7.081 | 25.4 | 2.34 |
| 3 | 270.2 | 50 | 3.34 | 25.4 | 1.06 |
| 4 | 186.6 | 50 | 2.71 | 25.4 | 0.6 |
| 5 | 190.5 | 50 | 3.82 | 25.4 | 0.9 |
| Mean | 244.9 | 50 | 4.2 | 25.4 | 1.25 |
| SD | 52.4 | 00 | 1.7 | 00 | 0.67 |

Table A.8 Summary of G_{IC} values for adhesively bonded sandwich panel using acrylic and epoxy adhesive

| Sample | Peak Load (N) | Mode 1 interlaminar fracture toughness G_{IC} (N/mm) | Mode 1 interlaminar fracture toughness G_{IC} (J/m ²) |
|---------|---------------|--|---|
| Epoxy | 244.9 | 1.25 | 12500 |
| Loctite | 939.8 | 5.5 | 5448.9 |

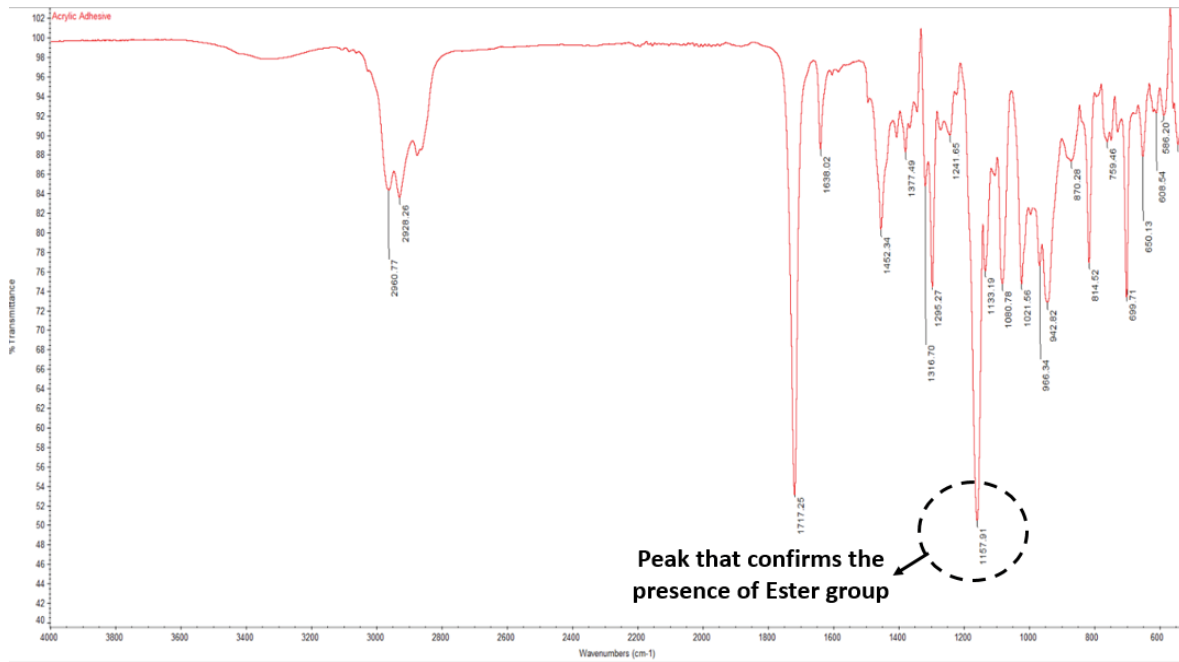


Figure A.4 FTIR transmittance versus wavenumber plot for acrylic adhesive

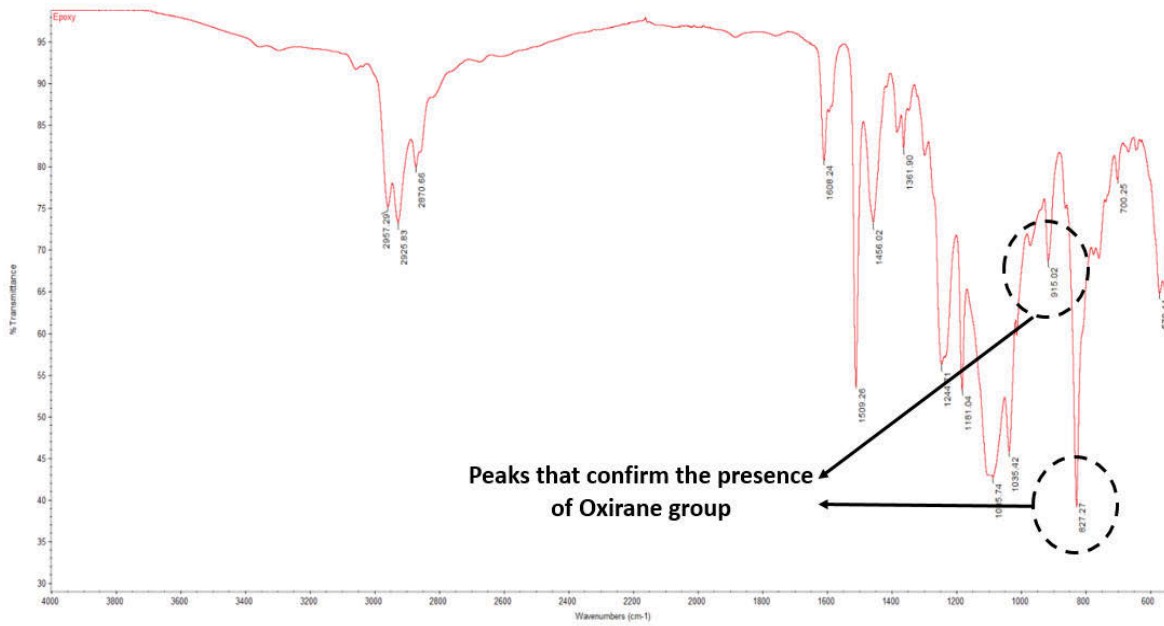


Figure A.5 FTIR transmittance versus wavenumber plot for epoxy adhesive

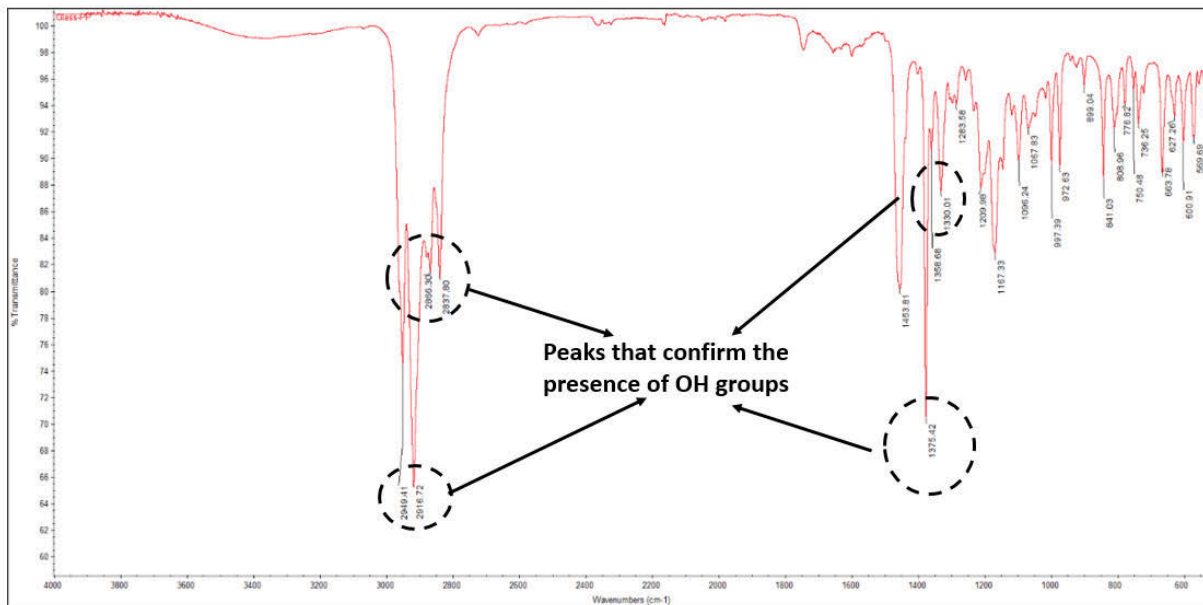


Figure A.6 FTIR transmittance versus wavenumber plot for glass-PP surface after plasma treatment

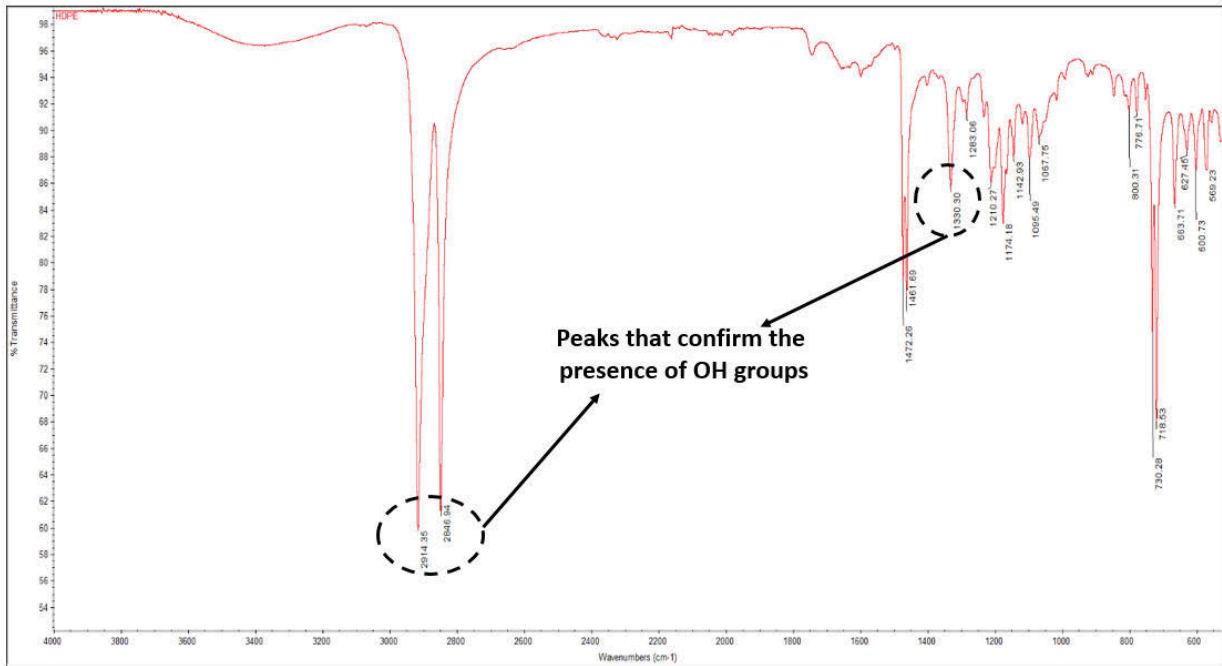


Figure A.7 FTIR transmittance versus wavenumber plot for HDPE surface after plasma treatment

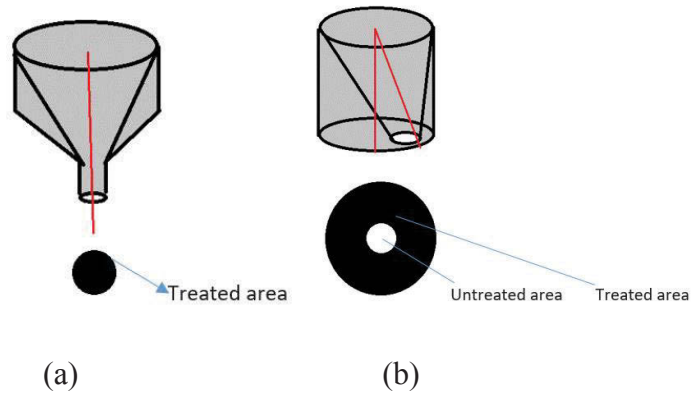


Figure A.8 Schematic of plasma stream coming out (a) from nozzle #10147 (b) from nozzle #22826

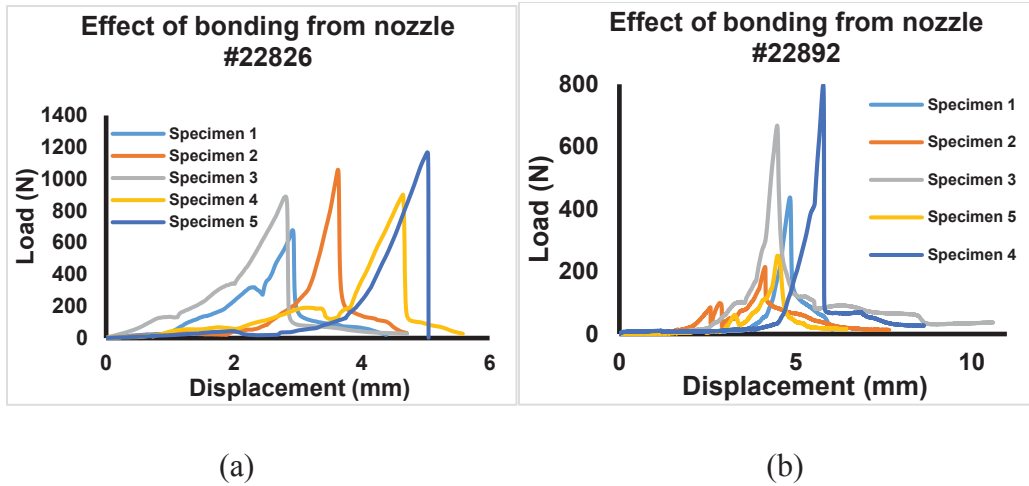


Figure A.9 Load- displacement curves from ASTM D5528 testing for adhesively bonded sandwich panels with plasma treatment from nozzle (a) 22826 (b) 22892

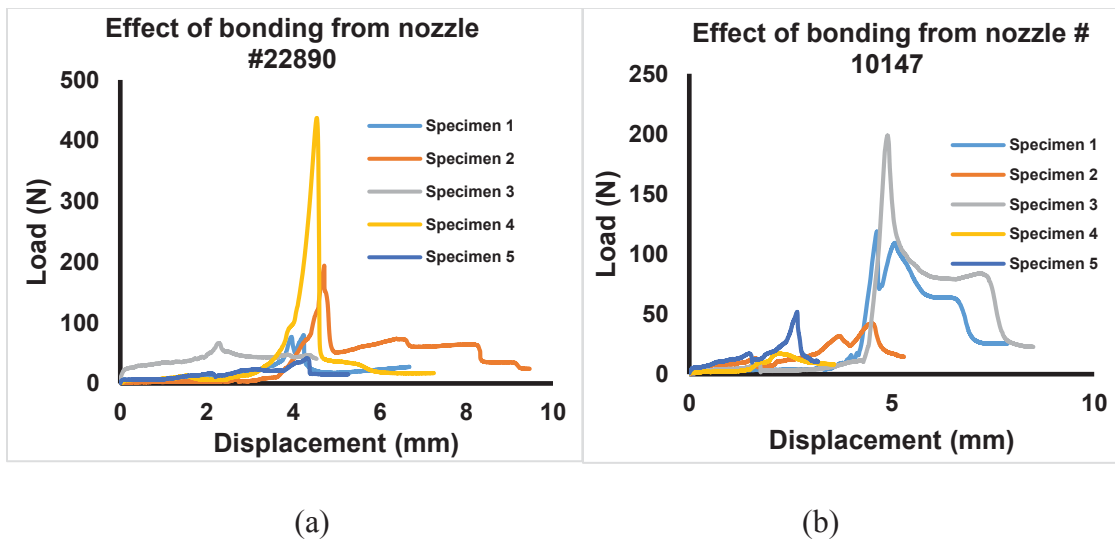


Figure A.10 Load- displacement curves from ASTM D5528 testing for adhesively bonded sandwich panels with plasma treatment from nozzle (a) 22890 (b) 10147

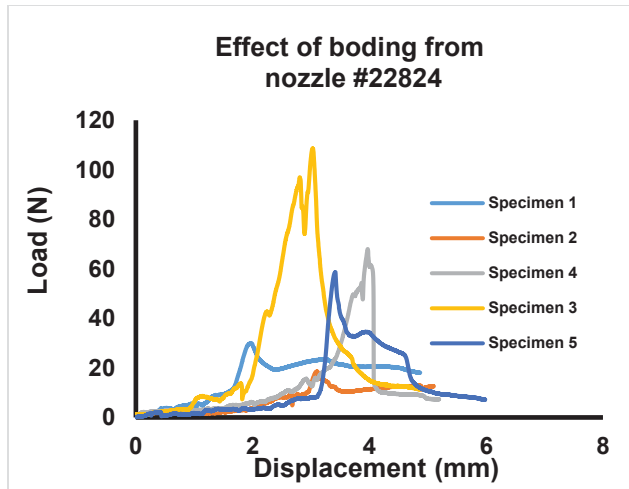


Figure A.11 Load- displacement curves from ASTM D5528 testing for adhesively bonded sandwich panels with plasma surface pre-treatment from nozzle 22824

Table A.9 G_{1c} calculations for adhesively bonded sandwich panel with plasma surface pre-treatment from nozzle #22826

| G_{1c} calculations of the adhesively bonded glass-PP and HDPE sandwich panels after plasma treatment from nozzle #22826 | | | | | |
|--|----------------------------|---|---|--------------------------------------|---|
| | Peak Load (N) P | Delamination length (mm) a | Load point displacement (mm) g | Specimen width (mm) b | Mode 1- Interlaminar fracture toughness G_{1c} (N/mm) |
| 1 | 678.9 | 50 | 4.4 | 25.4 | 3.5 |
| 2 | 1058.8 | 50 | 4.7 | 25.4 | 5.9 |
| 3 | 890.2 | 50 | 4.7 | 25.4 | 4.9 |
| 4 | 902.5 | 50 | 5.6 | 25.4 | 5.9 |
| 5 | 1168.4 | 50 | 5.0 | 25.4 | 6.9 |
| Mean | 939.8 | 50 | 4.8 | 25.4 | 5.5 |
| SD | 185.9 | 00 | 0.45 | 00 | 1.3 |

Table A.10 G_{Ic} calculations for adhesively bonded sandwich panel with plasma surface pre-treatment from nozzle #22892

| G_{Ic} calculations of the adhesively bonded glass-PP and HDPE sandwich panels after plasma treatment from nozzle #22892 | | | | | |
|--|----------------------------|---------------------------------------|---------------------------------------|------------------------------|---|
| | Peak Load (N) P | Delamination length (mm) a | Load point displacement (mm) g | Specimen width (mm) b | Mode 1- Interlaminar fracture toughness G_{Ic} (N/mm) |
| 1 | 437.3 | 50 | 6.1 | 25.4 | 3.2 |
| 2 | 214.2 | 50 | 7.7 | 25.4 | 2 |
| 3 | 667.6 | 50 | 10.6 | 25.4 | 8.4 |
| 4 | 797.3 | 50 | 8.7 | 25.4 | 8.2 |
| 5 | 250.9 | 50 | 6.4 | 25.4 | 1.9 |
| Mean | 473.5 | 50 | 7.9 | 25.4 | 4.7 |
| SD | 255.6 | 00 | 1.8 | 00 | 3.3 |

Table A.11 G_{Ic} calculations for adhesively bonded sandwich panel with plasma surface pre-treatment from nozzle #22890

| G_{Ic} calculations of the adhesively bonded glass-PP and HDPE sandwich panels after plasma treatment from nozzle #22890 | | | | | |
|--|----------------------------|----------------------------------|---------------------------------------|------------------------------|---|
| | Peak Load (N) P | Delamination length (mm)a | Load point displacement (mm) g | Specimen width (mm) b | Mode 1- Interlaminar fracture toughness G_{Ic} (N/mm) |
| 1 | 79.7 | 50 | 6.7 | 25.4 | 0.6 |
| 2 | 194.0 | 50 | 9.5 | 25.4 | 2.2 |
| 3 | 66.4 | 50 | 4.5 | 25.4 | 0.35 |
| 4 | 437.3 | 50 | 7.2 | 25.4 | 3.7 |
| 5 | 41.3 | 50 | 5.3 | 25.4 | 0.25 |
| Mean | 163.8 | 50 | 6.5 | 25.4 | 1.4 |
| SD | 163.8 | 00 | 2 | 00 | 1.5 |

Table A.12 G_{1c} calculations for adhesively bonded sandwich panel with plasma surface pre-treatment from nozzle #10147

| G_{1c} calculations of the adhesively bonded glass-PP and HDPE sandwich panels after plasma treatment from nozzle #10147 | | | | | |
|--|------------------------|-----------------------------------|---------------------------------------|------------------------------|---|
| | Peak Load (N) P | Delamination length (mm) a | Load point displacement (mm) g | Specimen width (mm) b | Mode 1- Interlaminar fracture toughness G_{1c} (N/mm) |
| 1 | 118.7 | 50 | 7.9 | 25.4 | 1.1 |
| 2 | 42.2 | 50 | 5.3 | 25.4 | 0.24 |
| 3 | 198.6 | 50 | 8.5 | 25.4 | 2 |
| 4 | 17.2 | 50 | 3.6 | 25.4 | 0.07 |
| 5 | 51.83 | 50 | 3.2 | 25.4 | 0.2 |
| Mean | 85.7 | 50 | 5.7 | 25.4 | 0.73 |
| SD | 73.43 | 00 | 2.4 | 00 | 0.8 |

Table A.13 G_{1c} calculations for adhesively bonded sandwich panel with plasma surface pre-treatment from nozzle #22826

| G_{1c} calculations of the adhesively bonded glass-PP and HDPE sandwich panels after plasma treatment from nozzle #22824 | | | | | |
|--|------------------------|-----------------------------------|---------------------------------------|------------------------------|---|
| | Peak Load (N) P | Delamination length (mm) a | Load point displacement (mm) g | Specimen width (mm) b | Mode 1- Interlaminar fracture toughness G_{1c} (N/mm) |
| 1 | 30 | 50 | 4.7 | 25.4 | 0.16 |
| 2 | 18.6 | 50 | 5.1 | 25.4 | 0.1 |
| 3 | 108.6 | 50 | 4.9 | 25.4 | 0.6 |
| 4 | 68 | 50 | 5.2 | 25.4 | 0.41 |
| 5 | 58.7 | 50 | 6 | 25.4 | 0.42 |
| Mean | 56.78 | 50 | 5.18 | 25.4 | 0.35 |
| SD | 35.32 | 00 | 0.5 | 00 | 0.21 |

Table A.14 Summary of G_{IC} values for adhesively bonded sandwich panels with plasma surface pre-treatment from five different nozzles

| Nozzle # | Peak Load (N) | Mode 1 interlaminar fracture toughness G_{IC} (N/mm) | Mode 1 interlaminar fracture toughness G_{IC} (J/m ²) |
|--------------|---------------|--|---|
| 10147 | 85.7 | 0.72 | 726.8 |
| 22892 | 473.5 | 4.79 | 4790 |
| 22890 | 163.8 | 1.42 | 1426.9 |
| 22826 | 939.8 | 5.5 | 5448.6 |
| 22824 | 56.78 | 0.35 | 350 |

Table A.15 Surface energies of glass/PP and HDPE surfaces after plasma treatment with five different nozzles.

| Surface energy (mN/m) of glass-PP and HDPE after plasma treatment from various nozzles | | | |
|--|-------------|----------|------|
| | Nozzle type | Glass-PP | HDPE |
| 1 | 22826 | 58 | 72 |
| 2 | 10147 | 30-32 | 52 |
| 3 | 22824 | 36-38 | 68 |
| 4 | 22890 | 52 | 42 |
| 5 | 22892 | 50-58 | 72 |

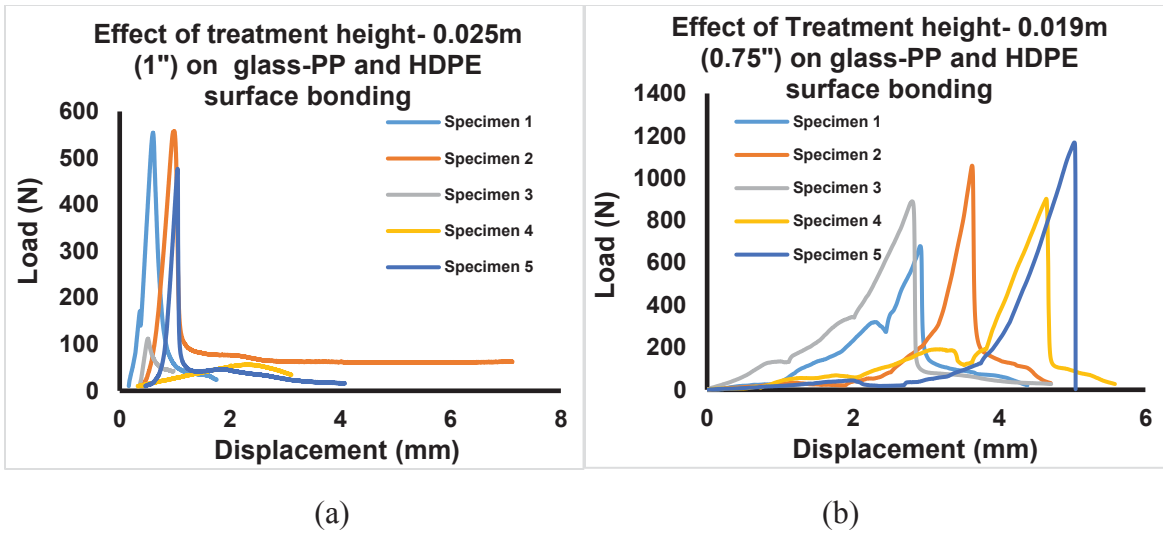


Figure A.12 Load- displacement curves from ASTM D5528 testing for adhesively bonded sandwich panels with plasma surface pre-treatment (a) from treatment height of 0.025m (1'') using nozzle #22826 (b) from treatment height of 0.019m (0.75'') using nozzle #22826

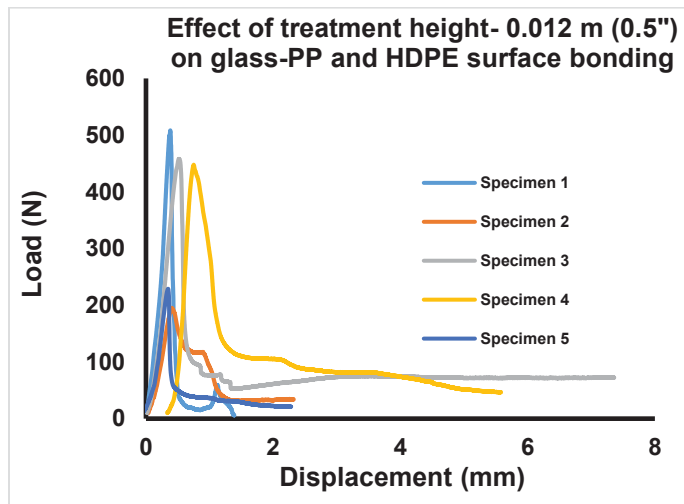


Figure A.13 Load- displacement curves from ASTM D5528 testing for adhesively bonded sandwich panels with plasma surface pre-treatment from 0.012m (0.5'') treatment heights using nozzle #22826

Table A.16 G_{Ic} calculations for adhesively bonded sandwich panel with plasma surface pre-treatment with treatment height of 0.0254m (1”) using nozzle #22826

| G_{Ic} calculations of the adhesively bonded glass-PP and HDPE sandwich panels after plasma treatment from treatment height of 0.0254m (1”) | | | | | |
|---|--------------------------------|---|---|--------------------------------------|---|
| | Peak Load (N) P | Delamination length (mm) a | Load point displacement (mm) g | Specimen width (mm) b | Mode 1- Interlaminar fracture toughness G_{Ic} (N/mm) |
| 1 | 554.2 | 50 | 1.757 | 25.4 | 1.2 |
| 2 | 557.6 | 50 | 7.122 | 25.4 | 4.7 |
| 3 | 112 | 50 | 0.975 | 25.4 | 0.13 |
| 4 | 56.7 | 50 | 3.113 | 25.4 | 0.2 |
| 5 | 476.7 | 50 | 4.082 | 25.4 | 2.3 |
| Mean | 351.4 | 50 | 3.4098 | 25.4 | 1.7 |
| SD | 246.7 | 00 | 2.3968 | 00 | 1.9 |

Table A.17 G_{Ic} calculations for adhesively bonded sandwich panel with plasma surface pre-treatment with treatment height of 0.019m (0.75”) using nozzle #22826

| G_{Ic} calculations of the adhesively bonded glass-PP and HDPE sandwich panels after plasma treatment from treatment height of 0.019m (0.75”) | | | | | |
|---|--------------------------------|---|---|--------------------------------------|---|
| | Peak Load (N) P | Delamination length (mm) a | Load point displacement (mm) g | Specimen width (mm) b | Mode 1- Interlaminar fracture toughness G_{Ic} (N/mm) |
| 1 | 678.9 | 50 | 4.4 | 25.4 | 3.5 |
| 2 | 1058.8 | 50 | 4.7 | 25.4 | 5.9 |
| 3 | 890.2 | 50 | 4.7 | 25.4 | 4.9 |
| 4 | 902.5 | 50 | 5.6 | 25.4 | 5.9 |
| 5 | 1168.4 | 50 | 5.0 | 25.4 | 6.9 |
| Mean | 939.8 | 50 | 4.8 | 25.4 | 5.5 |
| SD | 185.9 | 00 | 0.45 | 00 | 1.3 |

Table A.18 G_{1c} calculations for adhesively bonded sandwich panel with plasma surface pre-treatment with treatment height of 0.012m (0.5”) using nozzle #22826

| G_{1c} calculations of the adhesively bonded glass-PP and HDPE sandwich panels after plasma treatment from treatment height of 0.012m (0.5”) | | | | | |
|--|--------------------------------|---|---|--------------------------------------|---|
| | Peak Load (N) P | Delamination length (mm) a | Load point displacement (mm) g | Specimen width (mm) b | Mode 1- Interlaminar fracture toughness G_{1c} (N/mm) |
| 1 | 508.41 | 50 | 1.38 | 25.4 | 0.8 |
| 2 | 195.37 | 50 | 2.32 | 25.4 | 0.5 |
| 3 | 458.1 | 50 | 7.36 | 25.4 | 4 |
| 4 | 447.8 | 50 | 5.58 | 25.4 | 3 |
| 5 | 228.94 | 50 | 2.28 | 25.4 | 0.61 |
| Mean | 367.72 | 50 | 3.78 | 25.4 | 1.8 |
| SD | 144.34 | 00 | 2.55 | 00 | 1.6 |

Table A.19 Summary of G_{1c} values for adhesively bonded sandwich panels with plasma surface pre-treatment from three treatment heights nozzles # 22826

| Nozzle height | Peak Load (N) | Mode 1 interlaminar fracture toughness G_{1c} (N/mm) | Mode 1 interlaminar fracture toughness G_{1c} (J/m²) |
|----------------------|----------------------|--|---|
| 0.0254m (1”) | 351.4 | 1.7 | 1695 |
| 0.019m (0.75”) | 939.8 | 5.5 | 5449 |
| 0.012m (0.5”) | 367.7 | 1.8 | 1784 |

Table A.20 Surface energies of glass/PP and HDPE surfaces after plasma treatment using nozzle#22826 for three treatment heights.

| Surface energy (mN/m) of glass-PP and HDPE after plasma treatment from different height using nozzle#22826 | | |
|--|----------|------|
| Height of treatment (inches) | Glass-PP | HDPE |
| 1 | 40 | 72 |
| 0.75 | 58 | 72 |
| 0.5 | 46 | 72 |

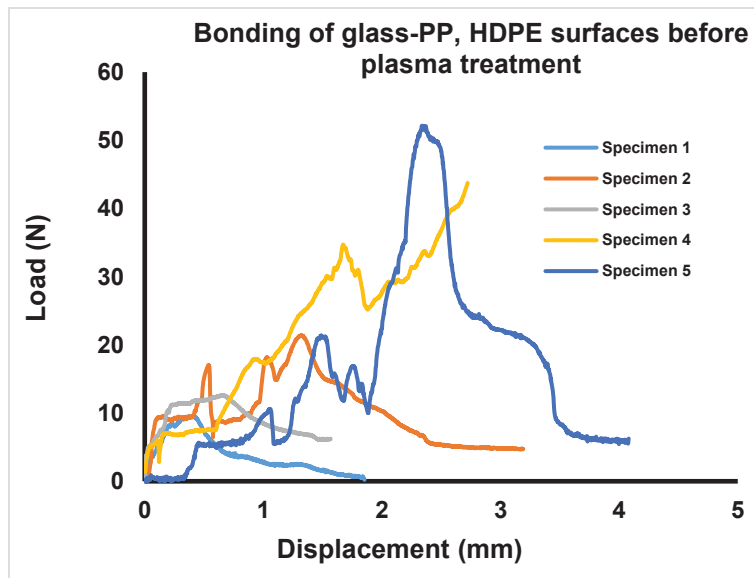


Figure A.14 Load- displacement curves from ASTM D5528 testing for adhesively bonded glass-PP and HDPE sandwich panels without plasma surface pre-treatment

Table A.21 G_{Ic} calculations for adhesively bonded glass-PP and HDPE sandwich panel without plasma surface pre-treatment

| G_{Ic} calculations of the adhesively bonded glass-PP HDPE surfaces before plasma treatment | | | | | |
|--|--------------------------------|---|---|--|--|
| | Peak Load (N) P | Delamination length (mm) a | Load point displacement (mm) g | Specimen width (mm) b | Mode 1- Interlaminar fracture toughness G_{Ic} (N/mm) |
| 1 | 9.6 | 50 | 1.8 | 25.4 | 0.02 |
| 2 | 21.4 | 50 | 3.2 | 25.4 | 0.08 |
| 3 | 12.6 | 50 | 1.6 | 25.4 | 0.02 |
| 4 | 43.7 | 50 | 2.7 | 25.4 | 0.14 |
| 5 | 52.1 | 50 | 4.0 | 25.4 | 0.25 |
| Mean | 27.9 | 50 | 2.7 | 25.4 | 0.1 |
| SD | 19.0 | 00 | 1.0 | 00 | 0.09 |

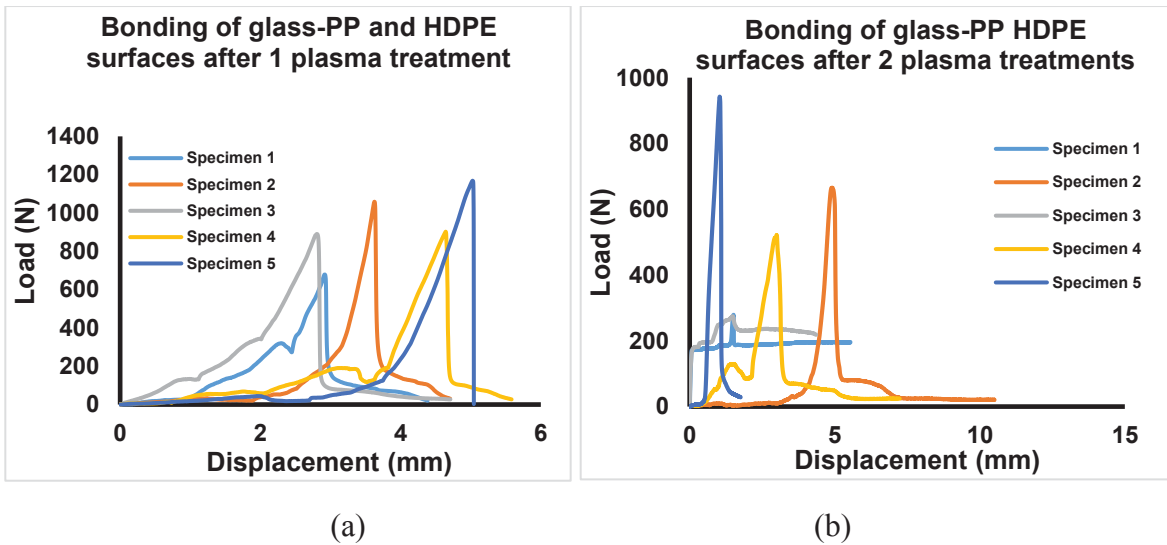


Figure A.15 Load- displacement curves from ASTM D5528 testing for adhesively bonded glass-PP and HDPE sandwich panels with (a) 1 plasma treatment (b) 2 plasma treatments

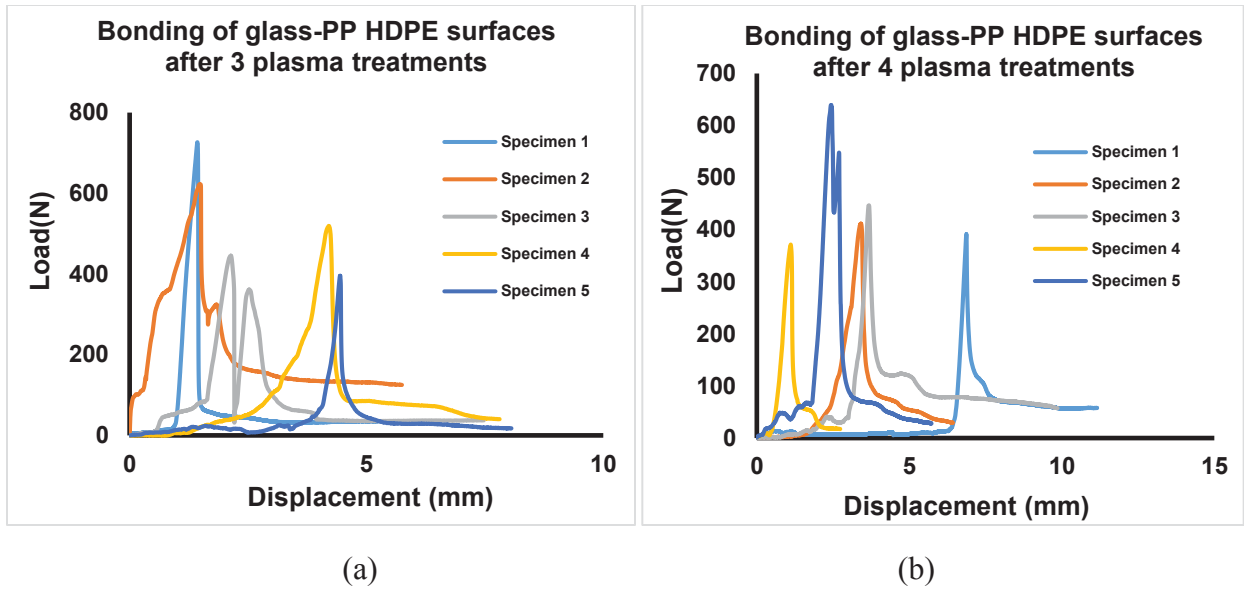


Figure A.16 Load- displacement curves from ASTM D5528 testing for adhesively bonded glass-PP and HDPE sandwich panels with (a) 3 plasma treatments (b) 4 plasma treatments

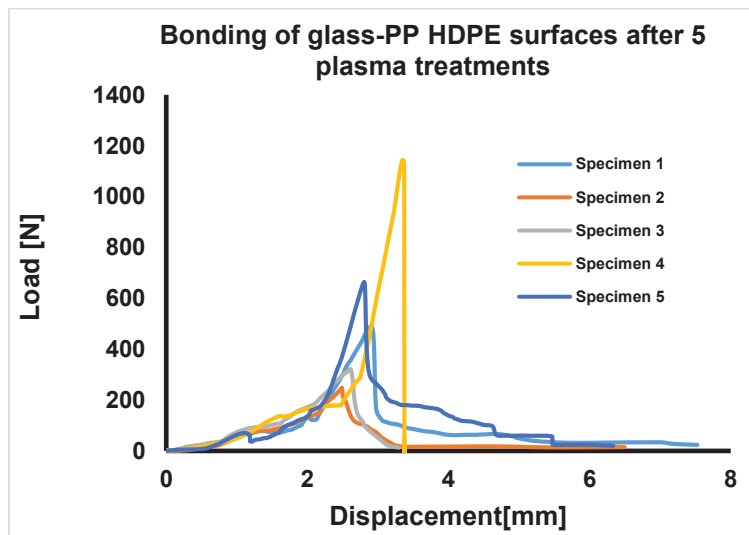


Figure A.17 Load- displacement curves from ASTM D5528 testing for adhesively bonded glass-PP and HDPE sandwich panels with 5 plasma treatments

Table A.22 G_{Ic} calculations for adhesively bonded glass-PP and HDPE sandwich panel with one plasma surface pre-treatment from nozzle# 22826

| G_{Ic} calculations of the adhesively bonded sandwich glass-PP and HDPE surfaces after 1 plasma treatment | | | | | |
|---|------------------------|-----------------------------------|---------------------------------------|------------------------------|---|
| | Peak Load (N) P | Delamination length (mm) a | Load point displacement (mm) g | Specimen width (mm) b | Mode 1- Interlaminar fracture toughness G_{Ic} (N/mm) |
| 1 | 678.9 | 50 | 4.4 | 25.4 | 3.5 |
| 2 | 1058.8 | 50 | 4.7 | 25.4 | 5.9 |
| 3 | 890.2 | 50 | 4.7 | 25.4 | 4.9 |
| 4 | 902.5 | 50 | 5.6 | 25.4 | 5.9 |
| 5 | 1168.4 | 50 | 5.0 | 25.4 | 6.9 |
| Mean | 939.8 | 50 | 4.8 | 25.4 | 5.5 |
| SD | 185.9 | 00 | 0.45 | 00 | 1.3 |

Table A.23 G_{Ic} calculations for adhesively bonded glass-PP and HDPE sandwich panel with two plasma surface pre-treatments from nozzle# 22826

| G_{Ic} calculations of the adhesively bonded sandwich glass-PP and HDPE surfaces after 2 plasma treatments | | | | | |
|--|------------------------|-----------------------------------|---------------------------------------|------------------------------|---|
| | Peak Load (N) P | Delamination length (mm) a | Load point displacement (mm) g | Specimen width (mm) b | Mode 1- Interlaminar fracture toughness G_{Ic} (N/mm) |
| 1 | 942.1 | 50 | 1.8 | 25.4 | 1.9 |
| 2 | 665.0 | 50 | 10.5 | 25.4 | 8.2 |
| 3 | 274.4 | 50 | 4.4 | 25.4 | 1.4 |
| 4 | 521.0 | 50 | 7.2 | 25.4 | 4.4 |
| 5 | 278.9 | 50 | 5.5 | 25.4 | 1.8 |
| Mean | 536.3 | 50 | 5.8 | 25.4 | 3.6 |
| SD | 281.2 | 00 | 3.3 | 00 | 2.9 |

Table A.24 G_{Ic} calculations for adhesively bonded glass-PP and HDPE sandwich panel with three plasma surface pre-treatments from nozzle# 22826

| G_{Ic} calculations of the adhesively bonded sandwich glass-PP and HDPE surfaces after 3 plasma treatments | | | | | |
|--|------------------------|-----------------------------------|---------------------------------------|------------------------------|---|
| | Peak Load (N) P | Delamination length (mm) a | Load point displacement (mm) g | Specimen width (mm) b | Mode 1- Interlaminar fracture toughness G_{Ic} (N/mm) |
| 1 | 726.5 | 50 | 5.4 | 25.4 | 4.7 |
| 2 | 622.2 | 50 | 5.7 | 25.4 | 4.2 |
| 3 | 445.5 | 50 | 7.5 | 25.4 | 3.9 |
| 4 | 519.1 | 50 | 7.8 | 25.4 | 4.9 |
| 5 | 396.6 | 50 | 8.0 | 25.4 | 3.8 |
| Mean | 541.9 | 50 | 6.9 | 25.4 | 4.3 |
| SD | 133.7 | 00 | 1.2 | 00 | 0.44 |

Table A.25 G_{Ic} calculations for adhesively bonded glass-PP and HDPE sandwich panel with four plasma surface pre-treatments from nozzle# 22826

| G_{Ic} calculations of the adhesively bonded sandwich glass-PP and HDPE surfaces after 4 plasma treatments | | | | | |
|--|------------------------|-----------------------------------|---------------------------------------|------------------------------|---|
| | Peak Load (N) P | Delamination length (mm) a | Load point displacement (mm) g | Specimen width (mm) b | Mode 1- Interlaminar fracture toughness G_{Ic} (N/mm) |
| 1 | 391.5 | 50 | 11.2 | 25.4 | 5.2 |
| 2 | 411.7 | 50 | 6.4 | 25.4 | 3.1 |
| 3 | 446.8 | 50 | 9.9 | 25.4 | 5.2 |
| 4 | 371.5 | 50 | 2.7 | 25.4 | 1.2 |
| 5 | 639.4 | 50 | 5.7 | 25.4 | 4.3 |
| Mean | 452.16 | 50 | 7.2 | 25.4 | 3.86 |
| SD | 108.28 | 00 | 3.4 | 00 | 1.68 |

Table A.26 G_{Ic} calculations for adhesively bonded glass-PP and HDPE sandwich panel with five plasma surface pre-treatments from nozzle# 22826

| G_{Ic} calculations of the adhesively bonded sandwich glass-PP and HDPE surfaces after 5 plasma treatments | | | | | |
|--|------------------------|-----------------------------------|---------------------------------------|------------------------------|---|
| | Peak Load (N) P | Delamination length (mm) a | Load point displacement (mm) g | Specimen width (mm) b | Mode 1- Interlaminar fracture toughness G_{Ic} (N/mm) |
| 1 | 490.5 | 50 | 7.5 | 25.4 | 4.4 |
| 2 | 248.0 | 50 | 6.5 | 25.4 | 1.9 |
| 3 | 321.5 | 50 | 3.3 | 25.4 | 1.2 |
| 4 | 1144.3 | 50 | 3.4 | 25.4 | 4.6 |
| 5 | 664.2 | 50 | 5.6 | 25.4 | 4.4 |
| Mean | 573.7 | 50 | 5.3 | 25.4 | 3.3 |
| SD | 357.2 | 00 | 1.9 | 00 | 1.6 |

Table A.27 Summary of G_{Ic} values for adhesively bonded sandwich panels with 0 through 5 number of plasma surface pre-treatments from nozzle # 22826

| Sample | Peak Load (N) | Mode 1 interlaminar fracture toughness G_{Ic} (N/mm) | Mode 1 interlaminar fracture toughness G_{Ic} (J/m^2) |
|--------------------|----------------------|--|--|
| Before treatment | 27.9 | 0.1033 | 103.3 |
| 1 treatment | 939.7 | 5.4489 | 5448.9 |
| 2 treatments | 536.2 | 3.575 | 3575 |
| 3 treatments | 541.9 | 4.274 | 4274 |
| 4 treatments | 452.1 | 3.86 | 3860 |
| 5 treatments | 573.7 | 3.29 | 3290 |



Figure A.18 Failed sandwich structure without surface treatment to glass-PP and HDPE surfaces



Figure A.19 Failed sandwich structure with plasma treatment to glass-PP and HDPE surfaces

Table A.28 Surface energies of glass/PP and HDPE surfaces before and after 1 through 5 number of plasma treatments using nozzle#22826

| Surface energy (mN/m) of glass-PP and HDPE before and after various number of plasma treatments | | |
|--|-----------------|-------------|
| # Treatments | Glass/PP | HDPE |
| 0 | 28 | 28 |
| 1 | 58 | 70-72 |
| 2 | 52-54 | 70-72 |
| 3 | 52-54 | 70-72 |
| 4 | 52-54 | 70-72 |
| 5 | 52-54 | 70-72 |

Table A.29 Effect of aging/time on the plasma treatment of glass/PP and HDPE surfaces

| Surface energy (mN/m) as a function of time | | | | | |
|--|-----------------|-------------|-------------|-----------------|-------------|
| Time | Glass-PP | HDPE | Time | Glass-PP | HDPE |
| 0 min | 58 | 72 | 24hrs. | 56 | 72 |
| 5 min | 58 | 72 | 2 days | 56 | 72 |
| 10 min | 58 | 72 | 3 days | 56 | 72 |
| 15 min | 58 | 72 | 4 days | 56 | 72 |
| 30 min | 58 | 72 | 5 days | 56 | 72 |
| 1 hr. | 58 | 72 | 6 days | 56 | 72 |
| 2 hrs. | 58 | 72 | 7 days | 54 | 72 |
| 3 hrs. | 58 | 72 | 8 days | 54 | 72 |
| 4 hrs. | 58 | 72 | 9 days | 54 | 72 |
| 5 hrs. | 58 | 72 | 10 days | 54 | 72 |

Table A.30 G_{Ic} calculations for adhesively bonded neat PP and HDPE sandwich panel before plasma surface pre-treatment

| G_{Ic} calculations of the adhesively bonded sandwich neat PP and HDPE surfaces before plasma treatment | | | | | |
|---|----------------------------|---------------------------------------|---------------------------------------|------------------------------|---|
| | Peak Load (N) P | Delamination length (mm) a | Load point displacement (mm) g | Specimen width (mm) b | Mode 1- Interlaminar fracture toughness G_{Ic} (N/mm) |
| 1 | 153.83 | 50 | 1.023 | 25.4 | 0.19 |
| 2 | 155.4 | 50 | 1.1 | 25.4 | 0.2 |
| 3 | 27.74 | 50 | 1.405 | 25.4 | 0.004 |
| 4 | 318.28 | 50 | 2.78 | 25.4 | 1.0 |
| Mean | 163.81 | 50 | 1.577 | 25.4 | 0.36 |
| SD | 119.09 | 00 | 0.818 | 00 | 0.47 |

Table A.31 G_{Ic} calculations for adhesively bonded neat PP and HDPE sandwich panel after plasma surface pre-treatment

| G_{Ic} calculations of the adhesively bonded sandwich neat PP and HDPE surfaces after plasma treatment | | | | | |
|--|----------------------------|---------------------------------------|---------------------------------------|------------------------------|---|
| | Peak Load (N) P | Delamination length (mm) a | Load point displacement (mm) g | Specimen width (mm) b | Mode 1- Interlaminar fracture toughness G_{Ic} (N/mm) |
| 1 | 286.43 | 50 | 11.368 | 25.4 | 3.9 |
| 2 | 325.24 | 50 | 5.687 | 25.4 | 2.2 |
| 3 | 214.94 | 50 | 13.558 | 25.4 | 3.5 |
| 4 | 119.26 | 50 | 10.798 | 25.4 | 1.5 |
| Mean | 236.46 | 50 | 10.352 | 25.4 | 2.8 |
| SD | 90.51 | 00 | 3.330 | 00 | 1.0 |

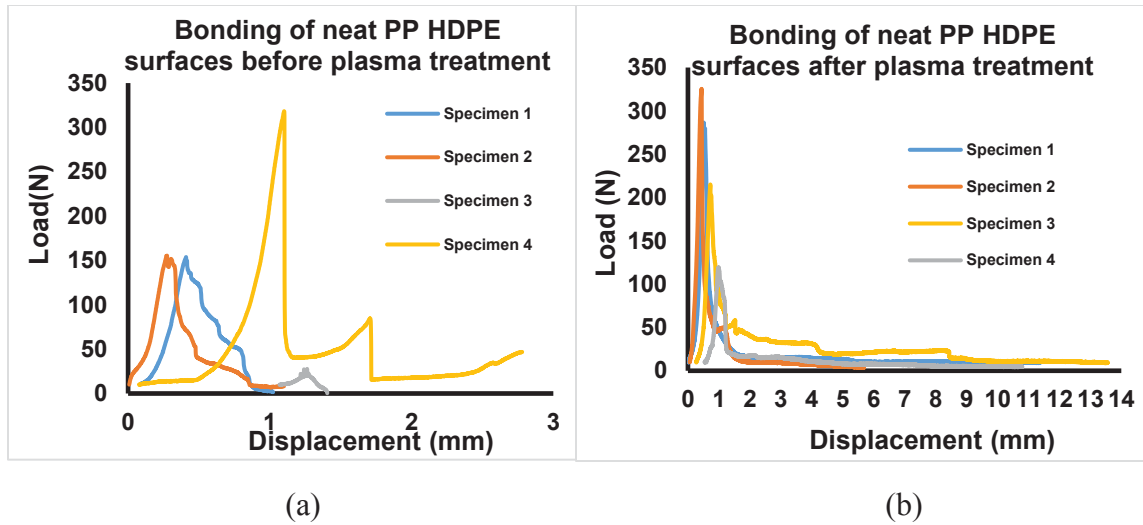


Figure A.20 Load- displacement curves from ASTM D5528 testing for adhesively bonded neat PP and HDPE sandwich panels (a) before plasma surface pretreatment (b) after plasma pretreatment

Table A.32 G_{Ic} calculations for adhesively bonded glass-PP and HDPE sandwich panel without plasma surface pre-treatment

| G_{Ic} calculations of the adhesively bonded glass-PP HDPE surfaces before plasma treatment | | | | | |
|---|------------------------|-----------------------------------|---------------------------------------|------------------------------|---|
| | Peak Load (N) P | Delamination length (mm) a | Load point displacement (mm) g | Specimen width (mm) b | Mode 1- Interlaminar fracture toughness G_{Ic} (N/mm) |
| 1 | 9.6 | 50 | 1.8 | 25.4 | 0.02 |
| 2 | 21.4 | 50 | 3.2 | 25.4 | 0.08 |
| 3 | 12.6 | 50 | 1.6 | 25.4 | 0.02 |
| 4 | 43.7 | 50 | 2.7 | 25.4 | 0.14 |
| 5 | 52.1 | 50 | 4.0 | 25.4 | 0.25 |
| Mean | 27.9 | 50 | 2.7 | 25.4 | 0.1 |
| SD | 19.0 | 00 | 1.0 | 00 | 0.09 |

Table A.33 G_{Ic} calculations for adhesively bonded glass-PP and HDPE sandwich panel after plasma surface pre-treatment

| G_{Ic} calculations of the adhesively bonded sandwich glass-PP and HDPE surfaces after 1 plasma treatment | | | | | |
|---|------------------------|-----------------------------------|---------------------------------------|------------------------------|---|
| | Peak Load (N) P | Delamination length (mm) a | Load point displacement (mm) g | Specimen width (mm) b | Mode I- Interlaminar fracture toughness G_{Ic} (N/mm) |
| 1 | 678.9 | 50 | 4.4 | 25.4 | 3.5 |
| 2 | 1058.8 | 50 | 4.7 | 25.4 | 5.9 |
| 3 | 890.2 | 50 | 4.7 | 25.4 | 4.9 |
| 4 | 902.5 | 50 | 5.6 | 25.4 | 5.9 |
| 5 | 1168.4 | 50 | 5.0 | 25.4 | 6.9 |
| Mean | 939.8 | 50 | 4.8 | 25.4 | 5.5 |
| SD | 185.9 | 00 | 0.45 | 00 | 1.3 |

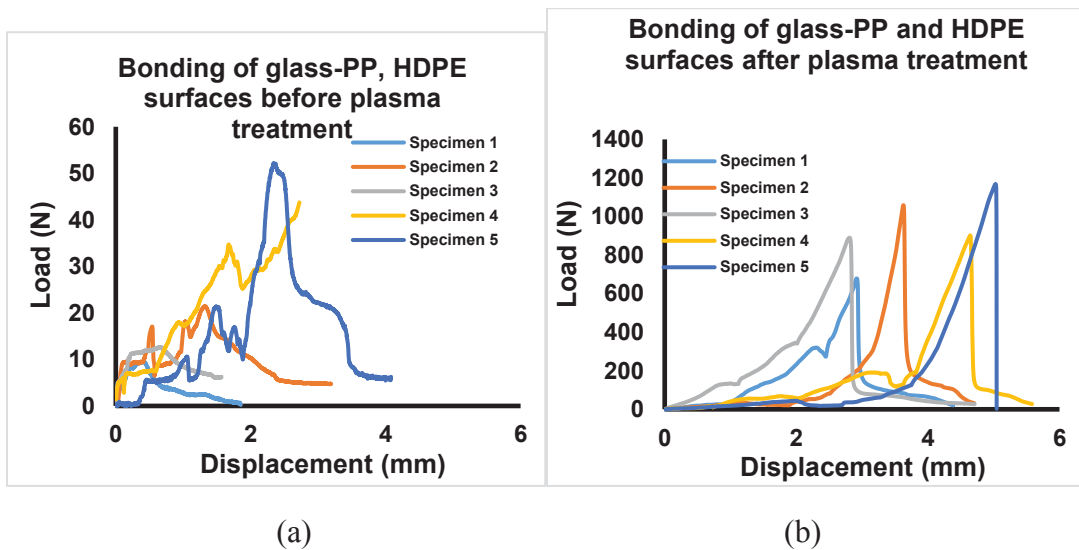


Figure A.21 Load- displacement curves from ASTM D5528 testing for adhesively bonded glass-PP and HDPE sandwich panels (a) before plasma treatment (b) after plasma treatment

Table A.34 Summary of G_{1C} values for adhesively bonded neat PP-HDPE and Glass-PP-HDPE sandwich panels before and after plasma treatment

| G_{1c} in N/mm | | |
|------------------------------------|---------------------|----------------------|
| | Neat PP-HDPE | Glass PP-HDPE |
| Untreated | 0.36 | 0.1 |
| Plasma treated | 2.8 | 5.5 |

Table A.35 Surface energies of glass-PP and neat PP surfaces before and after plasma treatment

| Surface energy (mN/m) of glass-PP, neat-PP and HDPE surfaces before and after plasma treatment | | |
|---|------------------|----------------|
| | Untreated | Treated |
| Glass-PP | 28 | 58 |
| Neat-PP | 28 | 46 |

Table A.36 Surface energies of glass-PP panels after plasma treatment

| Glass fiber wt % | Surface energy (mN/m) Before treatment | Surface energy (mN/m) After treatment |
|-------------------------|---|--|
| 64 | 28 | 58 |
| 58 | 28 | 58 |
| 47 | 28 | 56 |
| 36 | 28 | 52 |
| 31 | 28 | 52 |
| 16 | 28 | 48 |
| 13 | 28 | 48 |
| 0 | 28 | 46 |

Vita

Vidyarani Sangnal Matt Durandhara Murthy was born in Karnataka, India. She did her schooling in Davangere, Karnataka, India. After finishing her schooling in 2010, she attended Bapuji Institute of Engineering and Technology, Davangere, India (2010-2014) from where she graduated with a Bachelor degree in Chemical Engineering. In spring 2016, she started pursuing her Master's degree in Mechanical Engineering department at The University of Tennessee, Knoxville. She worked as Graduate Research Assistant with Dr. Uday Vaidya and Graduate Teaching Assistant with the Mechanical Engineering department at The University of Tennessee, Knoxville and obtained M.S degree in Mechanical Engineering in Fall 2017.